METAL-SUPPORTING POLYMER FOR SUPEROXIDE DISMUTASE MIMICS
AND
CONSTRUCTION OF METAL-BINDING TAG FOR PROTEIN PURIFICATION

THEERAPHON   PIACHAM

A THESIS SUBMITTED IN PARTIAL FULFILLMENT
OF THE REQUIREMENTS FOR
THE DEGREE OF MASTER OF SCIENCE
(MEDICAL TECHNOLOGY)
FACULTY OF GRADUATE STUDIES
MAHIDOL UNIVERSITY
2003

Thesis
entitled

METAL-SUPPORTING POLYMER FOR SUPEROXIDE DISMUTASE MIMICS
AND
CONSTRUCTION OF METAL-BINDING TAG FOR PROTEIN PURIFICATION

……………………………….
Mr.Theeraphon Piacham
Candidate

………………………………
Lect.Chartchalerm Isarankura Na Ayudhya,
Ph.D.
Major-Advisor

……………………………….
Assoc.Prof.Virapong Prachayasittikul,
Ph.D.
Co-Advisor

……………………………………………………
Assoc.Prof.Rassmidara Hoonsawat,
Ph.D.
Dean
Faculty of Graduate Studies

………………………………………………..
Asst.Prof.Rachada Kiatfuengfoo, Ph.D.
Chair
Master of Science Programme in
Medical Technology
Faculty of Medical Technology

Thesis
entitled

METAL-SUPPORTING POLYMER FOR SUPEROXIDE DISMUTASE MIMICS
AND
CONSTRUCTION OF METAL-BINDING TAG FOR PROTEIN PURIFICATION

was submitted to the Faculty of Graduate Studies, Mahidol University
For the degree of Master of Science (Medical Technology)
on
June 9, 2003

………………………………….
Mr.Theeraphon Piacham
Candidate

…………………………………
Lect.Chartchalerm Isarankura Na Ayudhya, Ph.D.
Chairman

……………………………… ………………………………….
Assoc.Prof.Virapong Prachayasittikul, Prof.Somsak Ruchirawat,
Ph.D. Ph.D.
Member Member

……………………………… ……………………………….
Asst.Prof.Byaporn Na Nagara, Lect.Ratana Lawung,
Ph.D. Ph.D.
Member Member

……………………………… ………………………………
Assoc.Prof.Rassmidara Hoonsawat, Assoc.Prof.Virapong Prachayasittikul,
Ph.D. Ph.D.
Dean Dean
Faculty of Graduate Studies Faculty of Medical Technology
Mahidol University Mahidol University

ACKNOWLEDGEMENTS

Publication Derived from this Master Thesis

METAL-SUPPORTING POLYMER FOR SUPEROXIDE DISMUTASE MIMICS AND METAL-BINDING TAG FOR PROTEIN PURIFICATION.

THEERAPHON PIACHAM 4338107 MTMT/M

M.Sc. (MEDICAL TECHNOLOGY)

THESIS ADVISORS: CHARTCHALERM ISARANKURA NA AYUDHYA, Ph.D., VIRAPONG PRACHAYASITTIKUL, Ph.D.

ABSTRACT

A Polymer-supported manganese catalyst possessing superoxide dismutase (SOD) activity was synthesized. Matrices consisting of either 4-vinylimidazole (4V) or 1-vinylimidazole (1V) in combination with methacrylic acid (MAA), which were expected to provide avidity to Mn (II) similar to that of the combination of histidine and aspartic acid residues at an active site of SOD, were selected as functional monomers to form a coordination sphere with template metal in a cross-linked polymer. All these matrices were prepared to form polymers through free radical polymerization, using excess amounts of the cross-linking monomer, ethyleneglycol dimethacrylate (EDMA). Mimicing the SOD activity of the polymers was assayed by measuring the inhibition of the photoreduction of nitro blue tetrazolium (NBT). It was anticipated that this catalytic activity would generate from the coordination between a metal center and a complex of three imidazole and one carboxyl groups as in the case of the native enzyme. Surprisingly, the polymer Mn-P1VMAA exhibited much higher activity than did the Mn-P4VMAA. Omitting one of the functional monomers (1V or MAA) resulted in a decrease in SOD activity. These findings strongly support a high potential for the application of the catalytic metal based-imprinted polymer for therapeutic use in the future.

The metal-binding tag was applied as a powerful approach for protein purification. The tagger was inserted into the protein of interest at the gene level. Based on the concept that polyhistidine bind tightly with a number of transition metals including Cu^{2+}, Ni^{2+}, Zn^{2+} and Co^{2+}, the hexahistidine-tagged GFPuv generated from the gene fusion technique here could be purified with Immobilized Metal Affinity Chromatography (IMAC) charged with zinc ions. Zinc ions rather than copper or nickel ions, were chosen as a linker on account of the very low adsorptivity of the native GFPuv. Although the purification fold of the H_6GFP was not greater than that of the native GFPuv, the H_6GFPuv was highly pure and the purified protein could easily be obtained in a one-step purification process. Furthermore, an enterokinase cleavage site (DDDDK) could also be inserted to allow for the removal of the hexahistidine sequence after purification in such a way that the fusion partner might interfere or disturb the properties of the native protein. However, neither the metal-binding region nor the enterokinase cleavage site affected either the fluorescent emission or the capacity to bind with the protease of the chimeric protease-binding GFPuv. These findings clearly indicate that the metal-binding tag could simply be fused to assist protein purification and the purified chimeric protease-binding GFPuv can directly be applied as a potential tool for protease detection in the future.

KEY WORDS: METAL/ POLYMER/ SUPEROXIDE DISMUTASE MIMICS/
                        CHIMERIC PROTEIN/ GREEN FLUORESCENT PROTEIN

การผลิตโพลิเมอร์ที่แสดงคุณสมบัติเป็นซุปเปอร์ออกไซด์ ดิสมิวเทส และ การสร้างสายเปปไทด์ที่มีคุณสมบัติใน
การจับจำเพาะกับโลหะเพื่อประยุกต์ใช้ในการทำให้โปรตีนบริสุทธิ์
(METAL-SUPPORTING POLYMER FOR SUPEROXIDE DISMUTASE MIMICS AND
METAL-BINDING TAG FOR PROTEIN PURIFICATION)

ธีรพล เปียฉ่ำ 4338107 MTMT/M

วท.ม. (เทคนิคการแพทย์)

คณะกรรมการควบคุมวิทยานิพนธ์: ฉัตรเฉลิม อิศรางกูร ณ อยุธยา, ปร.ด., วีระพงศ์ ปรัชชญาสิทธิกุล, Ph.D.

บทคัดย่อ

        โพลิเมอร์ที่จับกับโลหะแมงกานีสและแสดงคุณสมบัติเป็นซุปเปอร์ออกไซด์ ดิสมิวเทส ได้ถูกสังเคราะห์ขึ้น โดยใช้ฟังก์ชันนัล
โมโนเมอร์ 4-vinylimidazole หรือ 1-vinylimidazole และ methacrylic acid เป็นตัวจับแมงกานีส ซึ่งฟังก์ชัน
นัลโมโนเมอร์เหล่านี้มีคุณสมบัติคล้ายกับหมู่ฟังชันก์ของกรดอะมิโน histidine และ aspartic acid ที่จับอยู่โดยรอบโลหะ
ของเอนไซม์ซุปเปอร์ออกไซด์ ดิสมิวเทส โพลิเมอร์นี้ถูกเตรียมโดยวิธี free radical polymerization โดยใช้โมโนเมอร์ตัว
เชื่อมคือ ethylene glycol dimethacrylate โพลิเมอร์ที่มีคุณสมบัติเป็นซุปเปอร์ออกไซด์ ดิสมิวเทสถูกนำมาทดสอบเพื่อ
วิเคราะห์หาคุณสมบัติการเร่งปฏิกิริยา โดยใช้วิธี Nitro blue tetrazolium based assay จากผลการทดลองพบว่า คุณ
สมบัติการเร่งปฏิกิริยาของโพลิเมอร์เหล่านี้เกิดมาจากการจับกันระหว่างโลหะกับฟังก์ชันนัลโมโนเมอร์ เป็นที่น่าสนใจว่าโพลิเมอร์ที่
เกิดจากการจับกันระหว่างแมงกานีสและฟังก์ชันนัลโมโนเมอร์ 1-vinylimidazole และ methacrylic acid ให้ค่าการ
เร่งปฏิกิริยามากกว่าโพลิเมอร์ที่เกิดจากการจับกันระหว่างแมงกานีสและฟังก์ชันนัลโมโนเมอร์ 4-vinylimidazole และ
methacrylic acid นอกจากนั้นยังพบว่าฟังก์ชันนัลโมโนเมอร์ทั้งสองตัวคือ 1-vinylimidazole และ methacrylic
acid มีบทบาทที่สำคัญอย่างยิ่งต่อการเร่งปฏิกิริยาของโพลิเมอร์เหล่านี้ จากการศึกษาพบว่าโพลิเมอร์ที่จับกับโลหะที่แสดงคุณ
สมบัติเหมือนเอนไซม์นี้จะนำไปสู่การศึกษาปรับปรุงเพื่อประยุกต์ใช้ประโยชน์ต่อการรักษาในอนาคต

        สายเปปไทด์ที่มีคุณสมบัติจับกับโลหะได้ถูกนำมาประยุกต์ใช้ในการทำให้โปรตีนบริสุทธิ์ สายเปปไทด์นี้ถูกเชื่อมต่อเข้ากับ
โปรตีนที่สนใจในระดับยีน จากพื้นฐานที่ว่า polyhistidine จับแน่นกับโลหะทรานสิชัน อาทิ Cu^{2+}, Ni^{2+}, Zn^{2+} ้
Co^{2+} ดังนั้นโปรตีนลูกผสมระหว่าง hexahistidine กับโปรตีนเรืองแสงฟลูออเรสเซนต์สีเขียว(green fluorescent
protein) ซึ่งถูกสร้างมาจากวิธีทางพันธุวิศวกรรมนั้นสามารถทำให้บริสุทธิ์ได้โดยใช้ Immobilized Metal Affinity
Chromatography (IMAC) ที่มี Zn^{2+} เป็นโลหะตัวกลาง โดยโลหะนี้ถูกเลือกเป็นตัวจับกับโปรตีนลูกผสมเนื่องมาจาก
สามารถใช้เป็นตัวยืนยันคุณสมบัติการจับจำเพาะกับโลหะที่เกิดจากสายเปปไทด์มิใช่เกิดจากส่วนอื่นๆในโครงสร้างโปรตีน จากผล
การทดลองพบว่าระดับของความบริสุทธิ์ของโปรตีนลูกผสมเมื่อพิจารณาจากสัดส่วนความบริสุทธิ์ในแต่ละขั้นตอนนั้นยังให้ค่าที่ไม่
สูงนักแต่อย่างไรก็ตามความบริสุทธิ์ที่ได้นั้นเพียงพอต่อการนำไปใช้งานและยังสามารถทำให้บริสุทธิ์ได้ในขั้นตอนเดียว นอกจากนั้น
โปรตีนลูกผสมดังกล่าวยังถูกออกแบบให้มีตำแหน่งตัดจำเพาะด้วยเอนไซม์เอนเทอโรไคเนสเพื่อตัดสาย hexahistidine ทิ้งภาย
หลังขั้นตอนการทำให้โปรตีนบริสุทธิ์ ในกรณีที่สายเปปไปด์อาจมีผลรบกวนคุณสมบัติและการทำงานของโปรตีนนั้น แต่จากผลการ
ทดลองพบว่า สายเปปไทด์ที่มีคุณสมบัติจับกับโลหะและตำแหน่งตัดจำเพาะนั้นไม่มีผลรบกวนต่อคุณสมบัติการเรืองแสงของ
โปรตีนและคุณสมบัติการจับจำเพาะกับเอนไซม์โปรตีเอส ซึ่งจากผลการทดลองเหล่านี้แสดงให้เห็นว่า สายเปปไทด์ที่มีคุณสมบัติจับ
กับโลหะมีศักยภาพในการทำให้โปรตีนบริสุทธิ์ด้วยวิธีการที่ง่ายในขั้นตอนเดียว นอกจากนั้นโปรตีนเรืองแสงลูกผสมที่ถูกสร้างขึ้น
นั้นยังสามารถนำไปประยุกต์ใช้เป็นเครื่องมือในการตรวจติดตามที่มีประสิทธิภาพในอนาคต

CONTENTS

CONTENTS (continued)

CONTENTS (continued)

LIST OF TABLES

LIST OF FIGURES

LIST OF FIGURES (continued)

LIST OF FIGURES (continued)

LIST OF ABBREVIATIONS

Asp	Aspartic acid
ºC	Degree Celcius
Cu	Copper
Co	Cobalt
Cys	Cysteine
DNA	Deoxyribonucleic acid
e.g.	*exampli gratia*
et. al.	Et alii
Fe	Iron
g	Gram
GFP	Green fluorescent protein
Gly	Glycine
h	Hour
Hg	Mercury
His	Histidine
HPLC	High performance liquid chromatography
Ic50%	50% Inhibition Concentration
ICP-AES	Inductive coupled plasma atomic emission spectroscopy
IMAC	Immobilized metal affinity chromatography
Lys	Lysine
Mn	Manganese
MIPs	Molecular imprinted polymers
MIT	Molecular imprinting technology
MHz	Megahertz
MW	Molecular weight
mg	Milligram
ml	Millilitre
mmol	Millimole

LIST OF ABBREVIATIONS (continued)

μg	Microgram
μl	Microlitre
μmol	Micromole
min	Minute
M	Molar
Met	Methionine
nm	Nanometer
Ni	Nickel
NMR	Nuclear Magnetic Resonance
PAGE	Polyacrylamide Gel Electrophoresis
Phe	Phenylalanine
Pro	Proline
RNA	Ribonucleic acid
r.p.m.	Revolutions per minute
SDS	Sodium dodecyl sulphate
Ser	Serine
SOD	Superoxide dismutase
TAE	Tris acetate-EDTA buffer
Thr	Threonine
Tyr	Tyrosine
w/v	weight by volume
Zn	Zinc

CHAPTER I
INTRODUCTION

Molecular recognition is crucial for the functioning of living systems, where biological macromolecules including proteins (which may serve as enzymes, antibodies, and receptors), nucleic acids, and saccharides play decisive roles in biological activities. Since the recognition has to be based on simple interactions among chemical units, the challenge of synthesizing artificial molecules which are capable of molecular recognition has specially drawn into an attention.

Molecular imprinting is a technology in which recognition sites are created in a macromolecular matrix using a molecular template in a casting procedure. The selected molecule for printing is first allowed to form bonds with functional monomers. The resulting complexes are subsequently captured into a rigid two or three-dimensional network following polymerization. The print molecule is then removed to achieve the specific recognition sites in the polymer (1,2). Such a technique has been exclusively applied to imprint many bioactive organic compounds for variety of purposes (3-7). Imprinting of macromolecules is also exploring in quite a few laboratories (1). These include an imprinting of substrate of enzyme and anti-idiotypic of enzyme active site to generate polymer that mimics enzyme activity (8-10). It is known that catalytic activity of many metalloenzymes line on a correctly coordinated metal cofactor within the active site of the enzymes. Imprinting to mimics metalloenzymes activity is then falled into our interest. Since when metal ions are used as template, they are able to bring oriented and appropriated coordination groups into a multi-dentate structure that affords selective binding capability of the polymer towards the metal ion templates. Our study has been turning to superoxide dismutase, a scavenging enzyme cleaning up oxidative harmful free radical in the biological system. The manganese-based superoxide dismutase (Mn-SOD) from human mitochondria contains a Mn(II) coordination sphere and is able to catalyze the disproportionate of superoxide anions to produce hydrogen

peroxide (11).   To investigate the feasibility of building polymer based metalloenzyme mimics, we start to use metal ions (e.g. Mn^{2+}, Cu^{2+}, Fe^{3+}, Ni^{2+} or Co^{2+}) to assemble a similar coordination sphere in cross-linked polymer matrices. Catalytic activity of the metal-supported polymers has further been determined.   In the study of this thesis, construction of a binding site for metal ions to aid the process of protein or enzyme purification has also been in our scope of study.   The gene fusion technique is applied in an attempt to create the specific recognition site for metal ions onto the green fluorescent protein (GFP) along with a specific site for protease cleavage.   Effect of the fusion partner on binding capability to protease of the chimeric protease-binding green fluorescent protein is also investigated.

Therefore, the objectives of this study are

1. To investigate the feasibility of building polymer based superoxide dismutase mimics among various metal ions via molecular imprinting technique.

2. To determine the catalytic activity of the metal-supported polymer.

3. To construct a chimeric green fluorescent protein possesses dual characteristics of both metal-binding and binding avidity to protease by gene fusion technique.

4. To investigate the potentiality of applying the metal-binding tag for protein purification as well as the effect of the tagger on protease-binding avidity of the chimeric protein.

CHAPTER II
LITERATURE REVIEW

A. Molecular imprinting

1. Molecular imprinting concept

The concept of molecular imprinting could be described as a way of making artificial "locks" for "molecular keys". In the following picture, very simplistic views were demonstrated in figure 1.
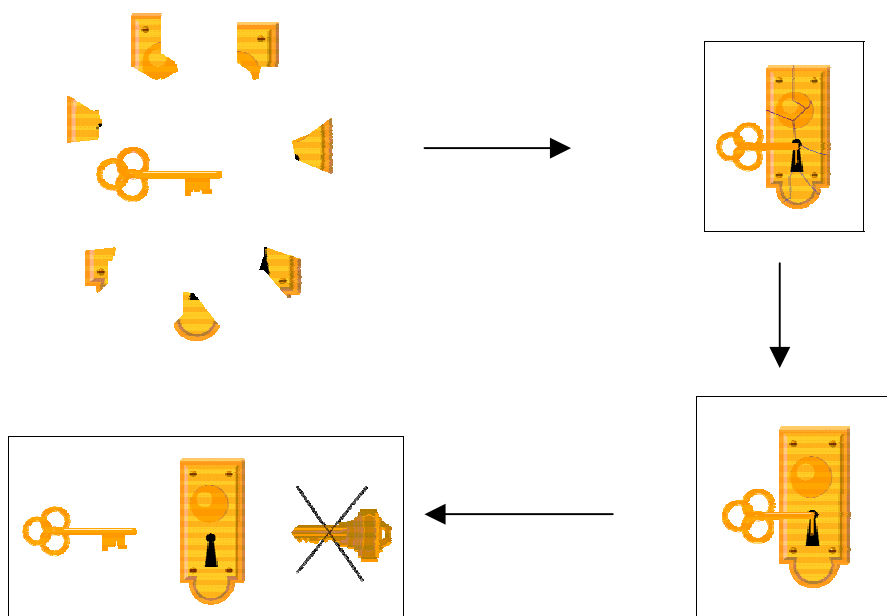
Figure 1 Molecular imprinting concept. The selected key molecule was in the first step mixed with a variety of lock building blocks. Then, the building blocks and the

key were allowed to, either firmly or loosely, attach to each other. The formed complexes between the key and the building blocks were subsequently "glued" together in order to fix the building block positions around the key. Removing the molecular key the leaves a construction which, if everything worked properly, was selective for the original key and would not recognize any other key (1, 2).

2. History

The emergence of molecular imprinting had its original source in the area of immunology when chemists attempted to explain the mechanism of antibody formation. One of the earliest inspirations that brought scientist to the concept of molecular imprinting came from Linus Pualing in 1940 who postulated mechanism for the formation of antibodies (12). The theory proposed that the great diversity in antibody formation was due to the formation of different three-dimensional configurations of the antibody polypeptide chain induced by the interaction with the antigens. Following these "instructive" theories on antibody diversity, the antibodies would be able to change their 3-D-structure in order to form as many interaction points as possible with the epitopes of the antigens. Thus, the antibody combining sites were "moulded" with the antigen as a template in a casting procedure, for instance, they were molecularly imprinted with the antigens (Figure 2).
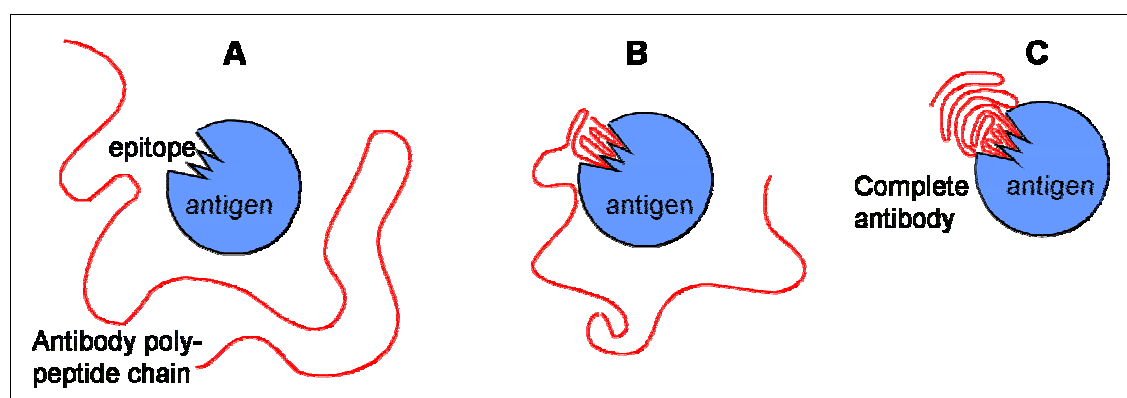
Figure 2 Antibody formation according to Pauling postulated. A) The nascent antibody polypeptide chain encountered the antigen. B) The polypeptide chain started to fold, directed by the structural prerequisites of the epitope. C) The guided antibody formation was complete (1, 2).

Later, these theories were found to be incorrect and their instructive models abandoned in favor of the more appropriate "clonal selective" theory of antibody formation. Nevertheless, their models laid the foundations for the area of molecular imprinting.   Following this hypothesis, his graduate student, Frank Dicket who carried out the imprinting experiments using a series of dye molecule mixed it with an acidic aqueous silica gel (13). After washing out the dye and drying the gel, the gel possessed some selectivity for template dye molecule but the imprints lost their recognition capability with time. During this period, molecular imprinting did not much progress, until Mosbach and coworker (14), who studied on the immobilization of enzymes and cells on their entrapments in polyacrylamide gel network as shown in the figure 3.
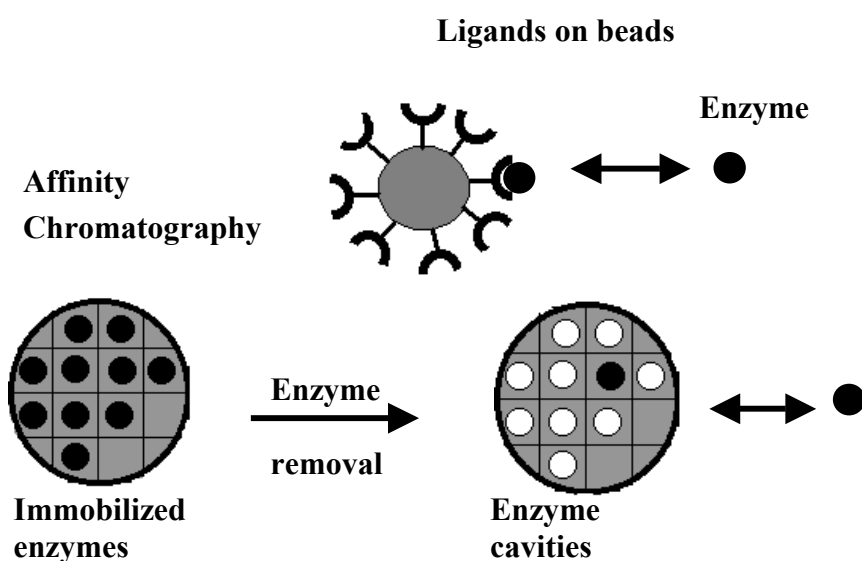
Figure 3 Connection between affinity chromatography, immobilized enzymes and the subsequent liberation of the cavities left behind by the enzyme (14).

These findings and the following research around affinity solid material led to the later approach of non-covalent molecular imprinting. In 1972, Takagishi and Klotz reported that polyethyleneimine, cross linked by disulfide bridges in the presence of methyl orange, exhibited slight memory for this template (15). Independently, Gunther Wulff and co-workers simultaneously reported chiral recognition of D-Glyceric-(p-vinyllanilide)-2,3-o-p-vinylphenylboronate, which was covalently incorporated in the polymer and subsequently hydrolysed (16, 17).(Figure4)
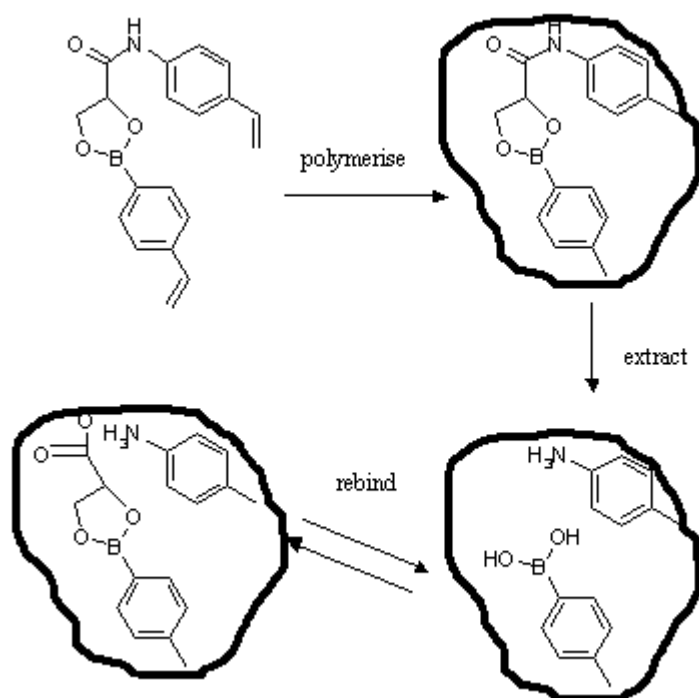
Figure 4 The first example of covalent imprinting, developed by Wulff group. The incorporation of a covalently modified template in polymer, and its subsequent removal by hydrolysis left a cavity that complements the non-modified template (D-glyceric acid) (16).

The independent development of a general non-covalent approach for imprinting in organic polymers by group of Mosbach (18) significantly accentuated the usefulness of and interest in this technique. By this approach the number of compounds those could be successfully imprinted increased dramatically, and the selectivity was achieved. Promising approach for the delicate task of imprinting in

aqueous solution and for the imprinting of macromolecule was based on metal-ion chelation between monomers and template (19-22).
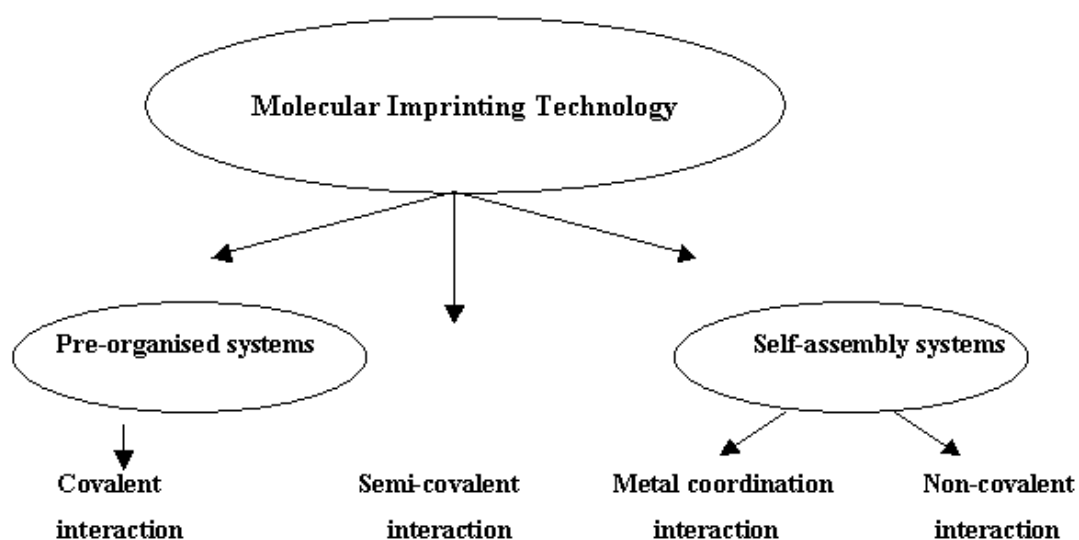
Figure 5 Two basic approaches of molecular imprinting: pre-organized approaches and self-assembly approaches (1, 2).

3. Principle of molecular imprinting

From the chemical point of view, there were two main approaches to achieve interactions between monomers and target templates, namely covalent and non-covalent interactions as shown in figure 6. Covalent imprinting was introduced by Wulff and coworkers while another, non-covalent imprinting was proposed by Mosbach group. Later, Whitcombe and co-workers generated a hybrid approach that combined two methods, covalent and non-covalent together, named semi-covalent (sacrificial) imprinting (23).(Figure 5)
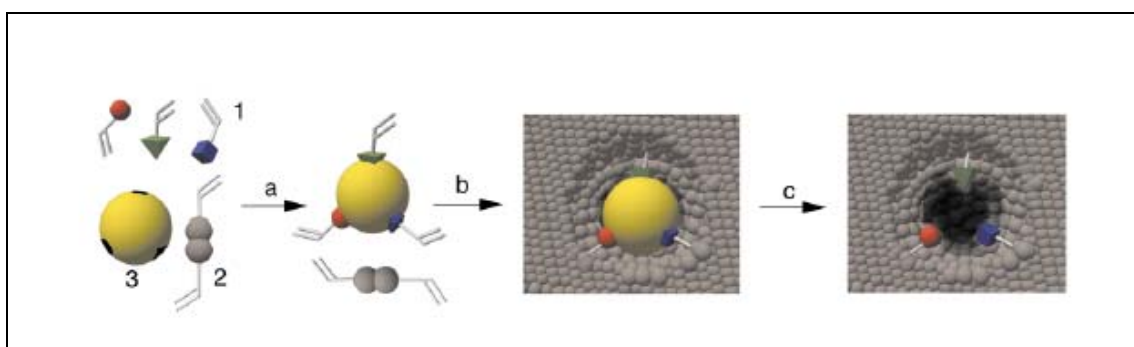
Figure 6 Schematic representation of the molecular imprinting principle.   1: Functional monomers, 2: cross-linker, 3: template molecule; a: assembly of the prepolymerisation complex, b: polymerisation, c: extraction of the template liberating the binding site (2).

3.1 The covalent approach (Pre-organised system)

In the covalent approach, the print molecule was coupled to a vinyl monomer, which this complex was reversible covalent linkage, so called pre-assembly complex.   Then polymerization was take place in large amount of cross-linker resulting in a rigid network. The template molecule could be readily extracted leaving behind cavities in the polymer that complemented the size and shape of the template and contained functionalized group left in cavities.   Reversible covalent bond formation and cleavage enabled association and dissociation of target molecule. Various kinds of chemical linkages were utilized in the covalent approach.   Among the most common types were boronic esters (8)(figure 7), Schiff bases (24) and ketals

(25). Covalent imprinting offered the possibility of defined template-monomer constructs thus controlling the stoichiometry of the imprinting cocktail. This might result in binding sites those were more homogenous than those obtained using non-covalent techniques (26).
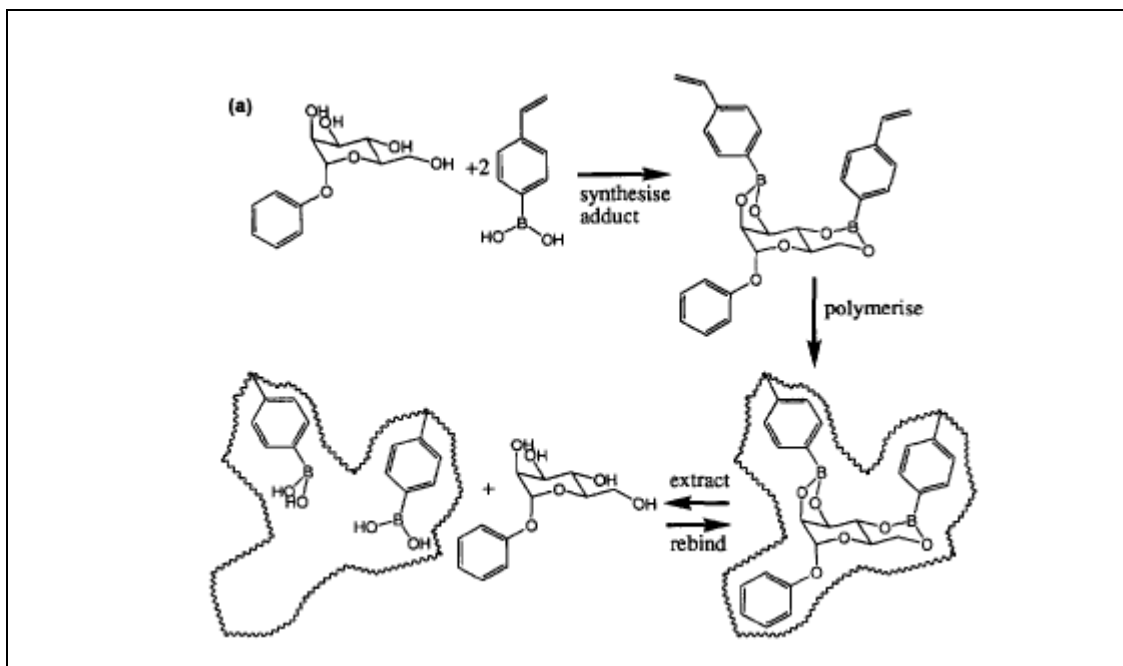
Figure 7 Covalent imprinting of α-D-mannoside using vinyl phenylboronic acid (8).

Covalent imprinting remained largely a niche method in the imprinting field. A major reason for that was the limited choice of potential monomers. The restricted and applicability was also a consideration. In addition, covalent approach involved in chemical synthesis of complex between templates versus functional monomer. This was limited by the availability to create suitable cleavage conditions. Furthermore, it was not always possible to couple functional monomers due to a lack of suitable functionality on the substrate.

3.2 The Semi-covalent approach

The semi-covalent approach was closely related to the covalent approach and was introduced by Whitcombe et al. (23). Figure 8 described the first published example of this approach where the template cholesterol was esterified with 4-vinylphenol to give a 4-vinylphenyl-carbonate ester. After co-polymerization of the template construct with excess cross-linker, the carbonate-bond was cleaved, releasing the template and a small sacrificial molecule, carbonic acid.   Following extraction of the template, the imprinted recognition site was bearing a phenolic residue oriented in a manner that allowed specific rebinding with the hydroxyl group of cholesterol.

In this hybrid concept, imprinting of template construct was imprinted in covalent fashion and rebinding relied on non-covalent, ionic interactions, so homogeneous binding sites should be ensured (covalent feature) and the equilibrium of substrate rebinding should be established quickly (non-covalent feature). However, the same limitations that were encountered in the covalent approach as chemical synthesis and cleavage still prevented the general applicability of this method.
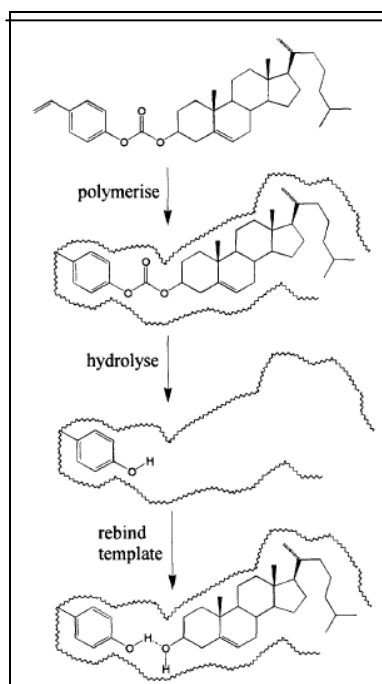
Figure 8 Semi-covalent approach published by Whitcombe et al (23).

3.3 The Non-covalent approach (Self-assembly systems)

The self assembly system utilized exclusively non-covalent or metal coordination interactions in the recognition of imprint species. By these approaches, functionally interactive monomers were allowed to self-assemble in complexes with the print species in solution prior to polymerization. These complexes were subsequently arrested through crosslinking into a rigid polymeric network.

3.3.1 Self-assembly by Non-covalent interaction

The greater the number of interactions between the imprint species and the functional monomers were available, the better recognition the artificial binding site would demonstrate. Typical interaction types were ionic interactions, hydrogen bonding, ¶-¶-interaction and hydrophobic interaction. Since these interactions were strongly dependent on the polarity of the solvent. The best imprint was made in organic solvent such as chloroform or toluene. When these normally weak interactions were established in solution, polymerization was then initiated and a molecular matrix was formed around the imprint species. The formed macromolecular architecture was thus complementary in shape and functionality to the imprint species as example in figure 9
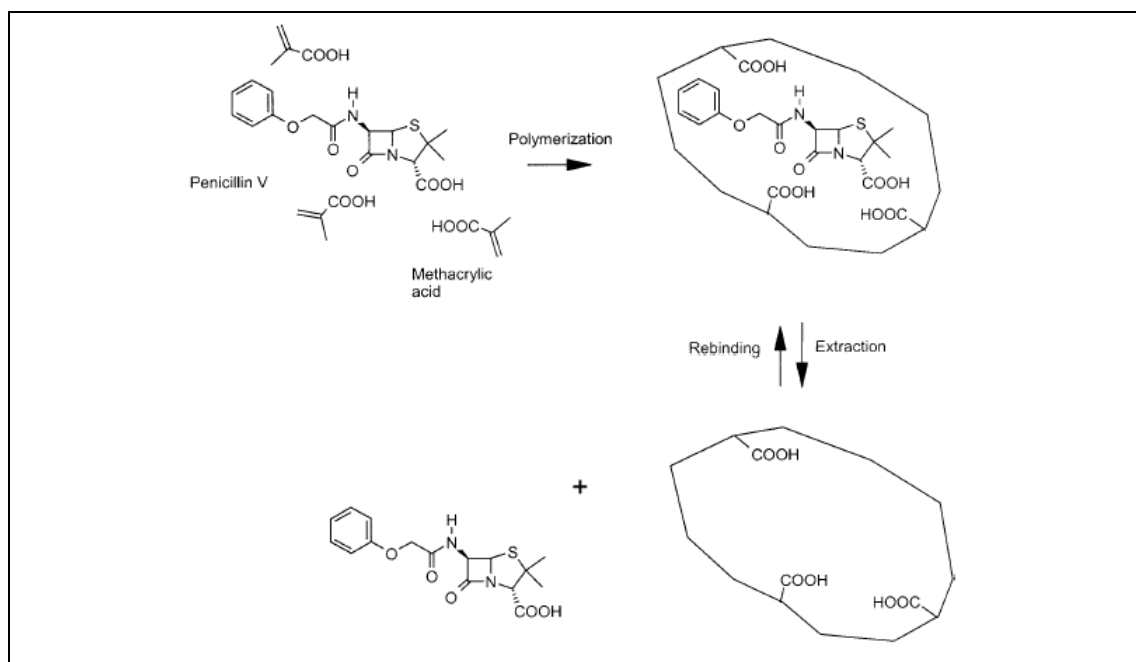
Figure 9 Schematic representation of a molecular imprinting process. Complexes, formed in solution by interactions between the print molecule (here penicillin V) and one or more functional monomer(s) (e.g., methacrylic acid), become fixed during polymerization with a cross-linker. Polymeric recognition sites were formed, complementary in shape and functionality to the print species (6).

After polymer formation the imprint molecule could be almost quantitatively recovered by mild extraction from the matrix. Association and dissociation of the original print molecule to the artificial binder took place without requiring any covalent bond formation or cleavage, with the target molecule simply diffusing in and out of the complementary sites.

3.3.2 Self-assembly by Metal coordination

In metal coordination systems strong metal ion chelating functionalities was utilized for organizing functional groups in the sites. The metal ions might after polymerization be exhaustively extracted from the matrix, e.g. by using of strong metal ion chelators like EDTA, and subsequently rebound to the sites by admission of metal solution. In most cases, this approach was used in attempts to construct molecular imprinting polymers selective against the imprinted metal ion template

compared to the other metal ions (27-30). Most examples following this approach was in the studies of absorption of transition metal ions, in particular Cu^{2+}, Co^{2+} and Zn^{2+}, by selective polymer.

The inspiration by the technique of immobilized metal ion affinity chromatography (IMAC), metal chelating interactions was used directly with organic molecules (21, 22, 31, 32). Certain metal ions, in particular transition metal ions, e.g. copper, cobalt and zinc, might form very strong coordination complexes with certain organic functionalities. Immobilization of the metal ions by chelating agents, such as iminodiacetic acid (IDA), rendered materials which were capable of binding certain proteins (32). Primarily, the imidazole group of histidine residues in proteins was utilized in chromatographic application, but other functionality such as indole-, mercapto-, and carboxyl groups might also form strong complexes. Following this methodology, immobilized metal monomer as vinylbenzyl iminodiacetic acid, was used to prepare molecular imprinted polymers against compounds comprising imidazole groups (Figure 10)
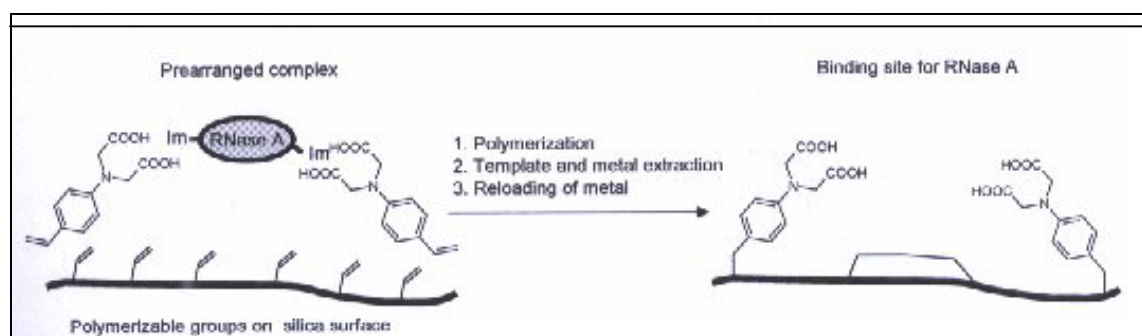
Figure 10 RNase A imprinting on the surface of methacrylate silica (32).

Although the versatility of this approach was restrained to but a few interaction systems, the interactions were very strong and might be used in aqueous systems where non-covalent bonds were very weak. Another advantage with this protocol was the possibility of changing the binding strength for polymerization or rebinding (32, 33). In this case, very strong complexes between imidazole groups,

metal chelators and Cu^{2+} ions were arrested by polymerization, but for chromatographic applications the Cu^{2+} ions were exchanged for Zn^{2+} ions which gave a weaker complex. This ion-switching provided a versatile tool for fine-tuning of the rebinding of ligands to the polymers.

In this elegant approach for highly selective polymers of defined architecture, the templates uses were various metal ions (22, 34). The area of metal ion templated polymers was received much less attention than organic compound templated polymers. However, recently there were some interesting works.   The researcher found that Zn^{2+} templated polymer (Figure 10), containing a sandwich arrangement of the well known 1,4,7-triazacyclononane (TACN) ligand, was found to be highly selective toward reintroduced Cu^{2+} in the presence of Fe^{3+}, Co^{2+}, Ni^{2+}, Zn^{2+} and $Mn^{2+.}$ While a similar Hg^{2+} templated TACN polymer was found to be highly selective for Hg^{2+} in the presence of Cd^{2+}, Pb^{2+}, Ag^+, Cu^{2+} and Fe^{3+} (35-37). (Figure 11)
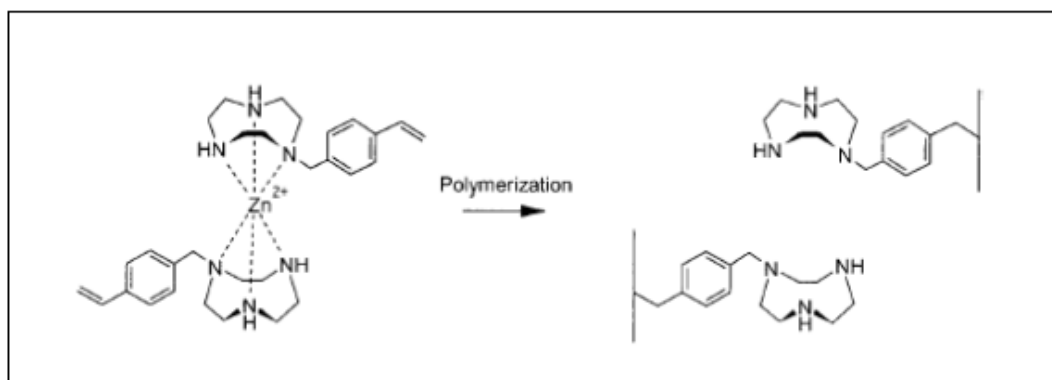
Figure11 Zn^{2+} templated polymer (37).

4. Molecular imprinting polymer system composed of:

4.1 Print molecule

Print molecules were originally chosen solely for the purpose of demonstrating the concept of molecular imprinting, i.e. they were model compounds. Various textile dyes, sugar derivatives and amino acid derivatives were examined, with convincing results reported from many different groups. However, it was in the early 1990's that molecular imprinting research become more focused. Real potential application began to be seriously investigated, with the chiral separation of pharmaceutical compounds being of particular interest. Generally, a print molecule should beard suitable functional groups for interaction with the functional monomers, to ensure stable complexion. Quite often, different interactions were utilized simultaneously to provide the optimal imprinting effect. There was literally no limit as to which print molecules might be used as templates, so long as they did not interfere with the chemical processes that gave rise to the final supporting matrix. In the case of free radical polymerization, this implied that no active (polymerisable) vinyl groups should be present in print molecule. It was known that imprinting effect varied with the print molecule. As general rule, rigid molecules carrying discrete functional groups were expected to give superior results (38).

For practical applications, the compound of interest (analyte) was generally used as the template for preparing the imprinting polymer. The structure and the chemical characteristics of template determined the nature of the imprinting approach that should be followed. If non-covalent imprinting was applicable, the chemical structure of template was used as starting point for selecting functional monomer candidates. For example, if the basic groups were present in the print molecule, methacrylic acid might provide strong ionic interactions between the charged print molecule and the monomer. When the print molecule was capable of forming complexes with certain metal ions, metal-chelating functional monomers might be better choice. If hydrophobic interactions were desired, the imprinting solvent could be adjusted according to enhance this effect, and so on.

4.2 The role of functional monomers

The functional monomer ultimately became the binding group in the imprinting polymer. Ideally it should form a stable complex with the print molecule in question during the polymerization process. In non-covalent imprinting, the selection of appropriate functional monomers was determined by the structure and functionality of the print molecule. Quite often multiple interactions of different nature could be exploited simultaneously, provided that the different monomers did not interact with one another stronger than with the template. Some of the functional monomer widely used for non-covalent imprinting was shown in figure 12. These included acidic monomers, basic monomers, hydrogen bond-forming monomer and metal-chelating monomers. Hydrophobic interactions were usually satisfied by the cross-linking monomer that intrinsically lipophilic. Whilst most of these functional monomers were themselves not optically active, there were a few examples where chiral functional monomer was used. Hosoya et al. used a racemic template and a chiral napthyl monomer to prepare an imprinted polymer that displayed selective binding of one enantiomer, *S-N*-(3,5-dinitrobenzoyl)-α-methylbenzylamine, and they demonstrated that the chiral discrimination of the polymer was due to the presence of the template molecule during polymerization (39, 40). Although chiral functional monomers were generally much more expensive, they might be conveniently used to prepare the desired chiral stationary phase when no optical pure print molecule was available.
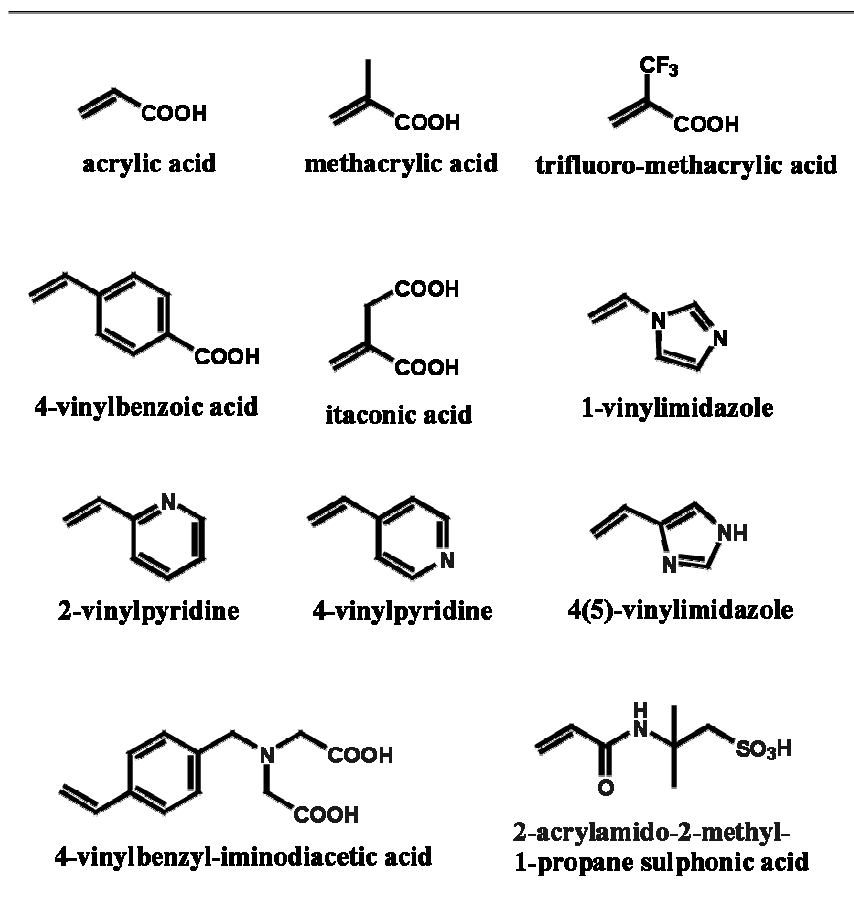
Figure 12 Representative functional monomers used in non-covalent molecular imprinting (39).

4.3 The role of cross-linking monomers

In many cases, high binding specificity was augmented by the rigid three-dimensional structure of the polymer, which was in turn ensured by the high cross-link density. For this purpose, a relatively large amount of cross-linking monomer was generally copolymerized with functional monomer. The distance between two adjacent linking points within the polymer network could be adjusted by using various cross-linkers. Figure 13 showed some of the cross-linking monomers that were used by different investigators. Because of the large proportion of cross-linker involved, the cross-linking monomer determined, to a large extent, the hydrophobicity of the imprinted polymer. This, in turn, affected the extent of non-specific binding.

Derivatives of divinylbenzene and acrylate cross-linkers were generally hydrophobic, whereas acrylamide-based cross-linkers were relatively hydrophobic.

4-divinylbenzene

N,N'-methylene-bisacrylamide

N,N'-phenylene-bisacrylamide

2,6-bisacrylamidopyridine

ethylene glycol dimethacrylate

trimethylolpropane trimethacrylate
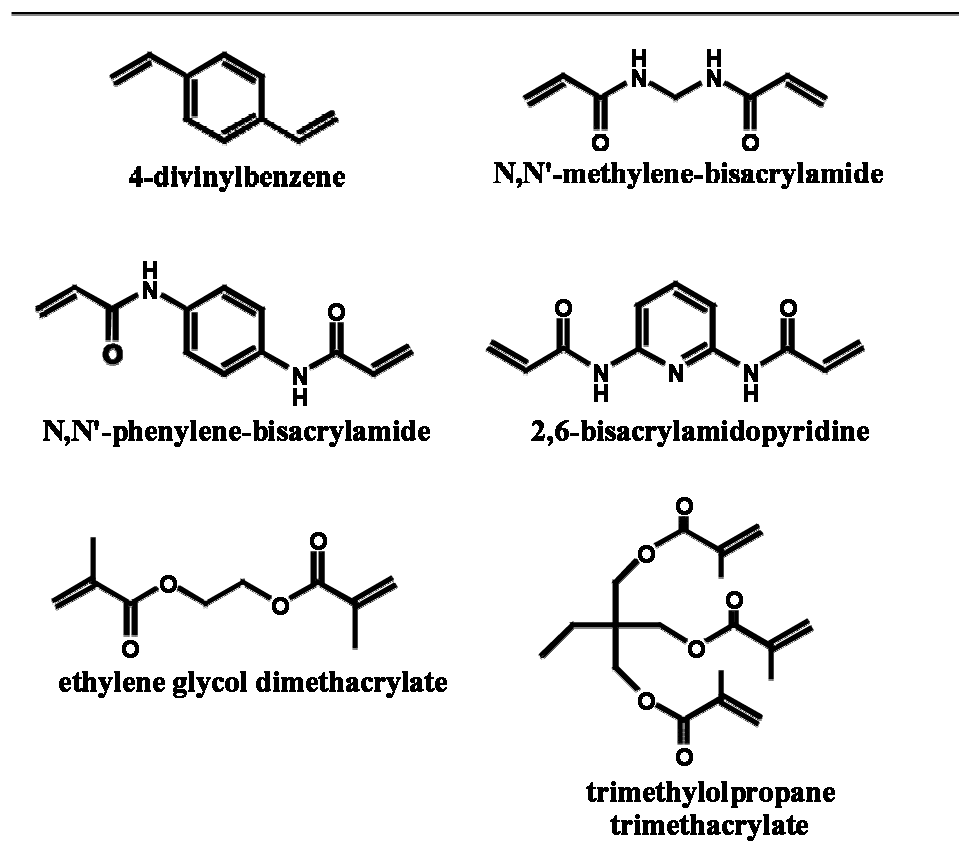
Figure 13 Cross-linking monomers commonly use for molecular imprinting (41).

Each cross-linking monomer affected the morphology of the imprinted polymer differently. For example, imprinted poly(MAA-co-TRIM) had larger average pore diameters and pore volumes than poly(MAA-co-EDMA) that were prepared under identical conditions (41). It was not universally the case that imprinted polymer prepared using cross-linkers with higher intrinsic cross-linking capability provided superior recognition specificity, although higher load capacities could be anticipated. The correct choice of cross-linker depended on the structure of print molecule, the polymer morphology required, as well as the desired application. The best choice of cross-linker was often arrived at through trial and error.

Appropriate levels of cross-linking were important in maintaining the binding specificity of an imprinted polymer. When the levels were too high, the loading capacities of the polymers were reduced and the diffusion of substrates into the imprinted cavities during rebinding might also be hindered. At the other extreme, when the functional groups were not sufficiently fixed by cross-linking, i.e. the levels of cross-linking were too low, the specific rebinding by the imprinted polymer also decreased. For the poly(MAA-co-EDMA) system, calculated as the molar fraction of the cross-linker, cross-linking densities between 80-90% were most commonly used, and this generally led to satisfactory recognition during rebinding analysis. However, a relatively low cross-linking did not necessarily sacrifice selective rebinding of substrate (42). As an example, 22.4% of cross-linker was used to prepare poly(MAA-co-EDMA) imprinted against Boc-L-Trp. When using the imprinted material as a chromatographic stationary phase, it was almost possible to baseline separation Boc-L-Trp from its enantiomer, Boc-L-Trp (43). For larger target molecules, diffusion kinetics might become a limiting factor, therefore a lower cross-linking density might be preferred.

4.4 Porogenic solvent

The solvent used in molecular imprinting not only helped to homogenize the reaction components prior to polymerization, but also had a profound influence on the surface area and porosity of the polymeric material obtained. While many inert solvents could be readily used for covalent imprinting, the non-covalent approach required that relatively apolar and poor hydrogen bond-forming solvents were used to maximize the non-covalent interactions between the print molecules and the functional monomers. The choice of the imprinting solvent was further limited by solubility of print molecule. For hydrophilic templates, a compromise between template solubility and imprinting effect usually needed to be made. Table1 listed the imprinting solvents commonly used in the non-covalent approach, together with their dielectric constants and hydrogen-bonding scales (44). If solubility of print molecule was satisfied, then solvents with lower dielectric constant, for example benzene, toluene, chloroform and dichloromethane, were preferred for imprinting using ionic

interactions.   When hydrogen bond interactions were utilized, solvent with lower hydrogen-bond acidity/basicity generally resulted in a better imprinting effect. Hydrophobic interactions could be utilized in aqueous environment, although they were employed simultaneously with other interactions during polymerization. It was worth nothing that many rebinding applications of non-covalent imprinted polymers took advantage of the hydrophobic effect, even though this was not the driving force for complexation in the imprinting step.

Porogenic solvents played an important role in determining the physical characteristics of the resulting material, i.e. the surface area and the porosity. With the methacrylic-based cross-linking monomer, EDMA, it was found that imprinted polymers prepared in acetonitrile had higher surface areas and pore diameters than those of polymers formed in chloroform (41). On the other hand, swelling of the imprinted polymers was most pronounced in chlorinated solvents, such as chloroform and dichloromethane (45). Although the dry state morphology varied greatly among polymers made in different solvents, Sellergren and Shea found that the swollen state morphology appeared to be more or less the same, due to the counter effect of different swelling capacities in the respective solvents. They concluded that polymer morphology was less important for the selectivity and the strength in substrate rebinding (46).

Table 1 Common solvents used for non-covalent molecular imprinting (41).

Solvent	Dielectric constant ε (20 °C)	Hydrogen-bond acidity	Hydrogen-bond basicity
Benzene	2.284	0	0.14
Toluene	2.379 (25 °C)	0	0.14
Chloroform	4.806	0.2	0.02
Dichloromethane	9.08	0.13	0.05
Acetonitrile	37.5	0.09	0.44
Acetone	20.7 (25 °C)	0.04	0.5
Tetrahydrofuran	7.6	0	0.51
Dimethylformamide	36.7	0	0.66
1-Proranol	20.1 (25 °C)	0.33	0.45
Methanol	32.63 (25 °C)	0.37	0.41
Water	78.54	0.35	0.38

4.5 Polymerization

Polymerization was generally performed overnight, usually with reaction for between 16 and 24 hours, and process was initiated by photo- or thermolabile initiators such as azobisisobutyronitrile (AIBN) or azobis(2,4-dimethylvaleronitrile) (ABDV). The conditions employed during polymerization therefore involved either UV-light (~336nm) or heat (40ºC or 60ºC). Some different polymerization conditions were compared with respect to MIPs selectivity in a study by O'Shannessy et al (47) in which it was shown that photochemical initiation and polymerization at 0ºC was advantageous as compared to thermal initiation, since it led to higher selectivity (due to higher stability of the monomer-template complexes). However, it was shown that thermal polymerization yielded MIPs with higher saturation capacity (46), and in that particular study, selectivity, as compared to that obtained by photochemical polymerization, was essentially unchanged. The other, cationic initiation was introduced to MIT (48). The polymers formed were highly rigid prior to further grinding step.

4.6 Template extraction and rebinding

The means for evaluating the recognition characteristics of these polymers differed, but the most common method was by chromatography. For this purpose, the bulk polymer was ground in mechanical mortar, sieved, and repeatedly sedimented to remove the finest particles, leaving a material that allowed packing into an HPLC column. Finally, the polymer was washed in polar solvent which disrupted the interactions between templates and polymer, and made the imprinted cavities accessible for interaction.

5. Characteristics of molecularly imprinted polymers

In the following some of the interesting physical and chemical characteristics of molecularly imprinted polymers were described (Table 2). These materials exhibited high physical and chemical resistance against external degrading factors. Thus, molecularly imprinted polymers were remarkably stable against mechanical stress and high temperature and pressure, resistant against treatment with acid, base or metal ions and stable in wide range of solvents (38). The storage endurance of the polymers was very high: storage for several years at ambient temperature led to no apparent reduction in performance. Further, the polymer could be used repeatedly, in excess of 100 times during periods of more than 8 months without loss of the "memory effect". In comparison with natural, biological recognition sites, which were often proteins, these properties were extremely advantageous.

Table 2 Characteristics of molecularly imprinted polymers.

Feature	Characteristics	Reference
Physical Stability	Resistant against mechanical stress, high pressure and elevated temperature	(78)
Chemical Stability	Resistant against acids-bases, various- organic solvents and metal ions	(78)
Storage Endurance	several years without loss of performance	(31)
Capacity	0.1-1 imprint molecule /g polymer	(32)
Imprint Memory	Repeated use >100 times	(27)
Binding Strength	mM range (determined by chromatography	(32, 45)
	nM range (determined by chromatography	(64)

6. Applications

The use of molecular imprinting for specific recognition of target molecules was demonstrated through numerous examples in several application areas. Given improved affinity and load capacity, imprinted artificial receptors would in many instances be able to replace their biological counterparts which were both difficult to produce and unstable in many environments.

6.1 Affinity separation

Molecular imprinted polymers could be used for various separation purposes. one of the most promising areas was the chiral separation of pharmaceutical compounds, particularly so given that increasingly the production of drugs with high enantiometric purity was demanded by administrative bodies, e.g. the FDA. Compared with conventional chiral stationary phases, imprinted polymers, when used in chromatographic mode, could separate racemates with pre-determined elution order. Although relatively large amounts of print molecule were required to prepare the tailor-made chiral selector in the first place, the polymer obtained were very stable under chromatographic conditions and could withstand repetitive use. In addition to various feasibility demonstrations, Kempe and Mosbach separated S-naproxen, an anti inflammatory drug, from the R-enantiomer using a polymer imprinting against the R-form (41). Haginaka et al. prepared imprinted polymer beads against the same template using a multi-step swelling method, and used the polymer beads for similar chiral separations (49-51). Ramstrom et al. prepared adrenergic receptor binging mimics using ephedrine and pseudoephedrine as templates, and demonstrated the chiral discriminating capabilities of these imprinted stationary phases for various adrenomimetic agents (45). The typical long-tailing peaks obtained from isocratic elution, which was mainly caused by the different affinities of the heterogeneous binding site, could be greatly sharpened by using gradient elution, and the resolution in many cases could be improved (52). Molecular imprinting was also combined with capillary electrophoresis (CE), and analytical technique that delivered high separation efficiency. MIP particles could either be physically entrapped within capillaries or

the imprinted stationary phase could be prepared in situ within the capillaries. A β-adrenergic antagonist, (R)-propranolol, and a local anaesthetic, (S)-ropivacaine, were successfully separated from their antipodes using imprints prepared by an in situ photo-initiated polymerization process (53, 54).   Alternatively, Walshe et al. used imprinted particles in the mobile phase as a chiral selector for separating (R)- and (S)-propranolol (55). As stated earlier, an important characteristic of imprints was their high affinity for target ligands. This feature was exploited in sample pre-treatment, using solid phase extraction (SPE) for the analysis of trace compounds such as drugs, metabolites, pesticides and other molecules of environmental concern.   Pre-concentration and clean up could be readily achieved using imprinted polymers as selective affinity media, by applying relatively large volumes of sample solution to the polymer followed by washing and elution steps. Pentamidine, a drug used for the treatment of AIDS-related pneumonia, was enriched 54 times from a sample solution with a physiological concentration of 30 nM. In condition experiment, an enrichment factor of only 14 was obtained when an anti-benzamidine MIP was applied under the same conditions (56).   Many off-line applications, in which the pre-treatment of sample was decoupled from the quantification step, were applied to various analyzes, such as the β-adrenergic antagonist, (R)-propranolol (57), and the triazines atrazine (58) and simazine (59).   Recently, an on-line solid-phase extraction was also investigated, in which serum theophylline was determined with a detection limit of 120 ng/mL using molecularly imprinted solid-phase extraction with pulsed elution (60). For SPE application, it was important that the imprinted polymer be free from any detectable residual templates prior to use, otherwise a potential problem, template leaking, might occur during the sample pre-treatment and led to erroneous results. To circumvent this problem, Andersson et al. introduced a strategy in which they used a structural analogue of the target compound sameridine (a local anesthetic and analgesic drug) as the template for the preparation of group-specific adsorbent. Since the analogue was readily separated from sameridine in subsequent gas or liquid chromatography, the uncertainty caused by possible template leakage was erased (61).

6.2 Artificial receptors for ligand binding assays

The wide variety of techniques developed for the determination of analytes based on their specific recognition by an antibody, included various configurations of immunoassays (62). Molecularly imprinted polymers were certainly very different from antibodies; they were large, rigid and insoluble, whereas antibodies were small, flexible and soluble. However, MIPs shared with antibodies one of their most important features, the ability to selectively bind a target molecule. Therefore, they could conceivably be employed in immunoassay-type binding assays in place of antibodies.
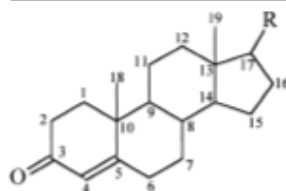
This was first demonstrated by Mosbach's group with a MIP based assay for the bronchodilator theophylline and the tranquilliser diazepam (63). The theophylline assay, not only showed a very good correlation with an antibody-based enzyme immunoassay currently used in analytical laboratories in hospitals, but, surprisingly, even yielded a cross reactivity profile very similar to that of the natural monoclonal antibodies. From a selection of closely related substances, only 3-methylxanthine, which had one methyl group less than theophylline, was bound to the polymer to some extent (7% binding as compared to theophylline), whereas caffeine, which had one additional methyl group, showed virtually no binding. This molecularly imprinted sorbent assay was developed for several other compounds such as drugs, (64, 65) herbicides (66, 67) and corticosteroids (68). Andersson and co-workers were showed that MIP assays could even be performed directly with diluted blood plasma (69).

6.3 Screening chemical libraries, Drug discovery

In recent years, combinatorial chemistry became more and more prominent as a tool in drug discovery and continued to contribute much in the pursuit of novel lead compounds in the pharmaceutical industry. In contrast to rational drug design, combinatorial approaches searched for lead molecule within defined collection of diverse compounds, either of chemical or biological origin. This needed to use of

efficient methods for the screening of the combinatorial libraries (70, 71). Among the most important screening strategies were the receptor binding assays (72) in which the use of biomimetic receptors such as imprinted polymer could be exploited. In 1998, Ramstrom et al. used a small steroid library to demonstrate the feasibility of using imprinted polymers for screening purposes.   An abiotic receptor for 11α-hydroxyprogesterone selectively bound the target compound from a background composed of twelve closely related structures (figure14). Screenings of mixture, as well as individual tests were demonstrated to be possible (73).

Steroid structures

Compound	R	Other substituents
11-α-Hydroxyprogesterone (1)	$COCH_3$	11α-OH
11-β- Hydroxyprogesterone (2)	$COCH_3$	11β-OH
17-α-Hydroxyprogesterone (3)	$COCH_3$	17α-OH
Progesterone (4)	$COCH_3$	
4-Androsten-3,17-dione (5)	=O	
1, 4-Androstadiene-3,17-dione (6)	=O	Δ^1
Corticosterone (7)	$COCH_2OH$	11β-OH
Cortexone (8)	$COCH_2OH$	
11-Deoxycortisol (9)	$COCH_2OH$	17α-OH
Cortisone (10)	$COCH_2OH$	11=O, 17α-OH
Cortisone 21-acetate (11)	$COCH_2OAc$	11=O, 17α-OH
Cortisol 21-acetate (12)	$COCH_2OAc$	11β-OH, 17α-OH

Figure 14 11α-hydroxyprogesterone's closely related structures (73).

For the new way to shape the new drug Mosbach et al. reported the new technique called anti-idiotypic imprinting (or double imprinting), they made a polymeric "mold" that fitted around a known inhibitor of the clinically interesting enzyme kallikrein.   They removed the inhibitor, leaving a molecular imprinted polymer with a cavity shaped like the inhibitor. Condensation reactions between pairs of small building-block compounds capable of binding to opposite halves of the cavity were then used to form addition products that resembled the shape and activity of inhibitor (9, 10). (figure15)
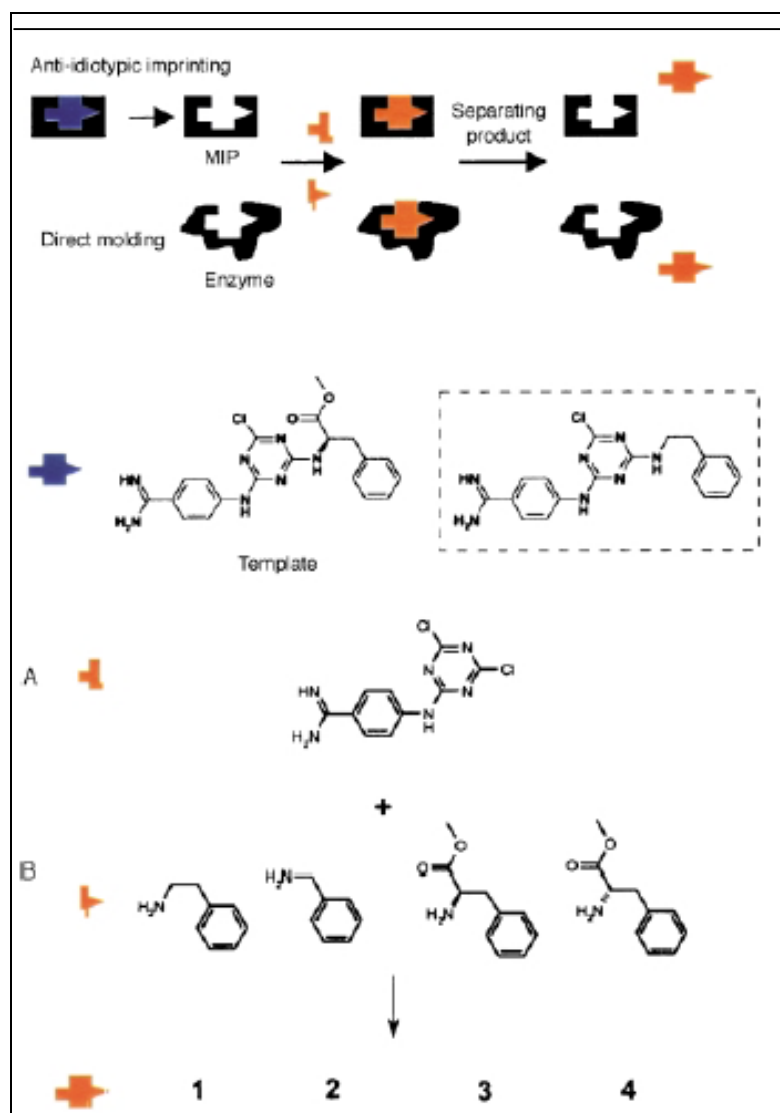
Figure 15 Schematic representatives of the anti-idiotypic imprinting approach and direct molding approach used. After removal of the template (in gray) from MIP (in black), the binding cavity was used to direct the assembly of the reactants (in light gray) to give products mimicking the original template (10).

6.4 Biomimetic and chemical sensors

In chemical sensors and biosensors, a chemical or physical signal was generated upon the binding of the analyte to the recognition element, a transducer then translated this signal into a quantifiable output signal.   The same general principle applied if an MIP was used as the recognition element instead of a biomolecule.   Certain general properties of the analyte (such as its IR spectrum) or changes in one or more physico-chemical parameters of the system (such as mass accumulation or adsorption heat) upon analyte binding were used for detection.   This principle was widely applicable and more or less independent of the nature of the analyte.   Alternatively, reporter groups might be incorporated into the polymer to generate or enhance the sensor response.   In other cases, the analyte might possess a specific property (such as fluorescence or electrochemical activity) that could be used for detection.   Because biosensors had very high specificity and ease of operation, the development of novel biosensors was one of the most intense research areas. However, unfortunately, the relatively poor stability of the biological entities often limited the lifetime of the corresponding sensor components.   There was an obvious opportunity therefore for artificial receptors prepared by molecular imprinting to function in place of natural receptors.   Biomimetic sensors based on molecular imprinted recognition components were therefore being developed.   Table 3 listed some of the molecularly imprinted recognition components that were used in biomimetic sensors.   The durability and low maintenance conferred by the imprinted polymers was expected to encourage more investigations in this area.   While most sensing elements were composed of conventional imprinted particles placed physically close to the signaling device, the direct polymerization of imprinted polymers onto transducers was reported (74).

Table 3 Lists some of the molecularly imprinted recognition components that were used in biomimetic sensors.

Print molecule (analyte)	Detection method (transducer)	Reference
L-Phenylalanine anilide	Potentiometric	(75)
	Field-effect capacitor	(76)
L-Phenylalanine	Membrane permeability	(77)
Morphine	Amperometric	(78)
Dansyl-L-phenylalanine	Fluorescence (Optical fiber)	(79)
Benzyltriphenylphosphonium	Conductometric	(80)
Methyl-β-D-glucopyranoside	pH measurement	(81)
cAMP	Fluorescence	(82)
Theophylline	Surface plasmon resonance	(83)
Pinacolyl methyphosphonate	Luminescence (optical fiber)	(84)
6-[(4-Carboxymethyl)phenoxy]-5,12-naphthacene quinone	Microgravimetric quart-crystal-microbalance	(85)
Glucose	Quartz-crystal-microbalance	(74)
2,4-Dicchlorophenoxyacetic acid	Differential-pulse voltametry on screen printed electrodes	(86)

6.5 Enzyme mimics

The imprinting of synthetic polymers to give catalytically active materials (enzyme analogues) were investigated. While most reports were successful in the binding-related aspects, real artificial enzymes based on imprinted polymers, with comparable catalytic characteristics to natural enzymes, were still to realize (table 4). However, there were some examples in which MIPs catalyzed specific reactions with enzyme-like kinetics.

For preparing the catalytic MIPs, an approach broadly similar to the production of catalytic antibodies were followed. To raise a catalytic antibody, a transition state analogue (TSA), which might be coupled to a carrier, was used as an antigen to induce an immune response and antibody generation in the host. The antibody library was then subjected to a screening process to search for specific clones with the desired catalytic characteristics (87). Quite often binding of the TSA was achieved but no catalysis of the desired reaction was observed. It turned out that mere binding did not guarantee catalysis, since the correct arrangement of the catalytic residues in the antibody was important as well. Researchers working on catalytic antibodies explored a large antibody reservoir to find an active clone, and might use site-directed mutagenesis to introduce catalytic residues into the active site (88).

Polymeric catalysts could be similarly produced in a relatively easy manner through molecular imprinting, by using analogues of the substrate, transition state, or product as templates. In all the examples, a transition state analogue was used that formed complementary interactions with the functional monomers, so that specific binding sites could be created and catalytic groups introduced therein. An important feature in enzyme and the substrate interaction was to raise the substrate into the transition state conformation. If successfully exploited this induced fit feature was expected to deliver highly efficient imprinted enzyme mimics.

Table 4 Representation of the examples of enzyme mimics based on molecular imprinting technology

Print molecule (TSA)	Reaction catalyzed	Catalytic group	Reference
p-Nitrophenol methylphosphonate	Hydrolysis of p-nitrophenyl acetate	Imidazole	(89)
N-Benzylisopropylamine	β-Elimination	Carboxyl	(90)
Phenyl 1-benzyloxy-carbonylamino-3-methyl-pentylphosphonate	Hydrolysis of *p*-nitrophenyl *N*-carbobenzoxy-L-lucinate	L-histidyl	(91)
Phosphonate derivative	Hydroxy of D/L-Boc-Phe-ONP	Serine esterase catalytic triad	(92)
Dibenzoylmethane	Aldol condensation	Pyridine-cobalt(II)	(93)
Chloraendic anhydride	Diel-Alder reaction	Carboxyl	(94)
Phosphonic acid monoester	Alkaline hydrolysis	Benzamidine	(95)
Indole	Benzisoxazole isomerization	Pyridine	(96)

B. Superoxide dismutase

Superoxide was a major factor in radiation damage, inflammation, tumor promotion, and re-perfusion injury. Fortunately, we were evolved an effective defense system against the toxicity of $O_2^{\bullet-}$, such as superoxide dismutase (SOD) and catalase.

In 1969, McCord and Fridovich first reported that the erythrocyte protein functioned as superoxide dismutase enzyme (97). Generally, there were three groups of SOD; each had different metal in the active site. According to the metals, they were termed as CuZnSOD, MnSOD and FeSOD, and in additional new finding NiSOD. Acting as one of the most important antioxidants, all SODs catalyzed the dismutation of $O_2^{\bullet-}$ as.

$$O_2^{\bullet-} + 2H^+ \longrightarrow H_2O_2 + O_2$$

1. General aspects of Superoxide dismutase

1.1 Superoxide dismutase

Superoxide dismutase (SOD) enzymes were ubiquitous in living systems (11). These enzymes served a vital role in defending oxygen-utilizing life forms from oxidative damage (11). The naturally occurring superoxide dismutase (SOD) enzymes appeared in many forms in both animals and plants. Cu/Zn-containing forms were found in the extracellular spaces of mammals, as well as in the cytosols of eukaryotic cells, the periplasms of gram-negative bacteria, and the plastids of plants. Mn-containing forms of SOD were found in the mitochondria of all mammalian cells and in *E. coli*; while all anaerobic prokaryotes, if they possessed SOD activity, would contain Fe SOD exclusively (11). All obligate aerobes possessed Mn SOD enzymes exclusively, and facultative anaerobes contained both. Additionally, a Ni SOD was discovered in *Streptomyces griseus* (178).

From the initial discovery by Fridovich and McCord that a class of serum copper- and zinc- containing proteins catalyzed the dismutation of superoxide to oxygen and hydrogen peroxide, (11,97) there were a tremendous amount of researches which were continued to elaborate the role that the SOD enzymes played in maintaining the health of organisms.   The SOD enzymes were a class of oxidoreductases which contained either Cu/Zn, Fe, or Mn at the active site and catalyzed this dismutation of the free radical superoxide, the one-electron reduction product of molecular oxygen (eq 1) (eqs 1 and 2, where M^n was the metalloenzyme in the reduced state and M^{n+1} was the enzyme in the oxidized state) to the non-radical products.   These enzymes performed this catalytic cycle of dismutation with incredible efficiency, i.e., at rates approaching diffusion controlled. For example, the mammalian Cu/Zn SOD's were shown to possess catalytic rates in excess of 2×10^9 $M^{-1}s^{-1}$, while the Mn and Fe SOD enzymes were shown to function at rates that were somewhat slower, approximately an order of magnitude slower depending on the source of the enzyme. The SOD enzymes were shown to have efficacy in animal models of disease states proposed to be, in part, mediated by superoxide, such as myocardial ischemia-reperfusion injury (98), inflammation (99), and cerebral ischemia reperfusion injury (100, 101). Further evidence for superoxide as a mediator of disease states continued to accrue, such as in ALS and neuronal apoptosis (102-106), cancer, and AIDS (107, 108).

$$O_2^{\cdot -} + M^{n+1} \longrightarrow O_2 + M^n \qquad \text{(Eq 1)}$$

$$HO_2^{\cdot} + M^n \longrightarrow H_2O_2 + M^{n+1} \qquad \text{(Eq 2)}$$
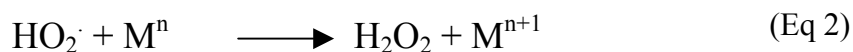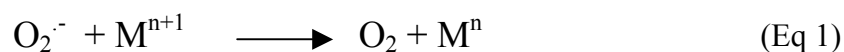
1.2 Protein structure of MnSOD

An example of SOD structure was demonstrated in figure 16
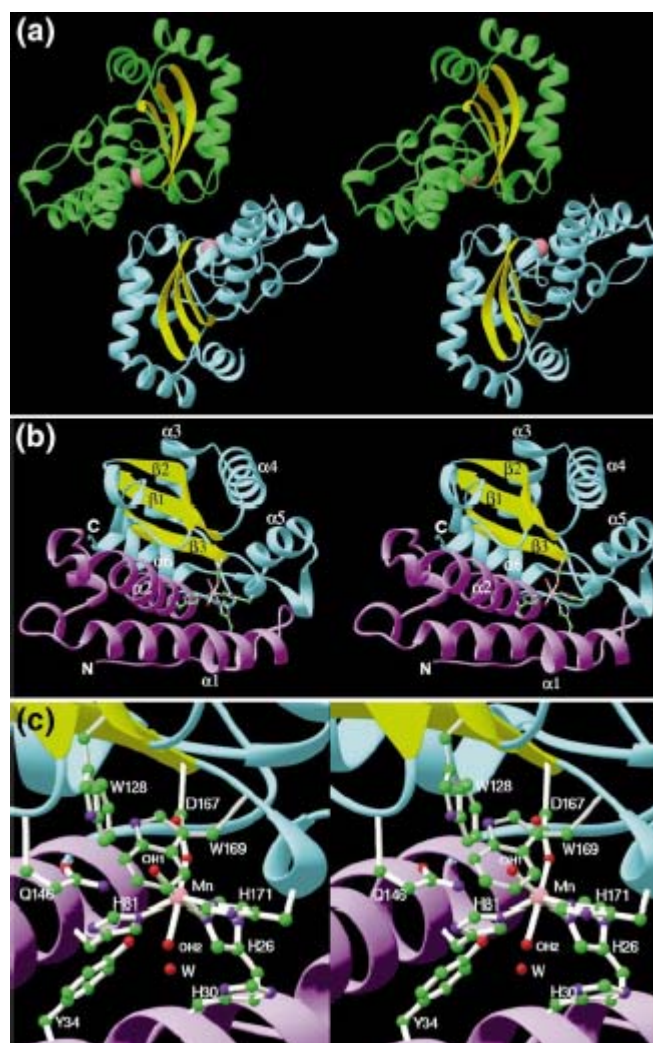
Figure 16 Stereopairs of ribbon diagrams of the MnSOD structure.   (a) The homodimer; monomers were colored yellow and green, and the active site manganese atom was indicated with a pink sphere.   (b) An individual monomer with pink manganese and six-coordinate active site.   The N-terminal a-helical domain was colored purple and the C-terminal a/b domain was colored with cyan a-helices and yellow antiparallel β-pleated sheets.   (c) Close-up view of the six-coordinate active site including the manganese ligands as well as the residues that neighbor the two hydroxide ligands (110).

1.3 **Active site geometry**
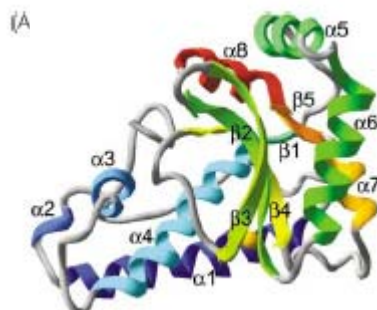
Figure 17 Monomer of Superoxide dismutase enzyme (109).

The metal-binding site of Mn- and FeSODs was highly conserved. It connected both domains via the metal ion and the corresponding residues were located on helices α1 (His90) and α4 (His145) of the N-terminal domain and on β4 (Asp228) and the following coil between β4 and α7 (His232) of the C-terminal domain. In addition to these three histidine residues and one monodentate aspartate, one water molecule ligated the central Mn(III) ion in a trigonal bipyramidal geometry (Figure 17,18).

Active site
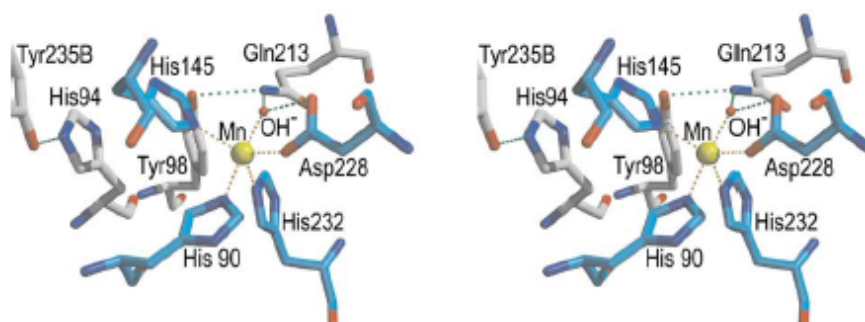
Figure 18 A stereo view of the active site of MnSOD. Residues coordinating the Mn ion were drawn with light blue carbon atoms; bonded to the Mn were depicted as broken red lines and the Manganese was in yellow. All but one amino acid residue (Tyr235B) shown were from chain A. Outer sphere residues form a hydrogen bonding network (broken green lines) surrounding the manganese-containing active site.

1.4 Sinificance of SOD on $O_2^{\bullet-}$ scavenging.
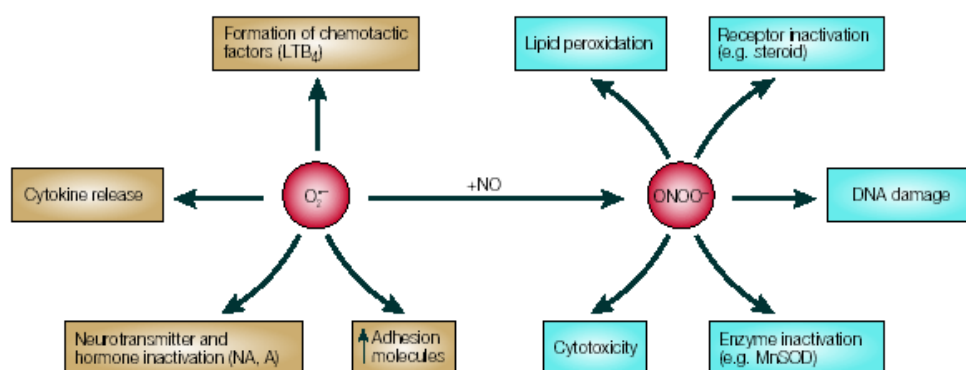
Figure 19 Biochemical effects of superoxide generation. Excessive production of superoxide ($O_2^{\bullet-}$) could lead to inflammation through various pathways, including generation of peroxinitrite (ONOO–). A, adrenaline; LTB4, leukotriene B4; MnSOD, manganese superoxide dismutase; NA, noradrenaline; NO, nitric oxide.

Some of the important pro-inflammatory roles for superoxide anions (Figure. 19) included: endothelial-cell damage and increased microvascular permeability (99); formation of chemotactic factors such as leukotrienes (for example, LTB4)(111, 112); recruitment of Neutrophils at sites of inflammation (113, 114); lipid peroxidation and oxidation; DNA single-strand damage (115); and formation of peroxynitrite ions (ONOO–) (116). Substantial circumstantial evidence implicated superoxide anions as mediators of inflammation, shock and ischemia–reperfusion injury. Superoxide anions deactivated catecholamine such as noradrenalin, an effect that was shown to account for the hypotension and hyporeactivity to exogenous catecholamines that were seen in severe septic shock (117). So, examples events above could disrupt by SOD, that scavenging superoxide radical before superoxide radical induced cascade effect.

C. Superoxide dismutase mimics

Most of the knowledge obtained about the roles of superoxide anion in diseases were gathered using the native superoxide dismutase enzyme (118, 119) and, more recently, by data generated in transgenic animals that overexpressed the human enzyme (VIDE INFRA). Protective and beneficial roles of superoxide dismutase were demonstrated in a broad range of diseases, both preclinically and clinically (120). For example, preclinical studies were revealed that superoxide dismutase enzymes had a protective effect in animal models of ischemia-reperfusion injury (including heart, liver, kidneys, brain)(121-125), transplant-induced reperfusion injury (126), inflammation (127), Parkinson's disease (128), cancer (129, 130), AIDS (131-133) and pulmonary disorders including asthma, chronic obstructive pulmonary diseases (134, 135) and Respiratory Syncytial Virus (RSV) infections (136). In some situations such as stroke or Parkinson's, the native enzymes did not show efficacy since they did not penetrate (because of their large size, MW 30 kDa) the blood brain barrier. Under these circumstances, used of transgenic animals that overexpressed the superoxide dismutase enzyme was led to some important observations. For instance, overexpression of the superoxide dismutase enzyme in rats was protective in animal models of stroke or Parkinson's (137). Most importantly, human clinical results with, Orgotein® (bovine CuZnSOD) showed promising results as a human therapy in acute and chronic conditions associated with inflammation, including rheumatoid arthritis and osteoarthritis as well as side effects (acute and chronic) associated with chemotherapy and radiation therapy (119, 138). Thus, in clinical trials, the use of the native enzyme supported the concept that removal of superoxide anion had a beneficial outcome. Although, the native enzyme showed excellent anti-inflammatory properties in both preclinical and clinical studies, in a variety of diseases, there were major drawbacks associated with its use. The main problem was the non-human origin of the enzyme: bovine. This inevitably gave rise to a variety of immunological problems. So, based on the concept that removal of superoxide anion modulated the course of inflammation, researcher tried to find the synthetic superoxide dismutase mimetics that served as pharmaceutical candidates in a variety of diseases as the native SOD enzyme was found to be effective.

Most catalytic SOD mimetics were designed with a redox active metal centre that catalyzed the dismutation reaction with $O_2^{\bullet-}$ in a manner similar to the active site metals of the mammalian (Cu or Mn) SODs. An ideal SOD mimetic should be stable, with high specificity for interaction with $O_2^{\bullet-}$ and with a high rate constant; it should also be nontoxic, much like the native SODs. Additionally, their size and charge could be exploited for targeting crucial cellular sites of oxidative stress.

It was recognized for many years that simple metal chelates could react with $O_2^{\bullet-}$. These included Mn-desferal (139), copper complexes of amino acids or anti-inflammatory drugs like indomethacin and salicylates (140), and manganese complexes of lactate, citrate or succinate (141). However, the rates of reaction of these chelates with $O_2^{\bullet-}$ were low and the complexes were unstable. The search for more potent and stable metal chelates was still appearing as active area. The resulting discovery the lead compound appeared the least three classes of metal-containing SOD mimetics including the metalloporpyrin (figure 20), the salen (figure 21) and macrocyclic (figure 22) SOD mimetics.
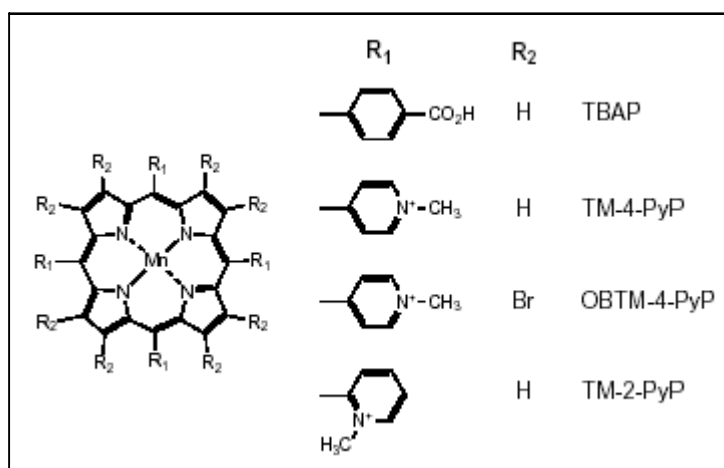
Figure 20 The structures of manganese meso-porphyrins commonly used as superoxide dismutase(SOD) mimics that included tetrakis-(4-benzoic acid) porphyrin (TBAP), tetrakis-(N-methyl-4-pyridyl) porphyrin (TM-4-PyP), β-octabromo-tetrakis-(N-methyl-4-pyridyl) porphyrin (OBTM-4-PyP) and tetrakis-(N-methyl-2-pyridyl) porphyrin (TM-2-PyP). The manganese moiety of the SOD mimetics functioned in

the dismutation reaction with O_2 by changing its valence between Mn(III) and Mn(II) (114).

EUK-8   **EUK-134**
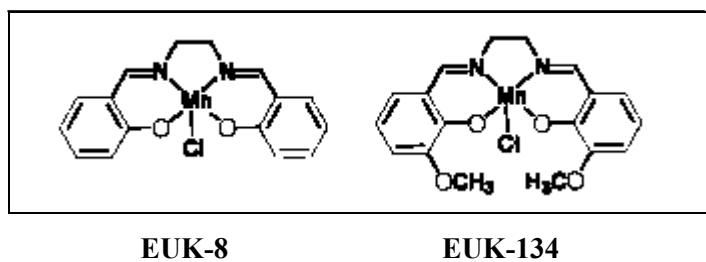
Figure 21 Mn (salen) structures (114).

M40403   **Mn(pentaazacyclopentadecane)([15]aneN$_5$)Cl$_2$**
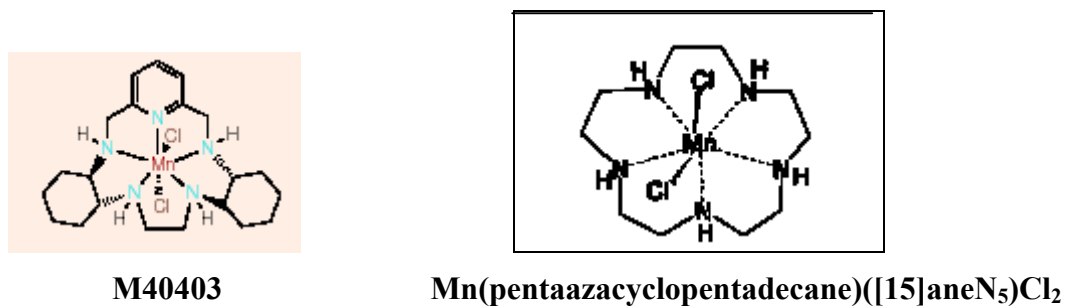
Figure 22 Macrocyclic compounds (114).

D. Gene fusion to facilitate purification of recombinant proteins

By genetic engineering it was possible to make gene fusions resulting in fusion protein having the combined properties of original gene product. Fusion could be made on either or both sides of the target gene depending on the specific application.   Many applications for fusion proteins in widespread areas of biotechnology were reported (142) including a facilitated purification of the target protein, meant to decrease proteolytic of target protein, displayed of proteins on surfaces of cells, phages or viruses, construction of reporter molecules for monitoring of gene expression and protein localization and to increase the circulation half-life of protein therapeutics.   However, the most frequent application of gene fusion was for the purpose of purification of recombinant proteins.

1. Affinity fusion partners

There was a great interest in developing methods for fast and convenient purification of proteins. For example, to facilitate functional and structural studies of proteins derived from the rapid growing number of genes coming out of genome programs such as the Human genome project, efficient and robust production and purification strategies were necessary.   For industrial production of recombinant proteins, simple and fast purification methods could drastically improve on the economy of the process. A powerful purification technique made possible since the introduction of genetic engineering was to purify the target protein by the use of genetically fused affinity fusion partner.   Such fusion proteins could often be purified to near homogeneity from crude biological mixtures by a single and fusion partner specific affinity chromatography step according to the basic principle shown in figure 23
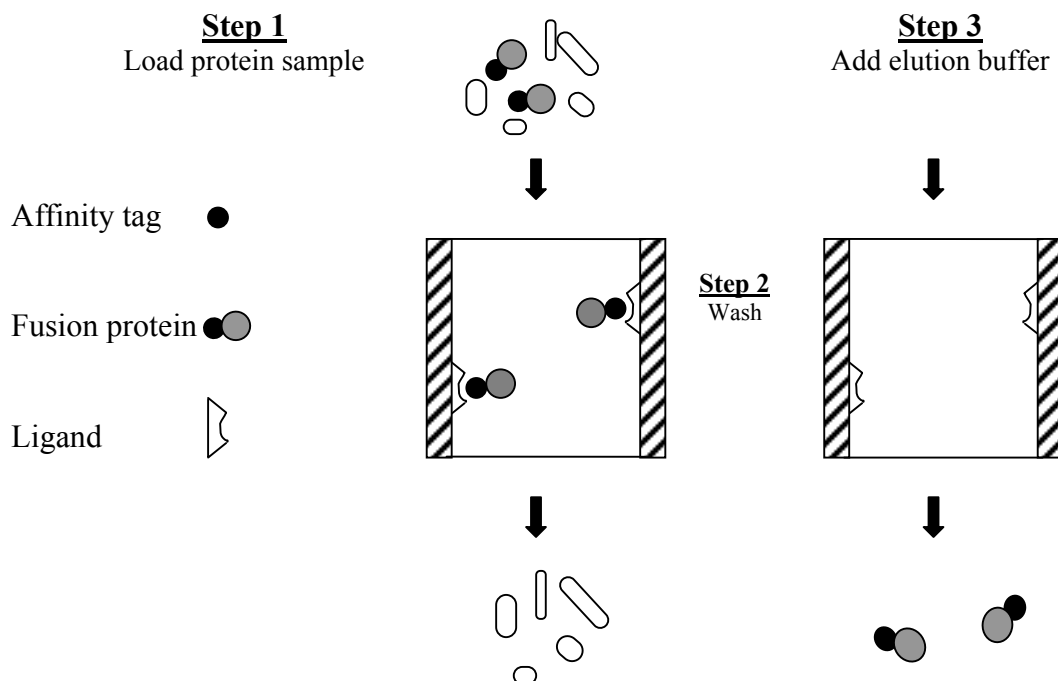
Figure 23 The basic principle for affinity purification of fusion proteins containing an affinity handle.

To date, a large number of different gene fusion systems were described involving fusion partner that ranged in size from one amino acid to whole proteins capable of selective interaction with a ligand immobilized onto a chromatographic matrix. In such systems, different types of interactions were utilized such as enzyme-substrates, bacterial receptors-serum protein, polyhistidines-metal ions and antibody-antigen.   The conditions for purification differed from system to system and environment of the target protein that tolerate was an important factor for deciding which affinity fusion partner to choose. Also other factors including costs for the affinity matrix, buffers and the possibilities to remove the fusion partner by site-specific cleavage were also important to consider. Numerous gene fusion systems for affinity purification were listed in Table 5, together with their respective elution condition.

Table 5 Fusion tags applied for protein purification and detection.

Peptide tag	Ligand	Utility
Polyhistidine	Nickel ions	Purifications [143]
FLAG peptide	Anti-FLAG antibody	Purifications/detection [144]
Strep-tag	Streptavidin	Purifications/detection [145]
In vivo biotinylated peptide	Avidin/streptavidin	Purifications/detection [146]
Polyaspartic acid	Anionic resins	Purifications [147]
Polyarginine	Cationic resins	Purifications [148]
Polyphenylalanine	HIC resins	Purifications [149]
Polycysteine	Thiols	Purifications [149]
Calmodulin-binding peptides	Calmodulin	Purifications/detection [150]

HIC, hydrophobic interaction chromatography.

2. Polyhistidine tags

A number of laboratories identified various alternative binding sites for intermediate metal ions that could be used as purification tags in recombinant proteins. In particular, peptide tags containing multiple histidines as $(His-X)_n$, $(His-X_3-His)_n$, where X was any amino acid, was fused to their C- or N-terminus of recombinant protein. These were proven helpful for the purification of recombinant proteins. The use of immobilized metal ion affinity chromatography (IMAC) to purify proteins fused with polyhistidine tags was a popular technology for the simple and cheap production of large amounts of pure industrial enzymes. Poly-His tagged proteins might be easily purified by IMAC (151). They were quite strongly adsorbed on these columns via interaction of poly-His tag with just one chelate. They might then be easily desorbed using imidazole or by lowering the pH.

3. Site-specific cleavage of fusion proteins

For certain applications it could be necessary to remove the affinity partner after purification. For example, a fusion partner could cause unwanted alter the conformation of protein. In addition, a fusion partner might complicate a structural determination of fused target protein. Several methods were described for site-specific cleavage of fusion proteins based on chemical or enzymatic treatment of the fusion protein. Due to the chemical cleavage methods were performed in harsh reaction that might lead to protein denaturation or amino acid sidechain modification and relatively unspecific, the enzymatic methods were to prefer before chemical methods, because they were generally more specific and the cleavage could performed under mild condition.

The enterokinase was used in many previous reports (152). A cDNA encoding the catalytic domain of bovine enterokinase was cloned and expressed both in mammalian cells and in *E. coli* (153). The enzyme possessed most of the characteristics of a universal cleavage reagent. It was highly active, worked over broad ranges of pH, denaturant levels or detergent concentrations, had high specificity for its pentapeptide recognition sequence (AspAspAspAspLys), and cleaved on the carboxy-terminal side of its recognition site, leaving no additional downstream residues on the cleaved product. The ready availability of recombinant enterokinase would greatly increase the utility of fusion gene expression technology.

E. Green fluorescent protein (GFP)

Green fluorescent protein, GFP, was a spontaneously fluorescent protein isolated from coelenterates, such as the Pacific jellyfish, *Aequoria victoria*. Its role was to transduce, by energy transfer, the blue chemiluminescence of another protein, aequorin, into green fluorescent light (154). The molecular cloning of GFP cDNA (155) and the demonstration by Chalfie that GFP could be expressed as a functional transgene was opened exciting new avenues of investigation in cell, developmental and molecular biology. Fluorescent GFP was expressed in bacteria (156), yeast (157), slime mold, plants (158, 159), drosophila (160), zebrafish, and in mammalian cells. GFP could function as a protein tag, as it tolerated N- and C-terminal fusion to a broad variety of proteins many of which was shown to retain native function (161). When expressed in mammalian cells fluorescence from wild type GFP was typically distributed throughout the cytoplasm and nucleus, but excluded from the nucleolus and vesicular organelles. However, highly specific intracellular localization including the nucleus, mitochondria (162), secretory pathway, plasma membrane and cytoskeleton (157) could be achieved via fusions both to whole proteins and individual targeting sequences. The enormous flexibility as a noninvasive marker in living cells allowed for numerous other applications such as a cell lineage tracer, reporter of gene expression and as a potential measured of protein-protein interactions.

1. Properties and structure of GFP

Green fluorescent protein was comprised of 238 amino acids. Its wild-type absorbance/ excitation peak was at 395 nm with a minor peak at 475 nm. The emission peak was at 508 nm. Interestingly, excitation at 395 nm led to decrease over time of the 395 nm excitation peak and a reciprocal increase in the 475 nm excitation band. This presumed photoisomerization effect was especially evidenced with irradiation of GFP by UV light. Analysis of a hexapeptide derived by proteolysis of purified GFP led to the prediction that the fluorophore originated from an internal

Ser65-Tyr66-Gly67 sequence which was post-translationally modified to a 4-(*p*-hydroxybenzylidene)- imidazolidin-5-one structure.   Studies of recombinant GFP expression in *E. coli* led to a proposed sequential mechanism initiated by a rapid cyclization between Ser65 and Gly67 to form a imidazolin-5-one intermediate followed by a much slower(hours) rate-limiting oxygenation of the Tyr66 side chain by O_2 as shown in figure 24
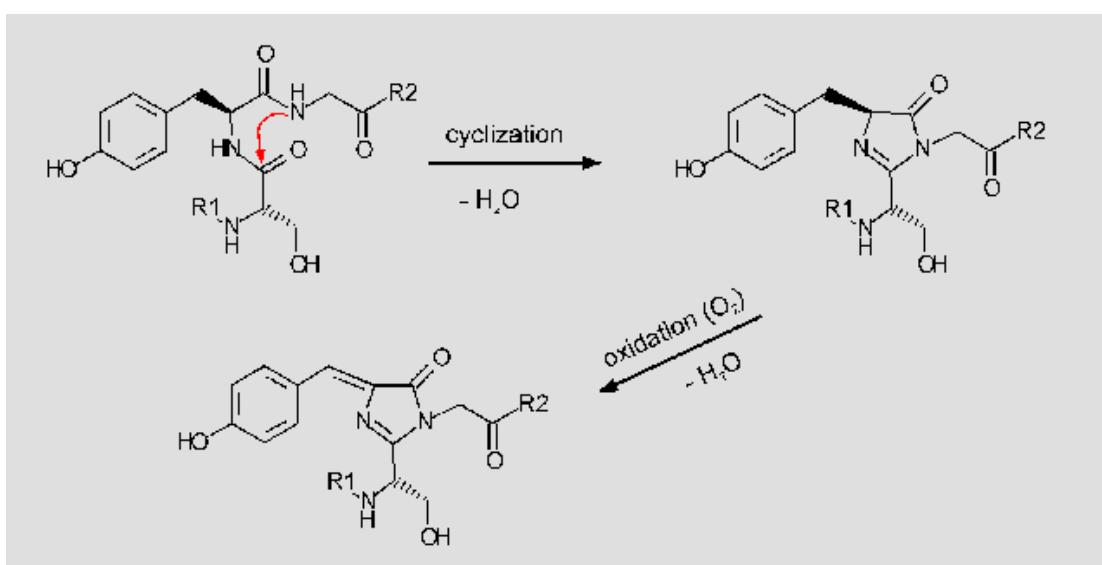
Figure 24 Cyclization mechanism of GFP chromophore (154).

2. GFP structure
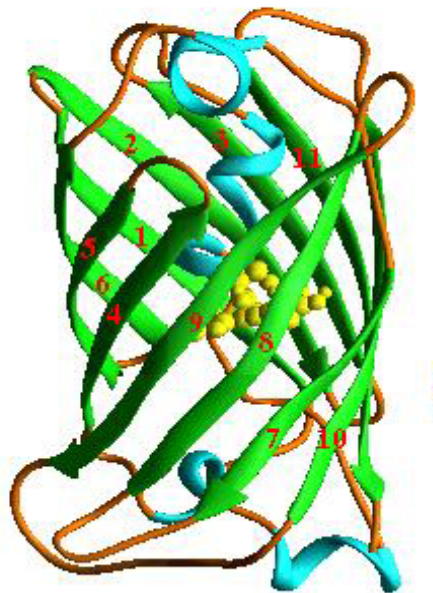
Figure 25 Green fluorescent protein structure (154).

GFP structure (figure 25) was named a beta-can protein. On the outside, 11 antiparallel beta strands (green) formed a very compact cylinder. Inside this beta-structure, there was an alpha-helix (blue), in the middle of which was the chromophore (yellow). There were also short helical segments (red) on the end of the can. The cylinder had a diameter of about 30 Å and a length of about 40 Å. Due to their structure, GFP was very resistant to denaturation condition. These included 6 M guanidinium hydrochloride, 8 M uria, varying pH (5.5-12), and various kinds of protease. Deletion of more than the N-terminal Met or more than seven amino acids from the C-terminus led to a total loss of fluorescence.

3. Application of Green Fluorescent Protein

GFP fluorescence was used to investigate remarkable array of properties and behaviors. The main reasons for this were that the chromophore of GFP was produced through an internal posttranslational autocatalytic cyclization that did not require any cofactors or substrates, fusion of GFP to a protein rarely affected the proteins activity or mobility, and GFP was nontoxic in most cases. GFP was resistant to heat, alkaline pH, detergents, photobleaching, chaotropic salts, organic salts, and many proteases. Mutants with optimized codon usage for mammals (154), plants, yeast (163), and fungi were created. GFP applications in cell biology and biotechnology (160), applications in plants, in transgenic plants, in fungal biology, in bacterial protein localization (164), in mouse embryos, visualizing protein dynamics in yeast, real-time molecular and cellular analysis, GFP as a vital marker in mammals (165). The production of transgenic animals such as mice (166), rabbits, and monkeys were attracted public attention and resulted in the formation of small companies proposing to produce fluorescent pets, Christmas trees, and flowers (167). Green mice and other animals were used as a source of green-tagged cells or organs for transplantation to make chimeric mice (165). In the followings, a summary of GFP laboratory applications was presented.

3.1 Fusion Tags

A fusion between a cloned gene and GFP could be created using standard subcloning techniques. The resultant chimera could then be expressed in a cell or organism. In this way GFP fusion tags could be used to visualize dynamic cellular events and to monitor protein localization (168, 169). GFP was ideally suited as a fluorescent fusion protein marker because it did not require the presence of any cofactors or substrates. The chromophore was produced in vivo, and in most cases the resultant chimera did not affect the localization or activity of the tagged protein.

For this reason GFP fusion proteins were the most common and successful application of GFP in biotechnology (156,160).

3.2 Reporter Gene

The first applications of GFP were as a reporter gene. Gene expression could be monitored by using a GFP gene that was under the control of a promoter of interest and measuring the GFP fluorescence which directly indicated the gene expression level in living cells or tissue. Green fluorescent protein was extensively used as a reporter gene (170, 171), especially in spatial imaging of gene expression in living cells (159, 172). However, its low sensitivity, due to the fact that there was no signal amplification, because each GFP had only one chromophore, had limited its use somewhat. The low sensitivity could be overcome by using sensitive photon counting devices; however, they were too expensive for routine uses (160).

3.3 Fluorescence Resonance Energy Transfer (FRET)

Fluorescence resonance energy transfer (FRET) was a nonradiative exchange of energy from an excited donor fluorophore to an acceptor fluorophore that was within 10-100 Å from the donor. In order for FRET to occur, the emission spectrum of the donor had to overlap with the excitation spectrum of the acceptor. The emission and excitation spectra of BFP and GFP overlapped as do the spectra of CFP and YFP, making them good potential FRET pairs. The efficiency at which the Foerster-type energy transfer occurred was steeply dependent ($1/r6$) on the distance between the fluorophores. Because any biochemical signal that changed the distance or orientation between the two fluorophores would affect the efficiency of FRET, it was a very useful technique for studying protein-protein interactions in vivo and in vitro (157, 169). The use of GFP in FRET-based applications were reviewed (169, 173).

3.4 Photobleaching

Photobleaching could be used to investigate protein dynamics in living cells. There were two methods based on photobleaching: fluorescence recovery after photobleaching (FRAP) and fluorescence loss in photobleaching (FLIP). By illuminating an area with high intensity illumination (bleaching) and monitoring the recovery of the resultant fluorescence loss (FRAP), the relative mobility of the GFP chimera could be determined. FLIP could be used to study transport of GFP fusion proteins between different organelles by repeatedly bleaching an area and monitoring the loss of fluorescence from outside the area. Applications of photobleaching GFP in cell biology were reviewed (174).

3.5 Metals

3.5.1. Reagentless Biosensors

Wild-type GFP had a strong affinity for Cu(II), less for Ni(II), and negligible interactions with Zn(II) and Co(II) (175). It contained 10 histidine residues, 5 of which were involved in secondary structures and unlikely to bind metal ions. His77, His81, and His231 were all within 7.5 Å of each other in the wild-type crystal structure of GFP (1EMF) and were proposed as a possible site for metal interaction (175). Since metal ions in the vicinity of a chromophore were known to quench fluorescence in a distance dependent fashion, a metal-binding GFP mutant was designed as a potential in vivo metal ion sensor. The 10C (T203Y, S54G, V68L, and S72A) GFP mutant was mutated to create two new mutants, one with a metal-binding site composed of two metal binding residues (S147H and Q204H) and the other mutant had a tricoordinate metal-binding site (S147H, S202D and Q204H). Both the metal-binding mutants displayed fluorescence quenching at much lower metal concentrations than the 10C variant.

3.5.2. Purification Aids

The affinity of GFPuv for Cu(II) and Ni(II) were used to purify and recover GFP using immobilized metal affinity chromatography (175). The simplest way of increasing GFP's metal affinity was to tag it with a polyhistidine. Ceramic hydroxyapatite was used to purify both proteins and DNA. A polyhistidine-tagged GFP was used to establish the effect of loading the hydroxyapatite with metal ions (176). The polyhistidine-tagged GFP did not show any binding to ceramic hydroxyapatite loaded with water, and there was no observable interaction between metal loaded ceramic hydroxyapatite and untagged GFP. However, the polyhistidine-tagged GFP showed strong binding to both Zn(II) and Fe(III) (176). A polyarginine-tagged GFP was used to demonstrate that polyarginine-tagged fusion proteins could be immobilized on flat surfaces, such as mica, for surface related spectroscopic and microscopic analysis (177).

3.6 Protein-Protein Interactions

Because any biochemical signal that changed the distance or orientation between the two fluorophores would affect the efficiency of FRET, it was a very useful technique for studying protein-protein interactions in vivo and in vitro (169). Luminescence resonance energy transfer (LRET) from *Renilla* luciferase to GFP was used to study protein-protein interactions in living cells. Protein-protein interactions could also be monitored by fluorescence gel retardation, fluorescence polarization assays, and affinity capillary electrophoresis (178). Fluorescence gel retardation was based on the fact that the electrophoretic mobility of a GFP protein chimera was higher than that of a complex formed by a protein-protein interaction between the GFP-protein chimera and another protein. Some of the drawbacks of fluorescence gel retardation were that it assumed that the protein-protein interactions remained at equilibrium throughout the electrophoresis and migration though the gel. Fluorescence polarization assays were based on the fact that a free GFP-protein chimera was likely to rotate more rapidly than a GFP-protein chimera interacting with another protein and would therefore had a lower rotational correlation time than its

bound counterpart.   Since fluorescence polarization assays could be performed in homogeneous solutions, in which the conditions could be controlled as desired, it was the preferred method over fluorescence gel retardation (178).   Attempts were currently underway to use GFP to characterize large numbers of protein-protein interactions in high-throughput settings.

CHAPTER III
MATERIALS AND METHODS

Materials

1. Apparatus

Autoclave, Model ss320 and 240, TOMY SEIKO Co.LTD, JAPAN.

Analytical balance, Model 1602 MPB, SARTORIUS, GERMANY.

Classical Lamp, PHILIPS Classical Tone lamp (60 W)

Refrigerated centrifuge, Model Avanti J-25, BECKMAN, USA.

Microcentrifuge, Model Biofuge A, HERAEUS CHRIST, WEST GERMANY.

Digital camera, Model Kodak DC 290, JAPAN

Electronic top loading balance, Model 1212 M, PRECISA, SWITZERLAND.

Electrophoresis unit, Model Mini-PROTEAN II, BIO-RAD LABORATORY Co, USA.

ELISA microtiter plate, NUNC, USA.

Fluorometer, Model FLx 800, BIO-TEK Instrument, INC, USA

Fraction collector apparatus, Model Hiload Pump P-50 based GradiFrac System, PHARMACIA BIOTECH, SWEDEN.

Freezer –86 °C, Model 958, FORMA SCIENTIFIC, USA.

Hot air oven, MEMMERT, WEST GERMANY.

Hot plate stirrer, Model SS3HC, CHEMLAB Co, ENGLAND.

Incubator, Model B-80, MEMMERT, WEST GERMANY.

Inducted Couple Plasma Atomic Emission Spectroscopy

Nuclear Magnetic Resonance (400 MHz), PERKIN ELMER

Shaking incubator, STUART SCIENTIFIC, ENGLAND.

pH meter, Model 611, ORIAN RESEARCH, ENGLAND.

Rocking Table

Safety cabinet, Model BH 120, GELMAN SCIENCES.

Skew cap glass tube

Sonicator, Model W380 Heat System Ultrasonic and Model XL Sonicator Ultrasonic Processor, HEAT SYSTEM INCORPORATION, USA.

Spectrophotometer, Model UV-2100, SHIMADZU CORPORATION, JAPAN.

Spectrophotometer, Model Junior II, COLEMAN, USA.

Vacuum Distillation apparatus

Vortex mixer, Model G560E, SCIENTIFIC INDUSTRIES INC, USA.
UV box, Foto/Phoresis I, FOTODYNE CORPORATION, USA.

Water bath

2. Chemical and biological reagents

Acrylamide, Prod no 89N35051, GIBCO BRL, USA.

Ammonium persulphate, Prod no 268990, AMERSCO, USA.

Ampicillin, Prod no A-9518, SIGMA, USA.

Argon gas

2,2' Azobiz(isobutyronitrile)

Bovine serum albumin, Prod no A7030, SIGMA, USA.

Bradford reagent, Prod no 500-0006, BIORAD-LABORATORIES, USA.

Calcium chloride, Prod no ART2381, E. MERCK, GERMANY.

Chelating Sepharose Fast Flow gel, Prod no 17-0575-01, PHARMACIA BIOTECH, SWEDEN.

Cobalt chloride, SIGMA, USA

Coomassie blue R 250, Prod no P0047213, AMERSCO, USA.

Copper sulfate, SIGMA, USA

Dialysis tubing, Prod no D-9527, SIGMA, USA.

Ethylenediaminetetraacetic acid, Prod no ED 4SS, SIGMA, USA.

Ethylene glycol dimethacrylate, SIGMA, USA

Ferric chloride, SIGMA, USA

Glacial acetic acid, Prod no 63, E. MERCK, GERMANY.

Glucose, SIGMA, USA

HEPES, SIGMA, USA

Hydrochloric acid, Prod no 317, E. MERCK, GERMANY.

Isopropyl-β-D-thiogalactopyranoside (IPTG), Prod no I-5502, SIGMA, USA.

Manganese Chloride, SIGMA, USA

Methacrylic acid, SIGMA, USA

Methanol, Prod no 6009, E. MERCK, GERMANY.

L-Methionine, SIGMA, USA

Molecular weight marker for SDS-PAGE, Prod no 161-0304, BIO-RAD LABORATORIES, USA.

Nickle chloride, SIGMA, USA

Nitro Blue Tetrazolium, SIGMA, USA

Nucleic acid molecular weight marker, NEW ENGLAND BIOLABS, USA.

Phenylalanine, MERCK, GERMANY

Potassium dihydrogen phosphate, SIGMA, USA

Polyethylene glycol 6000, Prod no 44271, BDH LABORATORY SUPPLIES, ENGLAND.

Restriction endonucleases, NEW ENGLAND BIOLABS, USA.

Riboflavin, MERCK, GERMANY

Sephadex G-75 gel filtration, PHARMACIA BIOTECH, SWEDEN.

Sodium chloride, Prod no K91113804 905, MERCK, GERMANY.

Sodium dodecyl sulphate (SDS), Prod no 0227, AMERSCO, USA.

Sodium Phosphate (Dibasic, Anhydrous), Prod no S-9763, SIGMA, USA.

Superoxide dismutase, SIGMA, USA

Trichloroacetic acid, SIGMA, USA

Triton X-100, MERCK, GERMANY

Trizma base, Prod no T1503, SIGMA, USA.

T4-DNA ligase, NEW ENGLAND BIOLABS, USA.

T4-Polynucleotide Kinase, NEW ENGLAND BIOLABS, USA.

N, N, N′, N′ Tetramethylenediamine (TEMED), Prod no 17-1312-01, PHARMACIA BIOTECH, SWEDEN.

Urocanic aid, SIGMA, USA

1-Vinylimidazol, MERCK, GERMANY

3. Bacterial Strains and Plasmid

3.1 *Escherichia coli* (*E. coli*) strain TG1 (lac-pro), *Sup* E, *thi*1, *hsd* D5/F′ *tra* D36, *pro* $A^+ B^+$, *lac*I, *lac*Z, M15 ; (ung^+, dut^+) was used as host. Plasmid pGFPuv (Clontech Laboratories, USA) was used for construction.

3.2 *Burkholderia pseudomallei* strain H10.

Methods

The Metals imprinted polymer catalyst useful as superoxide dismutase mimics were designed based on the concept of the active site coordination center in the active site of MnSOD and FeSOD enzymes. Metal coordinated with three imidazole nitrogen from three histidine residues, one oxygen from carboxylic acid and one oxygen from H_2O oriented as coordination sphere as seen in the active site (Figure 18). According to the active site, the 4(5)-vinylimidazole was chosen as mimicking to imidazole from histidine and methacrylic acid was mimicking to carboxylic acid of aspartic acid.

1. Synthesis of 4(5)-Vinylimidazole

Anhydrous urocanic acid was heated in vacuum in a distilling apparatus (Figure 26). The temperature was kept at 180 ºC for 30 minute then gradually increased the temperature to 220 ºC for 1 hour. The material was melted and begun to decompose as noticed by a decreased vacuum. On careful heating at 220-240 ºC, the product distilled as colorless syrup which crystallized in the receiver (179). The result product was subsequently investigated by ^1H NMR for determination of chemical structure.
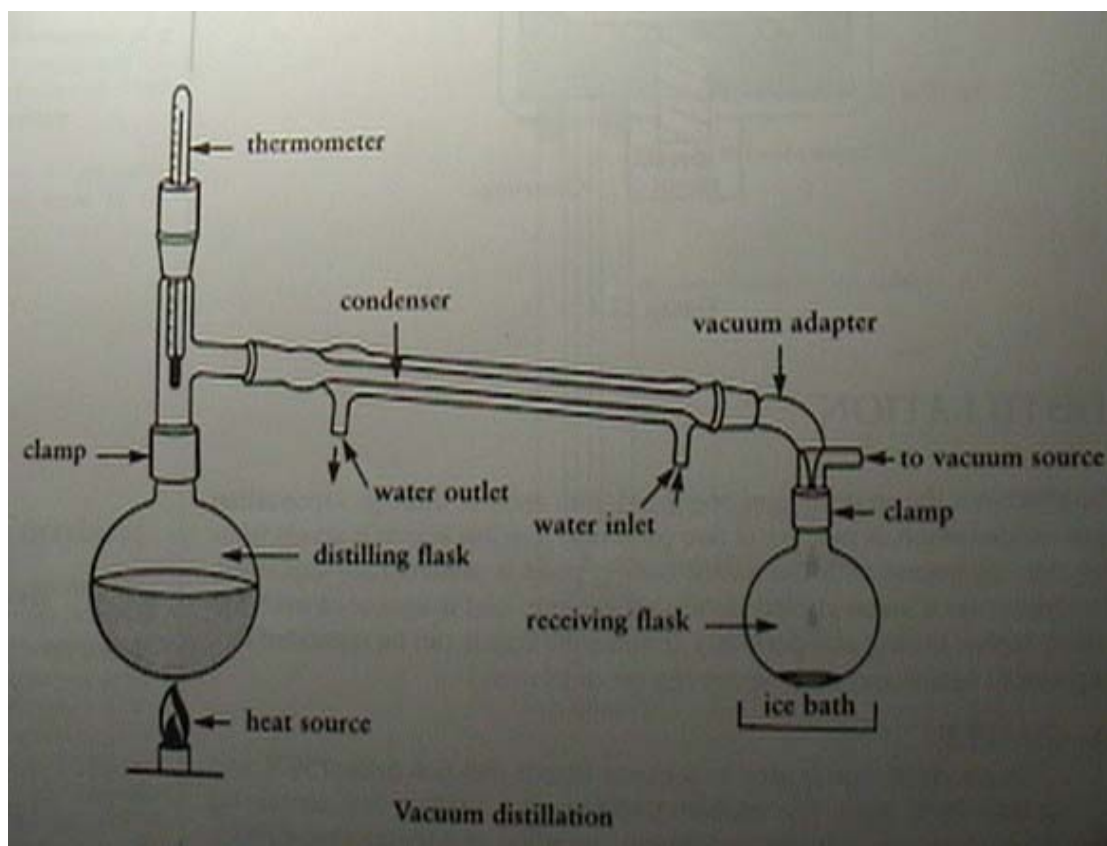
Figure 26 Distillation apparatus scheme (179).

2. Preparation of Metal template supported polymer

2.1. Preparation of the Metal -P4VM imprinted polymer using 4(5)-Vinylimidazole and Methacrylic acid as functional monomer.

Metal-P4VM imprinted polymer was prepared by using template-directed polymerization technique. Different metals ($MnCl_2$, $CoCl_2$, $FeCl_3$ and $NiCl_2$) were applied as the template. Each metal (100 μmol) was dissolved in 500 μL of porogen (methanol:water;9:1).   While the functional monomers, (4(5)-vinylimidazole (4V;300μmol) and methacylic acid (MAA;100 μmol)) were dissolved in 500 μL of the same porogen. All the metal and functional monomers were mixed together. Then, the mixture was incubated on rocking table for 1 hour. Then a crosslinker (ethylene glycol dimethacrylate;EDMA(4mmol)) was added to the solution and mixed together. The solution was subsequently transferred to a screw cap tube containing an initiator, (2,2'Azobiz(isobutyronitrile);AIBN) to yield a final concentration of 2% w/w initiator:monomer. The solution was then purged with Argon for 1 minute. The solution was started to polymerize by heating at 60 ºC for 24 hours. The resulting bulk polymer monolith was ground in mechanical mortar to obtain fine particle (1-10 μm) prior determination of SOD activity. Control polymer (Control P4VM) was also prepared for comparison by using all the components stated earlier except the metal templates.

2.2. Preparation of the Metal-P1VM imprinted polymer using 1-Vinylimidazole and Methacrylic acid as functional monomer.

Due to the difficulty to achieve the 4(5)-vinylimidazole in high amount, 1-vinylimidazole was selected as an alternative functional monomer that possessed nearly the same functional group of 4(5)-vinylimidazole. Preparation of the Metal-P1VM imprinted polymer was performed in a similar manner using 1-vinylimidazole.

3. Superoxide Dismutase Activity Assay

3.1. Superoxide dismutase activity assay by riboflavin-light-NBT based assay.

Superoxide dismutase activity was assayed by using an indirect method (riboflavin-light-NBT). A stock assay solution was prepared by mixing 27 mL of HEPES buffer (50 mM, pH 7.8), 1.5 mL of L-methionine (30 mg/mL), 1mL of NBT (1.41 mg/mL) and 750 µL of Triton X-100 (1% wt). One millilitre of stock solution was added to a microcentrifuge tube containing 5 mg of each imprinted polymers. Ten microlitre of riboflavin (44µg/mL) was then added to the solution and mixed by vortexing. The mixture was illuminated for 7 min under a PHILIPS Classic Tone lamp (60 W) in a light box, followed by an immediate centrifugation (9000 rpm, 1 min) to sediment the polymer particles. Visible absorbance at 550 nm of the supernatant was measured using a standard UV-VIS spectrophotometer. The extent of inhibition for NBT photoreduction was calculated as: $(Abs_{cont} - Abs_{test})/ Abs_{cont}$. The Abs_{cont} was defined as the absorbance value at 550 nm obtained from the metal-free polymer. Superoxide dismutase and $MnCl_2$ were used as positive control while the control polymer and the pure assay reagent were applied as negative control. (Fridovich, 1987) The reaction was performed in the dark room.

3.2. Determination of 50% NBT inhibition reduction of the Manganese-supported polymers

To determine 50% NBT reduction inhibition of the Mn-supported polymers, various amounts (0.5-10 mg) of the MnP4VM were applied for SOD activity assay and the 50% inhibition concentration was then calculated. For such experiment, the SOD enzyme (0.2275-9.1µg) was applied for comparison.

3.3. Effect of chelating agent on SOD activity of the imprinted polymer

The polymer Mn-P4VMAA (5 mg) was incubated with 1 mL of 0.1 mM EDTA in HEPES buffer (50 mM, pH 7.8) for 1 h. The polymer was then separated and the remaining activity was further analyzed.

4. Important role of functional monomer on SOD activity of the MIP

Role of the functional monomers on SOD activity of the MIP was investigated. Three different compositions of the functional monomers were selected as following: a) 1-Vinylimidazole (300 µmol)+MAA (100 µmol); b) 1-Vinylimidazole (400 µmol); c) MAA (400 µmol). These compositions were applied for preparation of the metal-supported polymers and the control polymers as previously described in section 2.1. SOD activity of these polymers was determined.

5. Evaluation of the reusability of MnP1VM.

Reusability of the MnP1VM as SOD mimics was evaluated by measuring the SOD activity of the polymer for three times. At each time, the MnP1VM was subjected to determine the remaining manganese ions via ICP-AES.

6. Construction and Expression of Genes

Cloning procedures were performed as described by Maniatis *et al* (181). Purification of DNA from agarose gel was done via Qiaquick DNA purification system (Qiagen).

6.1 Oligonucleotides preparation

An amino acid sequence Cys-Phe-Phe-Met-Pro-His-Thr-Phe-Cys, which was revealed as a protease binding peptide, was applied for code -reading to synthesize oligonucleotides (182). This sequence was previously obtained by selective binding of a phage library to the immobilized *Burkholderia pseudomallei*. The hexahistidine peptide, which was known to provide avidity to metal ions and applied as a potential tool for protein purification, was also accounted for decoding to synthesize oligonucleotide I. This oligonucleotide was designed to carry an enterokinase cleavage site for post purification process as represented in figure 27. All oligonucleotides were synthesized by the Bioservice Unit (BSU), National Science and Technology Development Agency (NSTDA), Thailand. To derive a double stranded genome, both of the synthesized complementary strands of the oligonucleotide (5′ → 3′ and 3′ → 5′) were dissolved in distilled water and diluted to an equal concentration (approximately 5 μM). Then 22.5 μl of each were mixed together and annealed by adding 5 μl of annealing buffer (10×) (10 mM Tris-HCl, 0.1 M NaCl, 1.0 mM EDTA, pH 7.8). Sample was incubated in a waterbath at 95 °C for 15 minute and further slowly cooled down to room temperature to allow hybridization. Finally, the oligonucleotide was treated with T4 Polynucleotide kinase in order to add a phosphate group at the 5′-terminal end. All oligonucleotides were readily applied for further gene construction.

The sequences of synthetic oligonucleotides were analyzed by the computational analysis (http://bioinfo.math.rpi.edu). This program provided the informative of appropriated inframe-fusion and restriction endonuclease sites created on a DNA sequence. However, it must be speculated that the predicted free energy of

mRNA folding (hairpin loop) had to be more than minus five as calculated from the RNA structure version 3.7 program.

Oligonucleotide I:

(5′-AGCTTACACCACCACCATCACCATGCGAGCTCTGATGACGATGATAA AGCCTGCA -3′ and 5′-GGCTTTATCATCGTCATCAGAGCTCGCATGGTGAT GGTGGTGGTGTA -3′)

Oligonucleotide II:

(5'-CTAGCTTGTTTCTTCATGCCGCACACTTTCTGTTCTAGAGCATCGATGG TAC -3′ and 5′- CATCGATGCTCTAGAACAGAAAGTGTGCGGCATGAAGAAA CAAG -3′)

6.2 Construction of DNA expression units (pH$_6$GFPuv and pH$_6$PBGFPuv)

In order to construct a chimeric gene providing hexahistidine region and green fluorescent protein (GFP), a pGFPuv plasmid was digested with *Hin*dIII and *Pst*I.   A fragment carrying the gfp gene was purified from 0.7% agarose gel electrophoresis. Synthetic oligonucleotide I encoding hexahistidine region carrying *Sac*I site was annealed to become double stranded DNA and subsequently inserted into the region between the *Hin*dIII and the *Pst*I sites within the multicloning sites of plasmid pGFPuv by using the T4 DNA ligase at 16 °C for 18 hours, yielding plasmid of pH6GFPuv (Figure 36).

To generate the pH6PBGFPuv, a plasmid unit that having a protease-binding region and GFP, synthetic oligonucleotide II encoding 1 region of protease binding peptide with *Cla*I site was inserted into the *Xba*I and the *Kpn*I sites of pH$_6$GFPuv. As shown in Figure 38, the *Xba*I site of synthetic oligonucleotide II was modified in order to generate a new *Xba*I site for further construction of multiple protease-binding regions. All chimeric genes were subsequently transformed into *E. coli* strain TG1 for further expression.

6.3 Preparation of competent *E. coli*

A colony of *E. coli* strain TG1 was inoculated into 5 ml of LB broth and culture was incubated for overnight with shaking (150 rpm) at 37 °C. Then 1 ml of culture was transferred into 100 ml of LB broth and further incubated at 37 °C until density of the cell reached 0.4 - 0.5 OD units at 600 nm. Culture was pelleted by spinning at 6,000 rpm for 5 min at 4 °C. Pellet was collected and resuspended in 30 ml steriled cold 50 mM $CaCl_2$ by gentle mixing on ice. Cells were further incubated on ice for 30 min. Cell pellet was harvested by centrifugation at 6,000 rpm for 5 min at 4 °C. Competent cell suspension was derived by carefully resuspending the pellet in 8 ml ice-cold 50 mM $CaCl_2$ and kept on ice until used.

6.4 Bacterial transformation

Transformation was initiated by mixing a ligation product with 0.2 ml of competent cell and kept on ice for 30 minutes. Sample was subsequently heated to 42°C for 2 min in waterbath. For recovery of the cell, a prewarm of 0.8 ml LB broth was added and incubated at 37 °C for 1 hour with shaking (150 rpm). The transformation was further accessed by spreading of 500 μl of the transforming suspension sample onto LB agar plates supplemented with 100 mg/L ampicillin. Plates were further incubated for 16-18 hours at 37 °C. Transformants were selected and plasmids were purified for further restriction endonucleases analysis and expression manipulation.

6.5 Restriction endonucleases analysis

To verify the inframe-fusing, all construction unit of the chimeric gene was checked via restriction endonucleases analysis. Since each synthetic oligonucleotide contained an insertional site for markers, the chimeric genes were therefore digested with marker restriction enzymes. For these circumstances, the pH_6GFPuv and the $pH_6PBGFPuv$ were digested with *Sac*I and *Cla*I, respectively. All digested samples

were accessed for the expected DNA fragments by subjection to agarose gel electrophoresis.

6.6 Agarose gel electrophoresis

DNA samples were mixed with loading buffer and applied into the slots of a 0.7% agarose gel submerging in TAE buffer. Electrical current was applied at 100 volts for 45 minutes at room temperature. Agarose gel was subsequently soaked in Ethidium Bromide solution (0.1 μg/ml). The DNA fragments in the gel was visualized under long wavelength UV light (354 nm) and photography of the fragments were performed. In all cases, standard λ/*Hin*dIII fragments were used as molecular weight markers.

6.7 Expression of constructed chimeric genomes

Transformants those harvested plasmid vector carrying constructed chimeric gene were grown to late exponential phase in LB broth at 37 °C with shaking (150 rpm). Ampicillin at concentration of 100 mg/L was included. Expressions of constructed genes were induced by 1 mM of isopropyl-β-D-thiogalactopyranoside (IPTG). Expressing gene products were always checked using appropriate procedure e.g. fluorescent properties.

7. Crude Chimeric Protein Preparation

Both native and chimeric GFPuv were harvested from culture of *E. coli* TG1 carrying constructed plasmids as previously described. Culture was spun at 6,000 rpm for 5 min and cell pellet was resuspended in sodium phosphate buffer, pH 7.4, containing 0.3 M NaCl. Cells were disrupted by sonic disintegration at output 6 for 20 sec (six times) with resting 40 sec in between and debris was removed by centrifugation at 10,000 rpm for 5 minute. The derived homogenates of native GFPuv was then heated to 65 °C for 15 min in order to precipitate other host proteins while

none of the chimeric His_6GFPuv and $His_6PBGFPuv$ was performed. Precipitate was removed by 5 minutes centrifugation at 10,000 rpm and the supernatant was attained as crude chimeric protein preparation prior to further purification by the Immobilized Metal affinity chromatography (IMAC).

8. Purification of Chimeric Protein

A metal Chelating Sepharose 6B column (0.7×8 cm) was charged with 20 mM of the desired metal ions. The column was washed with at least 5 column volumes of distilled water and equilibrated with phosphate buffer, pH 7.4 to the column. Crude extract was loaded at a flow rate of 0.58 ml/min.   Unbound material was removed by washing with 300 ml phosphate buffer. Bound protein was eluted by using 10 ml of 20 mM EDTA in phosphate buffer. Fractions were collected and those possessed greenish fluorescence were pooled and dialysed in 5×2 L of phosphate buffer. Fractions were stored at $-20\,°C$ until use. To the procedure herein, copper ion was charged to the affinity column for purification of native GFP while zinc ion was used for all chimeric proteins purification.

9. Partial purification of protease from *Burkholderia pseudomallei*

B. pseudomallei strain H10 was grown in defined chemical medium consisting of 85.6 mM NaCl, 14.4 mM K_2HPO_4 92 mM sodium monoglutamate, 24 mM valine, 8 mM phenylalanine, 70 M glucose, 1.33 mM $MgSO_4$, 0.14 mM $CaCl_2$, 0.0039 mM $FeSO_4$ and 0.0085 mM $ZnSO_4$.   Culture in 200 ml was initiated in 1 litre flask by inoculation of 2 ml overnight culture.   The culture was then incubated at 37°C with shaking 150 rpm for 48 hours.   The culture supernatant was collected by centrifugation at 7,000 rpm for 60 min and filtered through 0.45 μm millipore filter. Filtrate was concentrated by dehydration via polyethylene glycol.   Extracellular protease were purified by 20-80% ammonium sulphate precipitation and dialysed in 5×2 L Tris buffer. The partial purified protease was stored at -20 ºC

Protein contents were determined by dye-binding assay according to the method of Bradford (183), which was supplied as a kit by BioRad. Bovine serum albumin was used as standard protein

10. Polyacrylamide gel electrophoresis

Either native PAGE or SDS-PAGE were performed on 12% polyacrylamide gels in a Tris-glycine, pH 8.3 discontinuous buffer system. The protocol used was slightly be modified from Laemmli's method (184). Briefly, the separating slab gel was cast and polymerized at ambient temperature. Stacking gel of 4 % polyacrylamide was cast vertically over the slab gel. The electrophoretic buffer was added to the upper and lower reservoirs. Sample was mixed with loading buffer (4×) prior applying to the gel. Electrophoresis was performed at room temperature with constant voltage of 150 mV. Banding of protein was visualized by staining the gel in Coomassie brilliant blue R. For the case of native PAGE, fluorescent emission of GFP was determined by irradiation of standard long wave UV (354 nm) light source. Standard molecular weight markers were also included in the running.

11. Removal of the hexahistidine by enterokinase cleavage

Removal of the hexahistidine after protein purification was performed by the enterokinase cleavage assay. Assay was performed according to the manufacturer's instruction. The chimeric H_6GFP was incubated with enterokinase enzyme for 16 hours at 25 ºC. Mixture was subsequently loaded onto the IMAC-Zn^{2+} column. Fractions from all steps: crude after loaded; washing and elution were collected and subjected to electrophores on SDS-PAGE.

12. Binding of the chimeric Protease-binding GFP to *B. pseudomallei* protease.

Binding of the chimeric H_6PBGFP to *B. pseudomallei* protease was investigated by fluorescence gel retardation assay. Purified chimeric H_6PBGFP was

incubated at 25°C with partial purified protease for 15 minutes. Samples were mixed with loading buffer (4×) prior applying to the gel. The mixtures were loaded onto a SDS discontinuous polyacrylamide gel (184).   The gel was subjected to electrophoresis at constant voltage of 150 mV. After electrophoresis, the fluorescent was immediately observed under UV irradiation and the picture was taken by digital camera.   Binding interaction between the chimeric H_6PBGFP and protease was evidenced by decreasing of the protein mobility due to the complex formation.

CHAPTER IV
RESULTS

1. Synthesis of 4(5)-vinylimidazole

4(5)-vinylimidazole was successfully synthesized. Urocanic acid was become to be 4(5)-vinylimidazole by decarboxylation at 220 ºC as demonstrated in figure 27. The presence of 4(5)-vinylimidazole was subsequently confirmed by ^{1}H NMR spectra. A characteristic of proton peak was shown in figure 28.
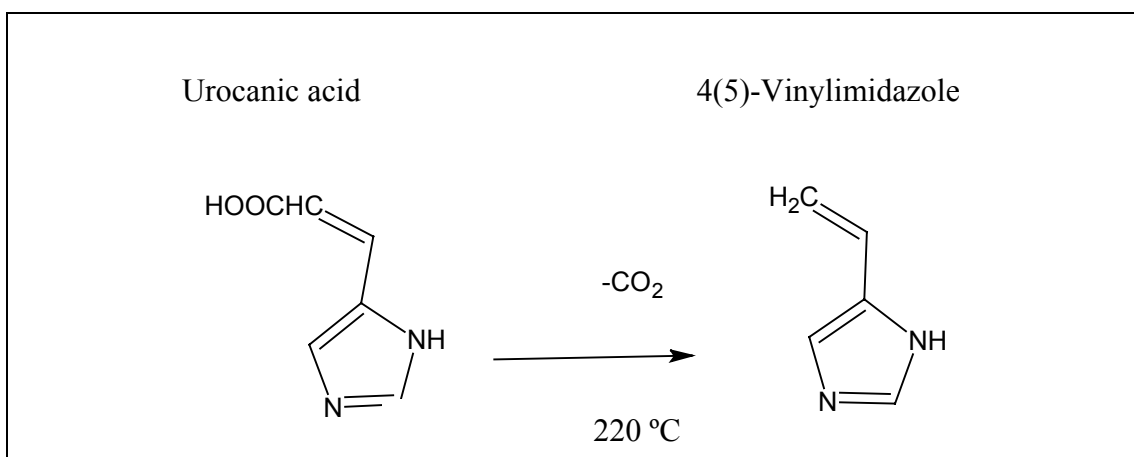
Figure 27 Urocanic acid was changed to be 4(5)-vinylimidazole by decarboxylation process.
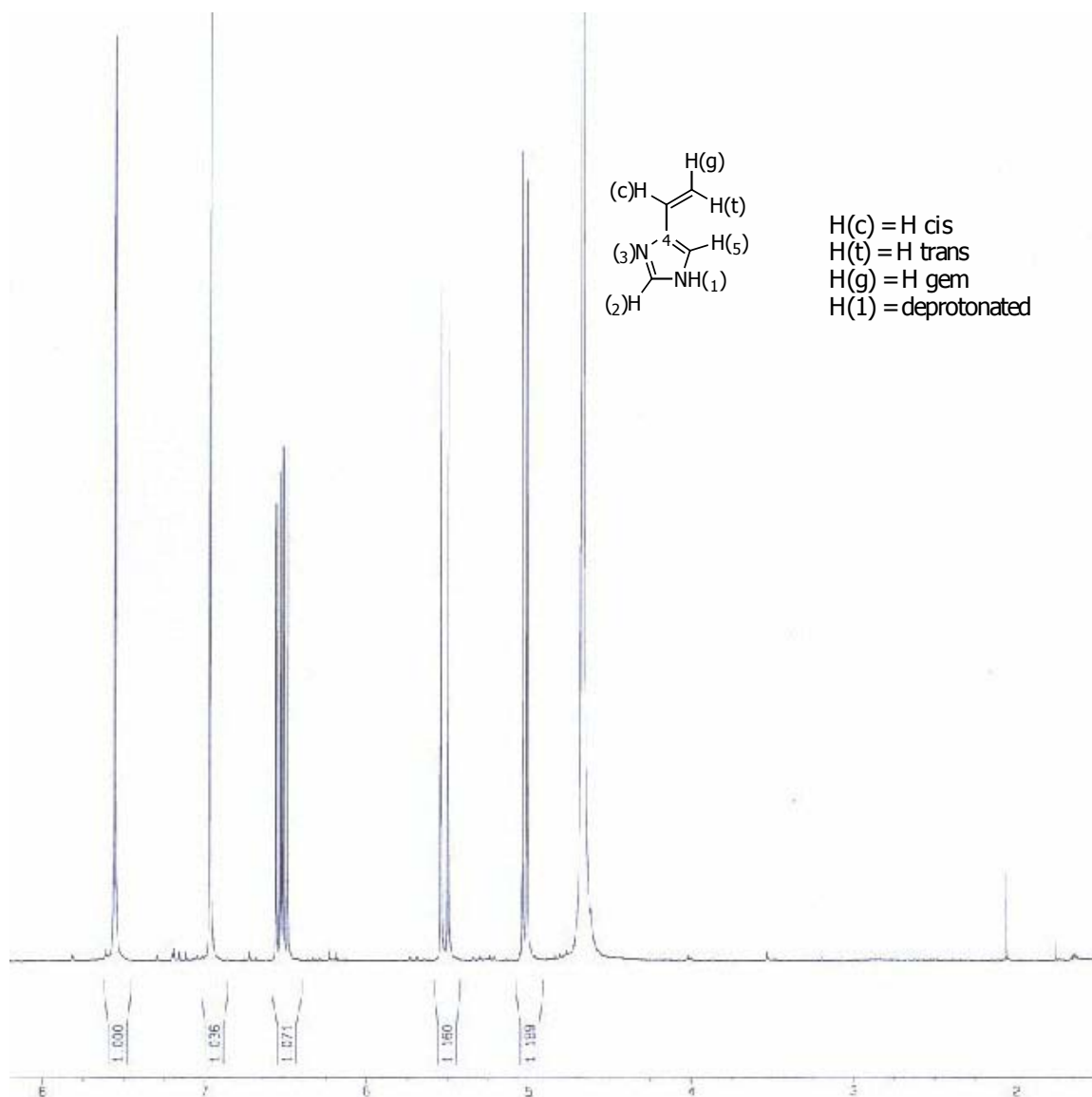
Figure 28 ^{1}H NMR spectrum of 4(5)-Vinylimidazole.

4(5)vinylimidazole: ^{1}H NMR (D$_2$O)   4.64 (dd,1 H, H,, J = 10.0 Hz, *Jgt* = 1.0 Hz), 5.52 (dd, 1 H, H,, *Ja* = 18.0 Hz), 6.52 (dd, 1 H, Hc), 6.97 (s, 1 H, Im H-5), 7.56 (s, 1 H, Im H-2).

2. Synthesis of a metal imprinted Polymer (MeP4VM)

Figure 29 demonstrated a scheme of metal imprinted polymer (MeP4VM) synthesis.   The MeP4VM was synthesized by using 4(5)-vinylimidazole and methacrylic acid served as functional monomers.   These polymers were then propagated by the crosslinking agent; ethylene glycol dimethacrylate (EDMA) and polymerized by thermally induced free radical polymerization.   The resulted polymer was stored until use.

Crosslinking (EDMA)

Free radical polymerization

(AIBN, 60 ºC, 24 hours)
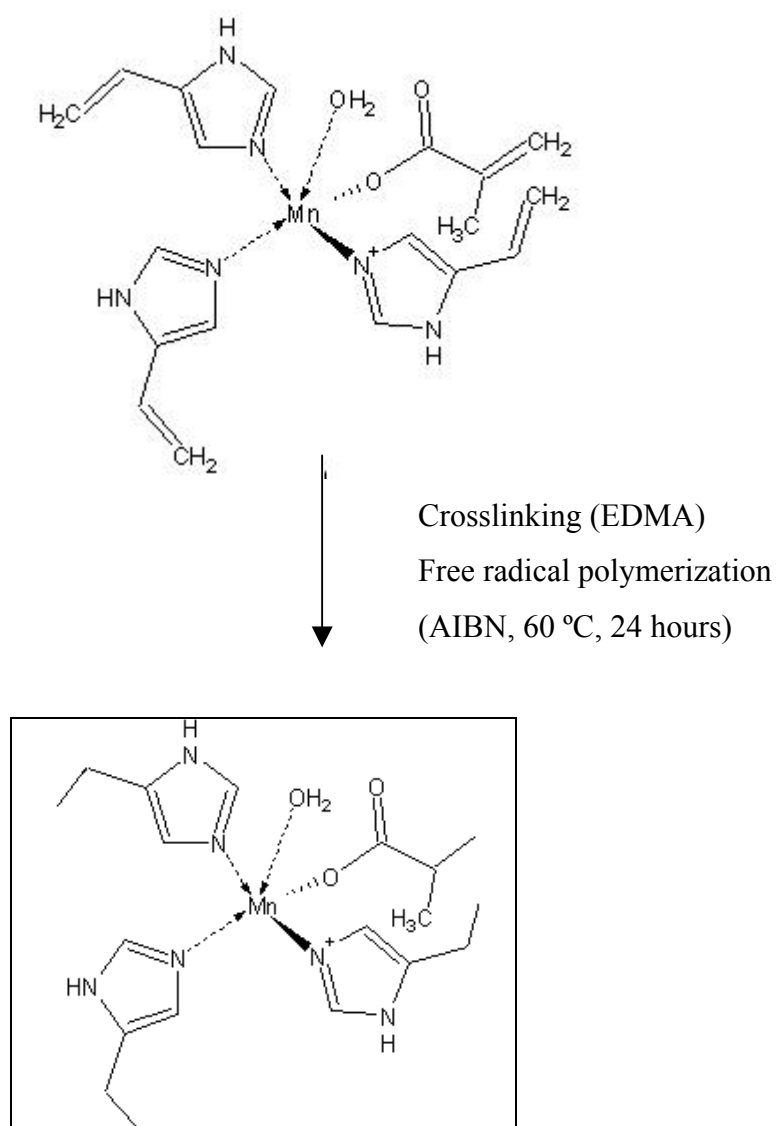
Figure 29 Scheme of the metal imprinted polymer(MeP4VM) synthesis

3. Determination of SOD activity

Superoxide dismutase activity of the MeP4VM was determined by riboflavin-light-NBT method, which was an indirect assay. Briefly, riboflavin (sensitizing dye) was activated by photon to be an excited state, which oxidized some electron donor e.g. L-Methionine. The dye was thereby reduced to a semiquinone which reduced O_2 to $O_2^{\cdot-}$. The $O_2^{\cdot-}$ radical, in turn, reduced NBT to an insoluble purple formazan. The insoluble formazan could be solubilized by using Triton® X-100 (detergent) as a stabilizer of formazan colloid, which was spectrophotometrically visible at 550 nm. Percentage of SOD activity was defined as 1 unit of SOD equal to concentration of enzyme or polymer that could inhibit the NBT photoreduction by 50%. As shown in figure 30, various amounts (0.2275-9.1μg) of SOD enzyme from bovine erythrocyte were applied for determination of 50% reduction inhibition. The result demonstrated that 1.1 μg of SOD was needed to inhibit 50% of the NBT photoreduction.

The catalytic metal imprinted polymer was applied as SOD mimics possessing SOD activity that catalyzed the dismutation of O_2^- to produce H_2O_2, leading to inhibition of O_2^- mediated NBT reduction. Therefore, superoxide dismutase activity of the MeP4VM was determined. Experiment was initiated by screening of the highest activity of the MeP4VM among various metals (MnP4VM, NiP4VM, FeP4VM and CoP4VM). SOD from bovine erythrocyte and $MnCl_2$ were applied as positive control while the control polymer without metal was used as negative control. As shown in table 6, the MnP4VM possessed the highest activity of reduction inhibition of 72.70% while the NiP4VM, the CoP4VM and the FeP4VM exhibited 22.9%, 28.95% and 11.6%, respectively. Therefore, various amounts (0.5-10 mg) of the MnP4VM were chosen to further determine the 50% NBT reduction inhibition. The 50% inhibition was determined by plotting the reduction of NBT at 550 nm versus MnP4VM amounts as shown in figure 31. The 50% inhibition was corresponding to the MnP4VM amount of 1.2 mg.

Effect of metal coordination complex on SOD activity of the MnP4VM was further investigated by using a chelating agent (0.1mM EDTA) (Table 7). A

pretreatment of the MnP4VM with EDTA led to a complete loss of SOD activity. Meanwhile, nothing effect was observed upon addition of EDTA to the control polymer (control P4VM). Furthermore, additional of excess amounts of $MnCl_2$ onto the control P4VM did not afford any SOD activity and free Mn(II) in solution only displayed a very low intrinsic activity. These findings strongly indicated that the majority of SOD activity was achieved from the metal-centered of imprinted polymers.

4. Synthesis of a metal imprinted polymer (MeP1VM)

1- Vinylimidazole (figure 32), which was provided as an alternative commercial available functional monomer, which was applied in combination with the MAA for construction of a metal imprinted polymer (MeP1VM). The 1-vinylimidazole possessed almost the same functional group as that of 4(5)-vinylimidazole, so this functional monomer was also brought into coordination complex and polymerization in a similar manner (figure 33).
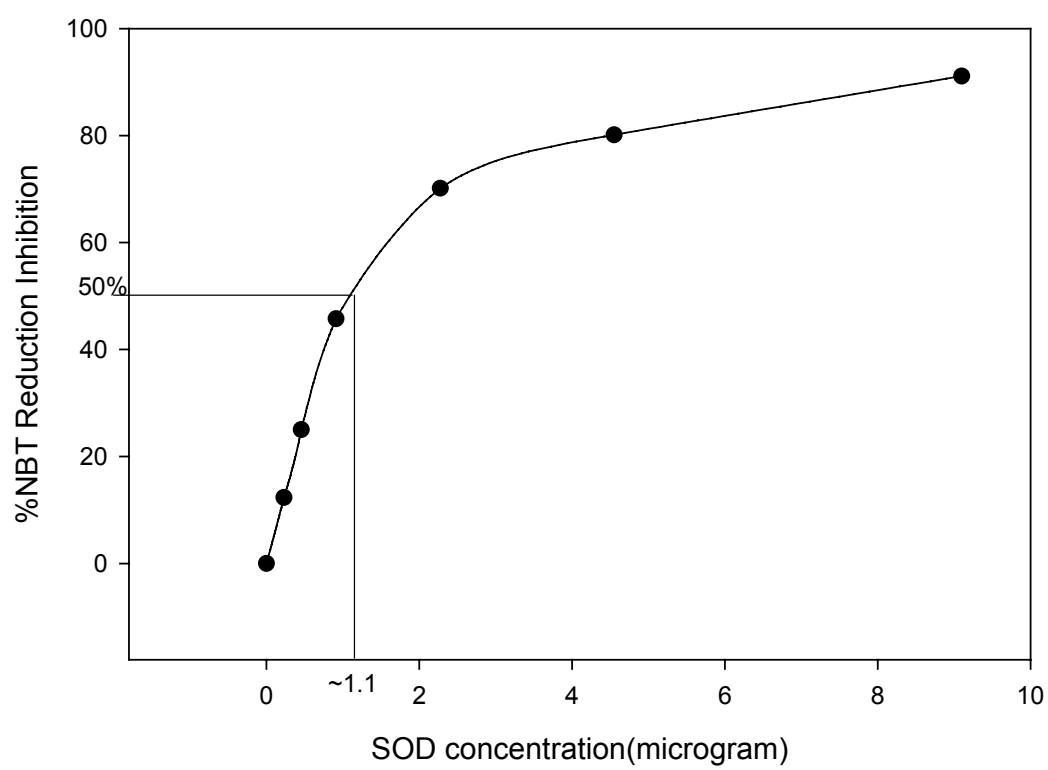
Figure 30 The plot of %NBT reduction inhibition versus SOD enzyme (µg)

Table 6 SOD activity determination of MeP4VM

MetalP4VM (5mg)	Absorbance[a] at 550 nm	% NBT reduction inhibition (SOD activity)
MnP4VM	0.0611	72.70%
NiP4VM	0.1726	22.90%
CoP4VM	0.1592	28.95%
FeP4VM	0.1978	11.60%
Control P4VM (negative control)	0.2238	0%
Bovine erythrocyte SOD;8.14µg (Positive control)	0.0553	75.29%

[a] the value given was the average of two samples
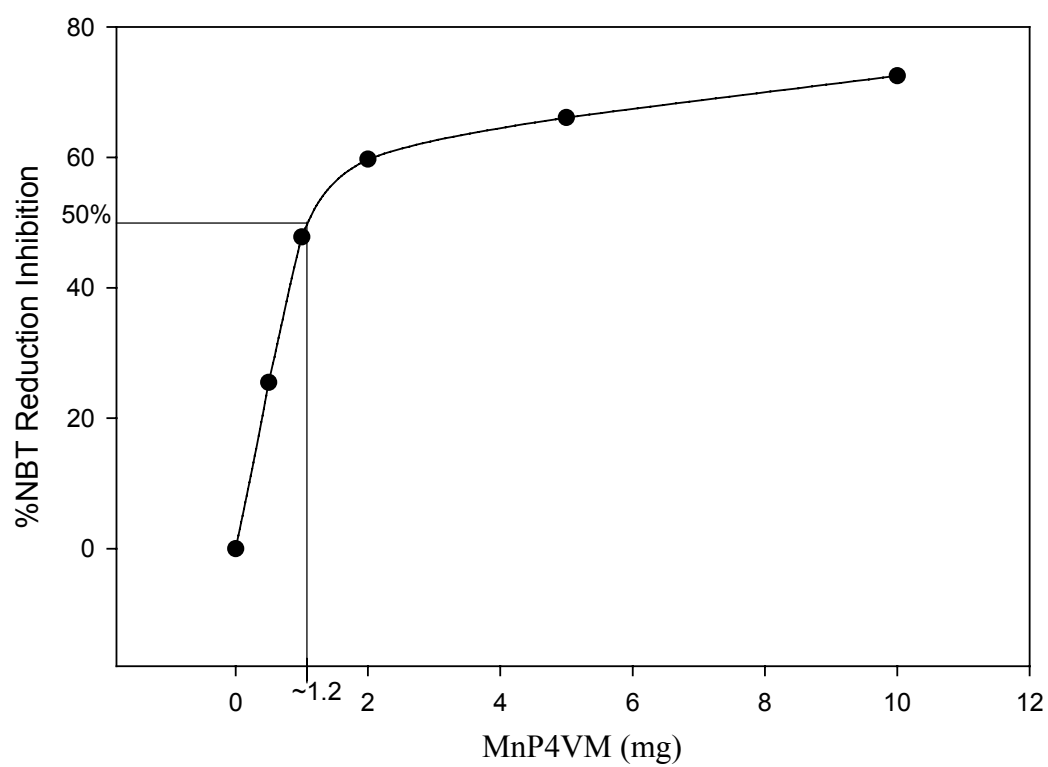
Figure 31 The plot of %NBT reduction inhibition versus MnP4VM amounts (mg)

Table 7 Effect of manganese coordination complex on SOD activity of the MnP4VM

Test	Absorbance[a] at 550 nm	SOD activity
MnP4VM (5 mg)	0.0835	Positive
MnP4VM (5 mg) (treated with 1 mL of 0.1mM EDTA)	0.3173	Negative
Control P4VM (5mg)	0.2947	Negative
Control P4VM (5mg) (treat with 1 mL of 0.1mM EDTA)	0.3104	Negative
Control P4VM (5mg) (loaded with 50µg MnCl$_2$)	0.3341	Negative
Control P4VM (1mg) (loaded MnCl$_2$ 10µg)	0.3472	Negative
MnCl$_2$ (50µg)	0.1972	Some
SOD (40.7µg)	0.0629	Positive
SOD (8.14µg)	0.0811	Positive
Reagent buffer (negative control)	0.4416	Negative

[a] the value given was the average of two samples
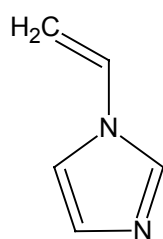
Figure 32 Chemical structure of 1-vinylimidazole

Crosslinking (EDMA)

 Free radical polymerization

(AIBN, 60 ºC, 24 hours)
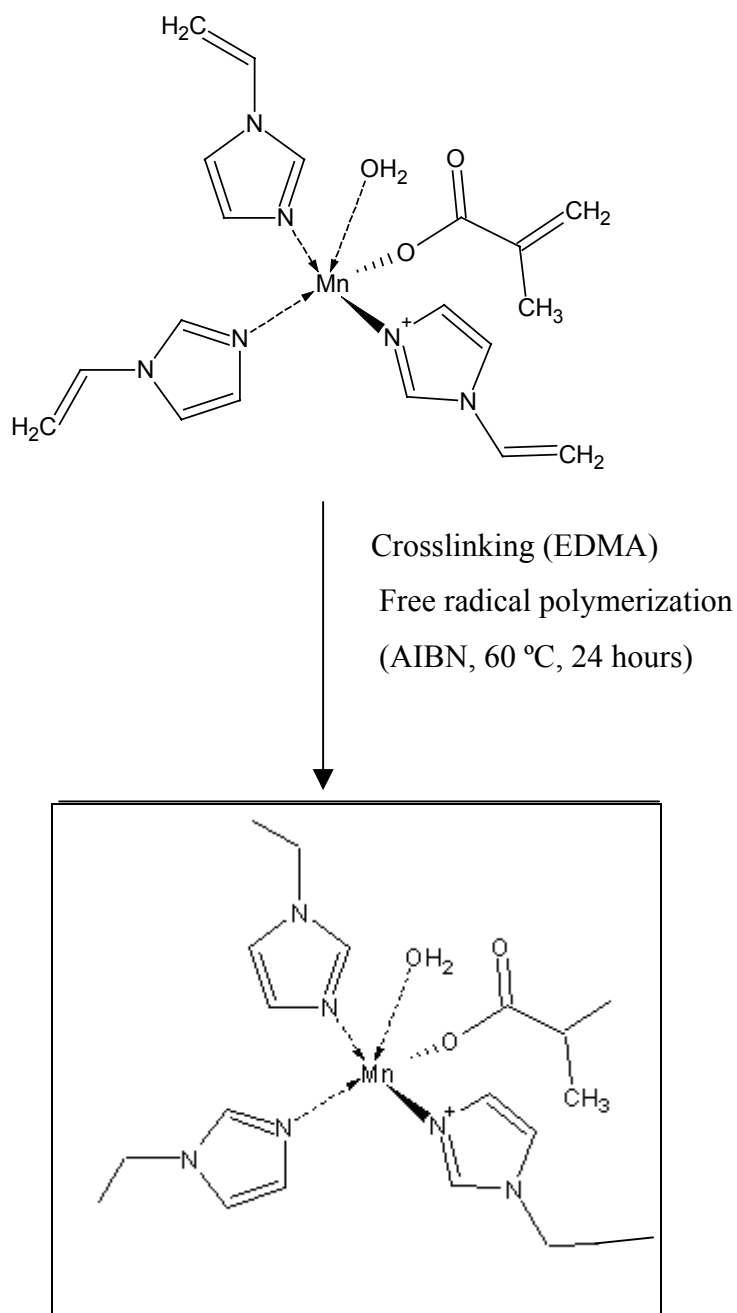
Figure 33 Scheme of the metal imprinted polymer (MeP1VM) synthesis

Determination of SOD activity of MeP1VM

Various metal templated imprinted polymers (MnP1VM, NiP1VM, CoP1VM, FeP1VM and CuP1VM) were constructed and assayed for SOD activity by Riboflavin- NBT photoreduction methods. It was found that the MnP1VM possessed the highest activity in % reduction inhibition (94.8%) while the CoP1VM and the CuP1VM possessed 77.09% and 55.34%, respectively.   The NiP1VM and the FeP1VM possessed 6.8% and 10.42%, respectively (Table 8).

The MnP1VM was chosen to further determine the 50% reduction inhibition by varying the amount of the polymer ranging from 0.125 mg to 10 mg while the control P1VM was also tested at the amount from 1 to 10 mg. The results were plotted between % NBT reduction inhibition and MnP1VM amount (figure 34). The plot indicated that the MnP1VM at 1.2 mg possessed 50% NBT reduction inhibition while the control P1VM exhibited no inhibition at all amounts tested.

5. Effects of functional monomer on SOD activity of MnP1VM

Effect of functional monomer on SOD activity of MnP1VM was studied. From our findings, the MnP1VM, which was generated from both 1-vinylimidazole and methacrylic acid, exhibited the highest activity (88.63%), while the MnP1V and the MnPM revealed the SOD activity of 48.32% and 62.43%, respectively.   These indicated the necessity of using both the 1-vinylimidazole and methacrylic acid to maintain the highest catalytic activity of the polymer. Furthermore, MnP1VM possesses higher SOD activity than MnP4VM.

Table 8 SOD activity determination of MeP1VM.

MetalP1VM (5mg)	Absorbance[a] (550nm)	% NBT reduction inhibition
MnP1VM	0.0203	94.80%
NiP1VM	0.3649	6.80%
CoP1VM	0.0897	77.09%
FeP1VM	0.3508	10.42%
CuP1VM	0.1762	55.34%
Control P4VM (negative control)	0.3916	0%
MnCl$_2$ (50µg)	0.1972	55.34%
SOD (8.14µg)	0.0811	81.63%
Reagent buffer (negative control)	0.4416	0%

[a] the value given was the average of two samples
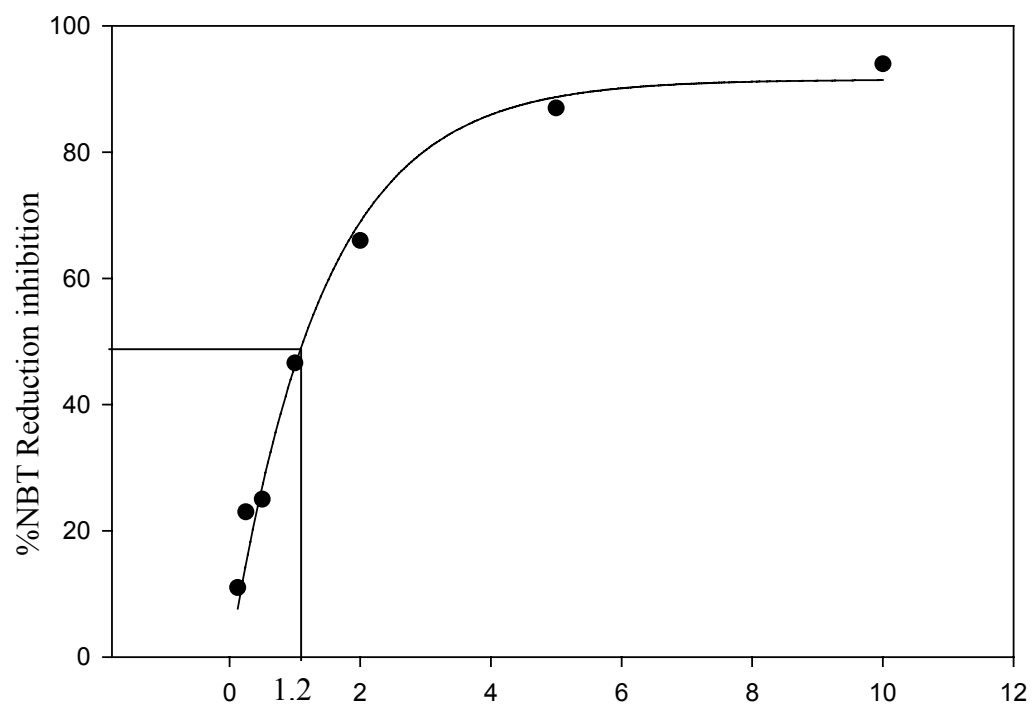
Figure 34 The plot of %NBT reduction inhibition versus MnP1VM amounts (mg)

6. SOD activity of reusage MnP1VM

This study explored the reusability of the MnP1VM as SOD mimics. Repeated use of the MnP1VM resulted in a reduction of activity *i.e.* the inhibition of NBT photoreduction decreased from the initial 89% to 79%, which was accompanied by a lowered amount of Mn(II) in the polymer (by 70%) as quantified by ICP-AES analysis. This inferred that less than 30% of manganese was able to form a stable complex with the ligand monomer. This was strongly evidenced by the fact that the remaining metal contents were in the similar level throughout all the second and third measurements.

Table 9 Effect of functional monomer on SOD activity of the metal-imprinted
polymer

Polymer (5mg)	Absorbance at 550 nm[a]	% NBT reduction inhibition
MnP4VM	0.0611	72.70%
MnP1VM (1-Vinylimidazole: MAA)	0.03325	88.63%
MnP1V (1-Vinylimidazole)	0.1571	48.32%
MnPM (MAA)	0.1529	62.43%
Control P1VM (1-Vinylimidazole: MAA)	0.2925	0%
Control P1V (1-Vinylimidazole)	0.3040	0%
Control PM (MAA)	0.4070	0%
MnCl$_2$ (50 µg metal content)	0.2211	positive
SOD (9.1µg)	0.0408	positive
Reagent buffer (negative control)	0.4597	negative

[a] the value given was the average of two samples

Table 10 MnP1VM, SOD activity in reusable polymer.

Sample	Concentration(mg)	SOD activity		
		1st round		3rd round
MnP1VM[a]	10	0.0313(90.95%)	0.0663(80.89%)[c]	
MnP1VM	10	0.0382 (88.99%)	0.0786(77.35%)	0.1359(60.84%)[d]
MnP1VM	10	0.0395 (88.62%)[b]		
MnP1VM	10	0.0412 (88.13%)		
$MnCl_2$	100 μg	0.0825		
Control P1VM	10	0.3432		
Control P1VM	10	0.3510		
Control P1VM (Average)		0.3471(0%)		
SOD (5 μg)		0.0895		
Reagent buffer (negative control)		0.3124		

Manganese content of the polymers determined by ICP/AES: a= 5.75 μg/mg;

b= 1.62 μg/mg; c= 1.27 μg/mg; d= 1.20μg/mg

7. Computational analysis on RNA structure and folding energy of designed gene sequences

The free energy of oligonucleotide1 encoding hexahistidine sequence was -4.4. The predicted RNA structure was shown in figure 35
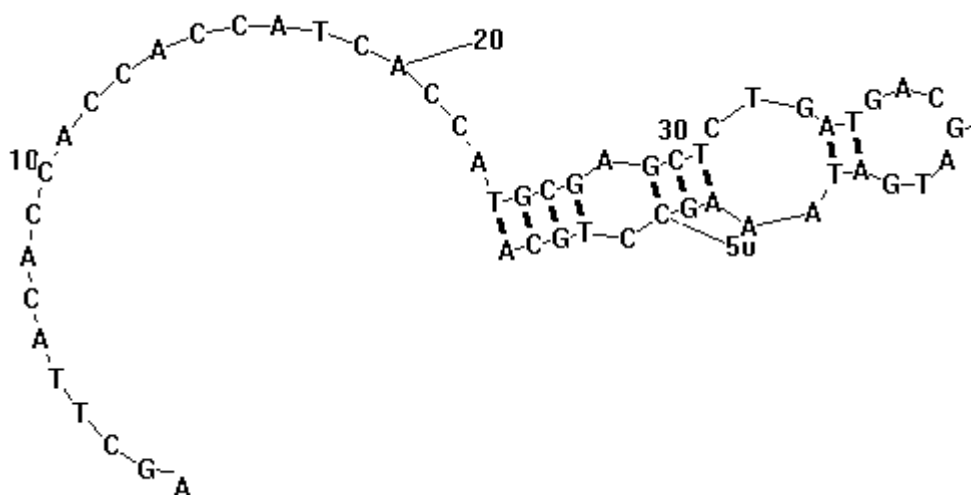
Figure 35 RNA structure prediction of oligonucleotide 1 encoding hexahistidine residues.

The free energy of oligonucleotide2 encoding the protease- binding sequence was -4.5. The predicted RNA structure was shown in figure 36
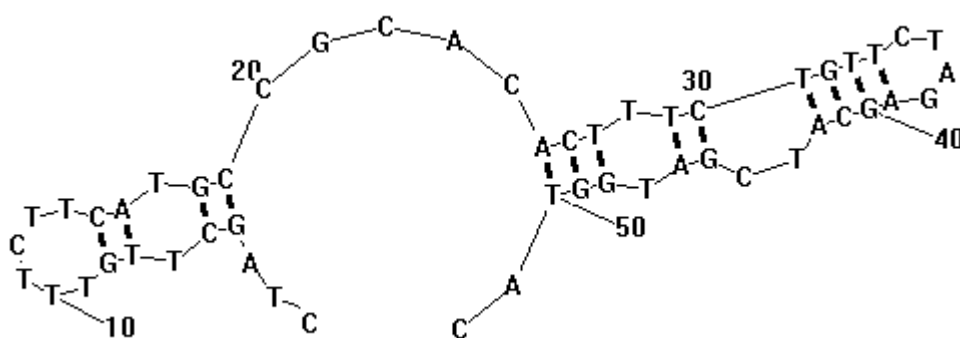
Figure 36 RNA structure prediction of oligonucleotide 2 coding for the protease-binding sequence.

All the predicted free energy of these two oligonucleotides were more than minus five, which was appropriated for chimeric gene expression.

8. Construction and Expression of Chimeric genes Encoding GFP having hexahistidine and Protease-Binding Region.

8.1 Construction of chimeric genes pH_6GFPuv and $H_6PBGFPuv$

Gene fusion technique was used as described in methods for construction of chimeric genes coding for GFP carrying hexahistidine and protease-binding sequence. Experiment was initiated by construction of a chimeric gene encoding GFP carrying hexahistidine. The plasmid pGFPuv was cleaved by *Hin*dIII and *Pst*I. Synthetic oligonucleotides encoding hexahistidine, which was known to be applied for protein purification via IMAC, was inserted into the *Hin*dIII and *Pst*I sites of the pGFPuv, generating a chimeric gene encoding hexahistidine green fluorescent protein as shown in figure 37. The resulting plasmid, pH_6GFPuv, was subsequently transformed into *E.coli* strain TG1. The green-fluorescent transformants were selected for verifying the inframe-fusing of chimeric gene by restriction endonucleases analysis. As shown in figure 38, the pGFPuv, which was applied as control, was cut with *Hin*dIII and *Sac*I, a single corresponding band was derived as represented in lane 3 and lane 4, respectively. Since the synthetic oligonucleotides were designed to carry the *Sac*I recognition site, therefore, when the purified plasmid from clones number 7, 9 and 11 were cut by *Sac*I this cleaved separately into two bands with different sizes (0.769 and 2.607 Kb) as represented in lane 7, 10 and 13, respectively. These results confirmed that the oligonucleotides encoding hexahistidine was inserted inframe into the GFPuv gene, generating the chimeric gene coding for the hexahistidine green fluorescent protein.

The chimeric pH_6GFPuv was further applied as a starting vector for further construction. The synthetic oligonucleotides that coded for protease-binding peptide (Cys-Phe-Phe-Met-Pro-His-Thr-Phe-Cys) was used for construction of a chimeric gene encoding GFPuv providing protease binding avidity. The pH_6GFPuv was cleaved by *Xba*I and *Kpn*I then the synthetic oligonucleotides were inserted into these sites yielding a chimeric gene encoding GFP having a protease binding region as shown in figure 39. The resulting plasmid was subsequently propagated by transforming into *E.coli* strain TG1. The green-fluorescent transformant colonies

were selected for restriction endonucleases analysis via *Cla*I.   Herein, the chimeric gene encoding hexahistidine GFP was applied as control. As shown in figure 40, the pH$_6$GFPuv was completely cut by *Xba*I as shown in lane 2. Since the oligonucleotide encoding protease-binding region carried the *Cla*I site, the inframe-fusing of five genes were checked via *Cla*I. The result showed that four clones were completely cut to obtain the molecular size of 3.409 Kb, as represented in lane 7, 10 and 13 of the upper part and lane10 in the lower part, respectively.

8.2 Chimeric gene expression.

All these chimeric genes were further expressed in *E. coli*. Expression of genes was simply detected in the culture upon UV light stimulation. Cell disruption was performed by sonic disintegration.   The chimeric protein was subsequently loaded to the IMAC column. The GFPuv and the PBGFPuv (182) were purified by heat treatment followed by IMACCu^{2+} while the H$_6$GFPuv and the H$_6$PBGFPuv were purified by IMACZn^{2+}. Table 11 detailed the results of each purification specific fluorescent activity of the H$_6$GFPuv (435x10^9 RFU/mg) was 3 folds higher than that of the GFPuv (173x10^9 RFU/mg).   While the fluorescent activity of GFPuv was approximately 17 folds higher than those of the PBGFPuv (10.1x10^9 RFU/mg) and the H$_6$PBGFPuv (11.4x10^9 RFU/mg). Fluorescent activities of the purified chimeric proteins were detected by Native-PAGE observed under UV light as shown in figure 41. SDS-PAGE was applied for molecular size estimation. As shown in figure 42, the GFPuv, the PBGFPuv, the H$_6$GFPuv and the H$_6$PBGFPuv, exhibited molecular weight of 30, 28, 33.7 and 34, respectively.

8.3 Removal of hexahistidine tail by Enterokinase cleavage

To investigate whether the hexahistidine could be removed after protein purification, the chimeric H$_6$GFP was incubated with enterokinase enzyme. The enterokinase cleaved specifically at the recognition sequence (DDDDK). As shown in figure 42, the binding capability to zinc ions of the chimeric H$_6$GFP was lost upon

addition of the enterokinase for 16 hours (lane 5). This finding was again supported by evidence that almost all of the proteins were retained in the wash fraction (lane 6-8). Meanwhile, omitting of the enterokinase addition resulted in a complete binding to the IMAC-gel and recovery of the protein was done by elution with chelating agent (lane 1-4). All the finding indicated that gene fusion technique was applied as a powerful tool for protein purification. Furthermore, the fusion partner could readily be removed to achieve the native protein after purification process.

8.4 Protease-binding avidity of the chimeric H_6PBGFP

To test the protease-binding avidity of the chimeric H_6PBGFP, the fluorescence gel retardation was applied. As represented in figure 43, binding of the H_6PBGFP to partial purified protease from *B. pseudomallei* led to the mobility shift of the fluorescent protein (lane 5) as compared to the control protein (lane 3). In addition, the H_6PBGFP lost its fluorescence upon thermal-induced denaturation (lane 4) while heating effect on the protease led to unfolding of protein which was unsuitable for binding interaction between these two proteins as represented in lane 6.
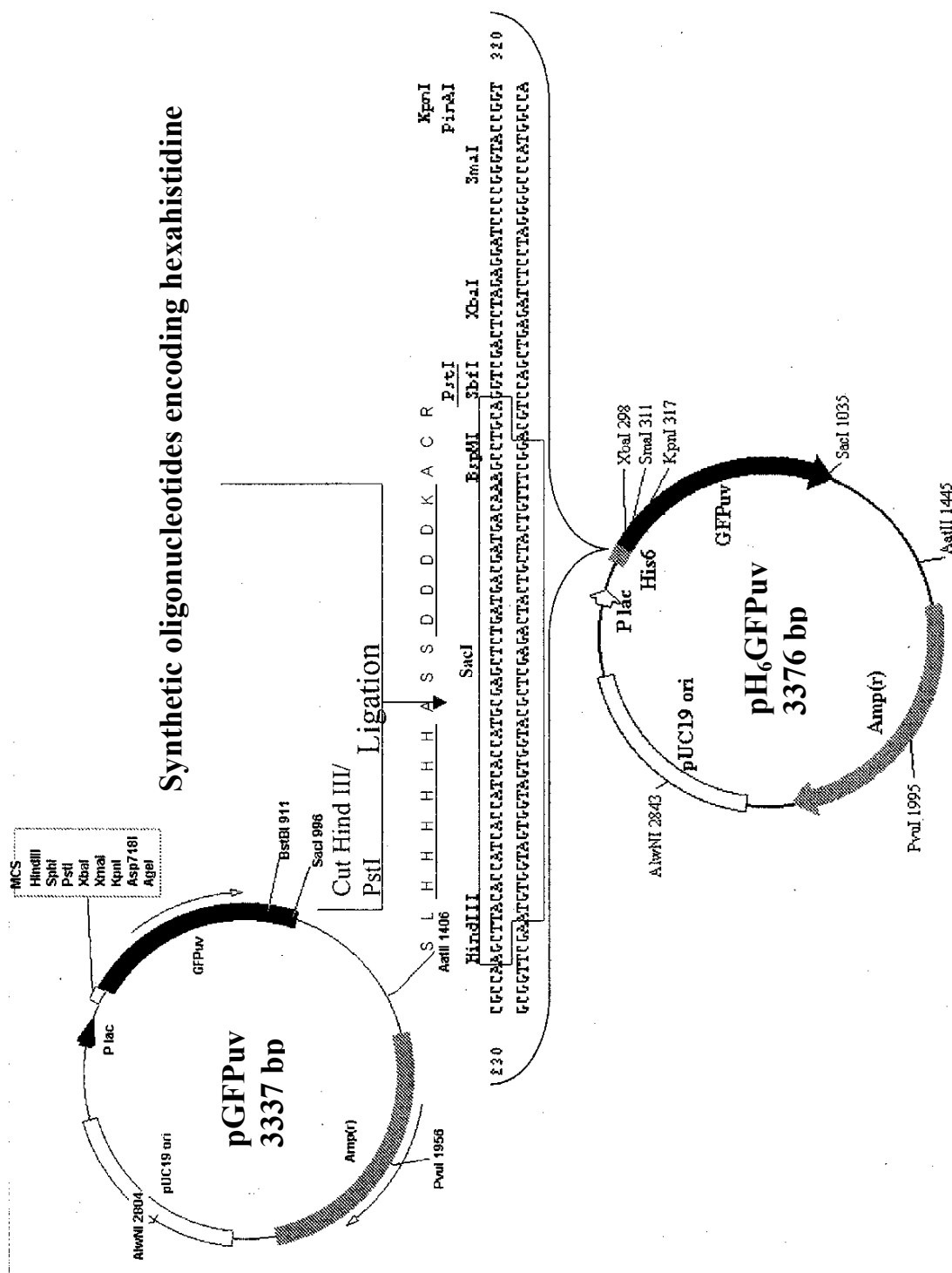
Figure 37 Construction of chimeric genes encoding pGFPuv carrying hexahistidine
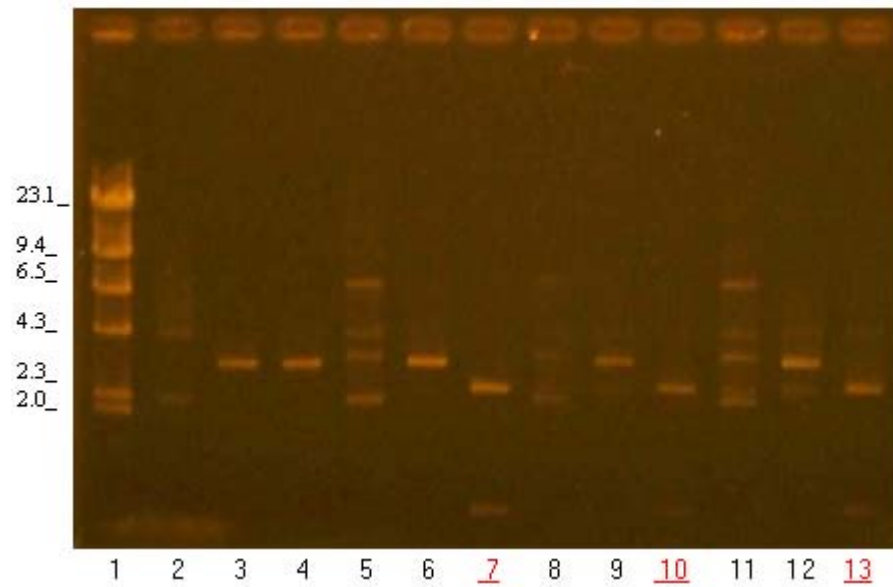
Figure 38 Restriction endonucleases analysis of chimeric genes endoding GFP carrying hexahistidine (pH$_6$GFPuv)

Lane 1	λ/*Hin*dIII marker	Lane 8	Clone 2 uncut
Lane 2	pGFPuv uncut	Lane 9	Clone 2 cut with *Hin*dIII
Lane 3	pGFPuv cut with *Hin*dIII	Lane 10	Clone 2 cut with *Sac* I
Lane 4	pGFPuv cut with *Sac*I	Lane 11	Clone 3 uncut
Lane 5	Clone 1 (uncut)	Lane 12	Clone 3 cut with *Hin*dIII
Lane 6	Clone 1 cut with *Hin*dIII	Lane 13	Clone3 cut with *Sac*I

Synthetic oligonucleotides encoding Protease-binding

pH₆GFPuv
3376bp

Xbai 298
Smai 311
KpnI 317
P lac
His6
GFPuv
pUC19 ori
AlwNI 2843
Amp(r)
PvuI 1995
AatII 1445

SacI 1035
Cut XbaI / KpnI

Ligation

L A C F F M P H T F C S R A S M V P
                                                 KpnI
      XbaI   ClaI   PinAI
SbfI   Mutated XbaI
GGTCGACTCTAGCTTCGTTTCTTCATGCCGCACACTTTCTGTTCTAGAGCATCGATGGTAC CGGTAG
CCAGCTGAGATCGAACAAAGAAGTACGGCGTGTGAAAGACAAGATCTCGTAGCTACCATGGCCATC
290   355

pH₆PBGFPuv
3409bp

SacI 266
HindIII 235
PstI 290
P lat
His6
PB
GFPuv
SacI 1068
pUC19 ori
AlwNI 2876
Amp (r)
PvuI 2028
AatII 1478

Figure 39 Construction of pH₆PBGFPuv Chimeric genes Encoding GFPuv having hexahistidine and Protease-Binding Region.
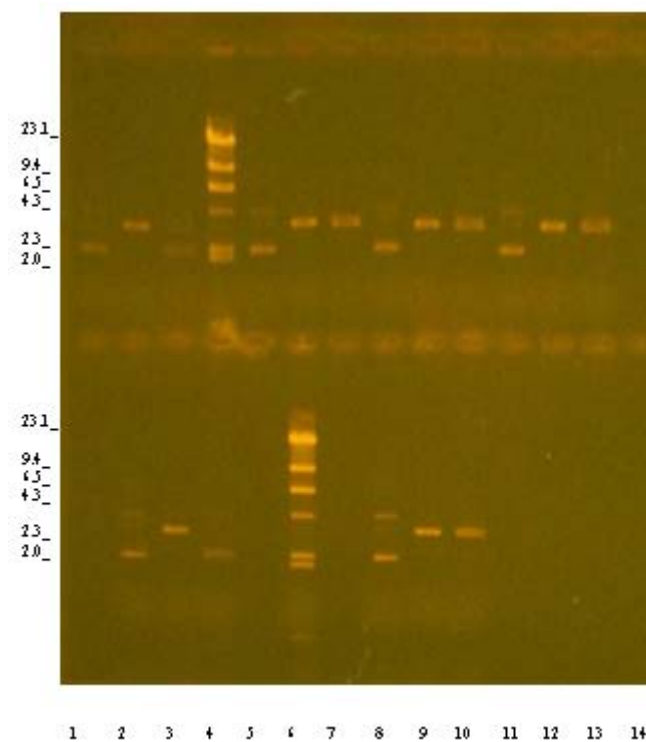
Figure 40 Restriction endonuclease analysis of chimeric genes coding for GFP carrying hexahistidine and protease-binding sequence (pH$_6$PBGFPuv)

TOP

Lane 1-3 pH 6GFPuv uncut, cut with *Xba*I, cut with *Cla*I

Lane 4 λ/ *Hin*dIII marker

Lane 5-7 Clone 1 uncut, cut with *Xba*I, cut with *Cla*I

Lane 8-10 Clone 2 uncut, cut with *Xba*I, cut with *Cla*I

Lane 11-13 Clone 3 uncut, cut with *Xba*I, cut with *Cla*I

BOTTOM

Lane 2-4 Clone 4 uncut, cut with *Xba*I, cut with *Cla*I

Lane 6 λ/ *Hin*dIII marker

Lane 8-10 Clone 5 uncut, cut with *Xba*I, cut with *Cla*I

Table 14 Purification Table

Protein	Volume (ml)	Protein content (mg/mL)	Total Protein (mg)	Total Fluorescence (RFU)	Specific activity (RFU/mg)	Purification fold
GFP						
Crude GFP	4	1.8	7.2	95.85×10^9	13.3×10^9	
Heated Crude GFP	3.5	0.46	1.61	93.01×10^9	57.8×10^9	4.35
IMAC	6	0.265	1.59	275×10^9	173×10^9	13
H$_6$GFP						
Crude H$_6$GFP	5	3.74	18.69	910×10^9	48.72×10^9	
IMAC	5	0.51	2.53	1101×10^9	435×10^9	8.93
PBGFP						
Crude PBGFP	5	1.87	9.35	6.2×10^9	0.67×10^9	
Heated Crude PBGFP	4.5	0.57	2.57	4.7×10^9	1.82×10^9	2.73
IMAC	6	0.17	1.01	10.2×10^9	10.1×10^9	15.2
H$_6$PBGFP						
Crude H$_6$PBGFP	4.5	2.58	11.63	14.5×10^9	1.25×10^9	
IMAC	5	0.28	1.498	17.1×10^9	11.4×10^9	9.12
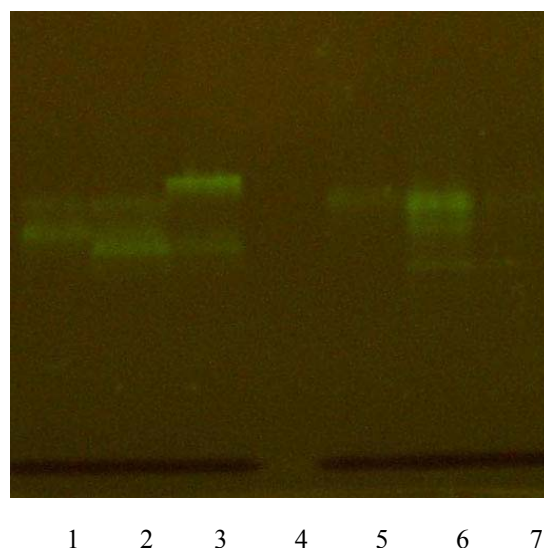
Figure 41 Native –PAGE of chimeric green fluorescent proteins, the GFPuv, the PB-GFPuv, the H_6GFPuv and H_6PBGFPuv

Lane 1   Purified native GFPuv (IMAC Cu^{2+})

Lane 2   Purified PB-GFPuv (IMAC Cu^{2+})

Lane 3   Purified H_6GFPuv (IMAC Zn^{2+})

Lane 5   Purified H_6PBGFPuv (IMAC Zn^{2+})

Lane 6   Purified H_6PBGFPuv (IMAC Cu^{2+})

Lane 7   Supernate of H_6PBGFPuv (IMAC Zn^{2+})
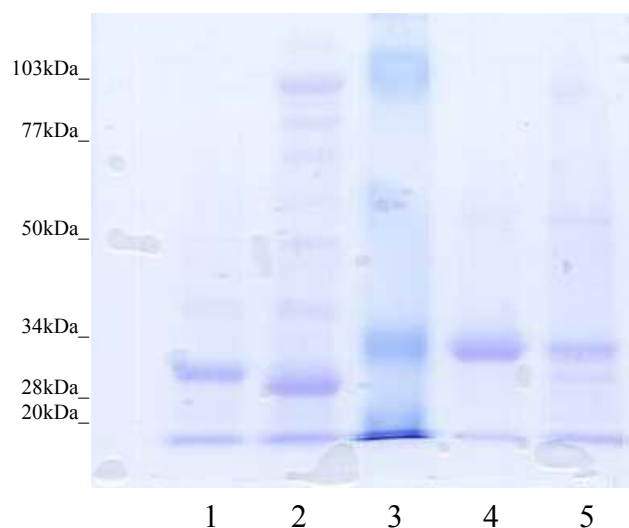
Figure 42 SDS-PAGE of chimeric proteins, the GFPuv, the PB-GFPuv, the H_6GFPuv and H_6PBGFPuv

Lane 1   Purified native GFPuv (IMAC Cu^{2+})

Lane 2   Purified PB-GFPuv (IMAC Cu^{2+})

Lane 3   Standard protein marker

Lane 4   Purified H_6GFPuv (IMAC Zn^{2+})

Lane 5   Purified H_6PBGFPuv (IMAC Zn^{2+})
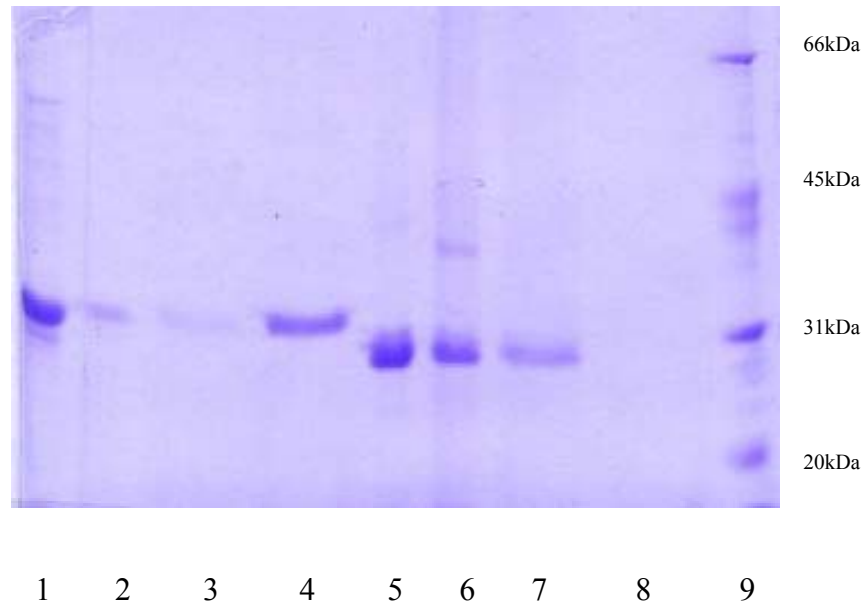
Figure 43 SDS-PAGE analysis of products of H$_6$GFPuv cleaved by enterokinase.

Lane 1 H$_6$GFP, 16 hours incubation without EK

Lane 2 H$_6$GFP, after loaded IMAC Zn^{2+}

Lane 3 H$_6$GFP, from wash fraction

Lane 4 H$_6$GFP, from elute fraction

Lane 5 H$_6$GFP and EK mixture, 16 hours incubation

Lane 6 H$_6$GFP and EK mixture, after load IMAC Zn^{2+}

Lane 7 H$_6$GFP and EK mixture, from wash fraction

Lane 8 H$_6$GFP and EK mixture, from elute fraction

Lane 9 Molecular Marker
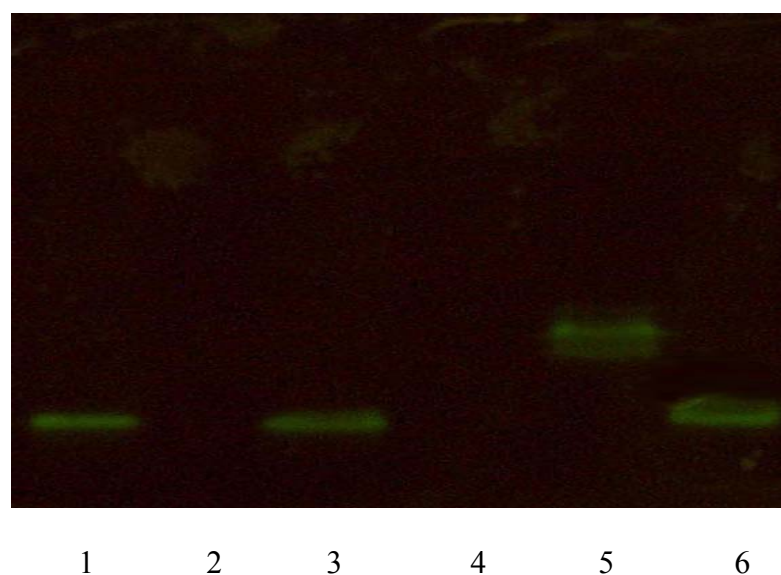
Figure 44 Binding capacity of Hexahistidine protease-binding green fluorescent
protein.

Lane 1   Purified H$_6$PBGFP

Lane 2   Marker

Lane 3   Purified H$_6$PBGFP

Lane 4   Heated Purified H$_6$PBGFP with Partial purified protease

Lane 5   Purified H$_6$PBGFP with Partial purified protease

Lane 6   Purified H$_6$PBGFP with Heated Partial purified protease

CHAPTER V
DISCUSSION

Synthesis of a polymer supported metal catalyst useful as a SOD mimic

Free radical is defined as any radical species those providing one or more unpaired electrons. They are unstable and highly reactive to other cellular components including proteins, lipids and lipoproteins, nucleic acids, carbohydrates etc. Involvement of free radical in several pathological condition (e.g. artherosclerosis, cancer, diabetes etc) has been evidenced (11,107,125). Meanwhile, scavenging and antioxidantion for the protection against the damaging effects of free radical in the biological system are extensively explored (11,119,120).

Superoxide dismutases (SODs) are among the major role player of scavenging activity. The enzymes catalyze the disproportionation of superoxide to yield molecular oxygen and hydrogen peroxide. Many researchers have focussed attention on developing and applying either the native enzyme or the SOD mimics in therapeutic approach. Degree of expression of SOD enzymes in cell culture and in whole animals has been well established to provide protection against the deleterious effects of a wide range of models of oxidative stress (185-187). Moreover, application of the purified native enzyme as a commercial product namely Orgotein$^{\circledR}$ (bovine Cu/Zn SOD) has extensively been investigated in clinical trial for decade (118,188,189). The Orgotein shows its efficacy to attenuate inflammation and pain of rheumatoid arthritis and osteoarthritis (190-195). It also possesses the protective effect against acute and chronic side effects associated with chemotherapy and radiotherapy (188,196). Despite the apparent clinical benefit, SOD enzymes suffer as drug candidates due to several reasons (as described in Chapter II), and have been removed from the market primarily because of immunogenic response. In addition, there are some limitations including the size of molecule (30 kDa), which is unable to penetrate the cellular component, as well as the short life span in vivo. Therefore,

there is an increasing trend of developing synthetic SOD mimics that may lead to circumvent all these problems. Searching for more potent and stable metal chelates has resulted in the discovery of at least three to four classes of metal-containing SOD mimetics. These include the salen, macrocyclic, metalloporphyrin and the compounds (kojic acid, 7-hydroxyflavone, desferoxamine) based SOD mimetics (114,197,204). For instance, the macrocyclic, M-40403 has been reported to have excellent therapeutic efficacy in a variety of cancer including skin and kidney cancers. In addition to its anticancer activity, the M-40403 and other related SOD mimetics have demonstrated favorable therapeutic effects in animal models of myocardial infarction, stroke, inflammatory bowel disease, rheumatoid arthritis, diabetic microangiopathies and septic shock and neurodegenerative disorder (114,197). Applying of these reactive compounds for clinical investigations can be benefit due to the cellular permeability, the lack of immunogenicity and the longer half life in blood circulation. Moreover, the potential to apply for oral delivery as well as the cost of goods can also be taken into an account. However, these are some limitations including the drawback interaction between the metal compound and a wide variety of reactive oxygen species, which may perturb some physiological processes. In addition, releasing of the active metal upon decomposition of the complex results in a huge toxicity to biological macromolecule.

In the present study, the newly catalytic polymers as superoxide dismutase mimetics have successfully been constructed by using the molecular imprinting technique. This is due in part to the selectivity of molecularly imprinted materials, the versatility of metal ligand coordination and the stability of the imprinted polymer. The metal imprinted polymers have been designed according to the metal coordination sphere at the active site as those of the enzymes in nature e.g. MnSOD and FeSOD. The metal coordination center of SOD enzyme contains existing ligands including three nitrogen from three imidazole groups of histidine residue and two oxygen from carboxylic group of aspartic acid and H_2O. Considering on the functional group existing at the active center leads to the selection of artificial functional monomers such as 4(5)-vinylimidazole or 1-vinylimidazole and methacrylic acid for mimicking the imidazole group and the carboxylic group, respectively. The 4(5)-vinylimidazole has already been selected as the first priority to

mimic the imidazole group. The imidazole group of 4(5)-vinylimidazole has two nitrogen groups that can play role on metal coordination reaction. However, synthesis of the 4(5)-vinylimidazole is laborious and the difficulty to achieve high amount of the compound is also taken into an account. Therefore, the 1-vinylimidazole has further been applied for such system. Although, the 1-vinylimidazole has only one group of nitrogen to form a complex with metal but the polymer (MeP1VM) possesses higher SOD activity than the MeP4VM at all metal tested (Table 9). This may be explained by the fact that in the natural enzyme system, the metal center is coordinated to histidine residues via the "pyridine nitrogen" (N-3) (192), which is better simulated by 1-vinylimidazole. Importantly, the functional monomer is also a critical role on catalytic activity of the imprinted polymer, the necessity of functional monomer has been determined. Omitting one of the functional monomer results in a markedly decrease of SOD activity. (Table 9) This clearly indicates that the MnMIP requires mainly 2 functional monomers to form complex with Mn in order to retain SOD activity. This is as well in good agreement with the enzyme in nature, which requires the correct folding of amino acids His 74, His 163, His 26, and Asp 159 in the active site. Unfolding or misfolding of the native protein results in a complete loss of activity (109,110).

This study explores a high possibility to develop the molecular imprinted polymer for clinical application as well as biotechnological aspect because of the ease of preparation, low cost and the reusability of the polymer. For such certain condition, the MnP1VM may further be applied as an immobilized enzyme mimic for scavenging of oxygen free radicals that have been generated from any sources such as cancer drug and chemical compounds. Upon implementation of the imprinted polymer into the biological system, the reactivity and toxicity to cellular compartments can be negligible. This is due in part to the stability of the polymer that prevents a release of free active metal to the system. However, improvement of the polymer needs to be geared for the future task. These include solubility, size, metal stability as well as the catalytic activity. The solubility of the polymer can be obtained by using a water soluble crosslinking agent. While the suspension polymerization technique may be useful in order to circumvent the sizing problem. The stability and activity improvement may obtain by searching for any other

functional monomers that provide high affinity to metal ions. For the biotechnological applications, the polymer supported metal (Mn, Co, Cu, Fe and Ni) catalyst will further be determined on their epoxidation ability and applied for compound synthesis (199). Furthermore, selectivity to metal ions and metal-binding capability of the polymer has to be investigated, which will be applied as a potential tool for metal remediation in the future.

Metal-binding tag as a powerful tool for protein purification

Although various classical separation procedures, which are based on the physicochemical properties of the protein, such as charge, size, and hydrophobicity, can be employed for purification of recombinant proteins. These procedures are often time consuming and laborious. Based on a particular property of an amino acid sequence that is fused to the recombinant protein as affinity tag, simple and rapid approaches for purification have extensively been developed (142). These include using the glutathione *S*-transferase and the maltose-binding protein as the fusion partners (201,202). Protein A is also a popular fusion system for purification of recombinant protein via immunoglobulin columns (200). Binding of biotin tag to avidin–agarose has been reported (203). The histidine tag has been applied for purification via metal chelate affinity chromatography for decade (151). Purification of protein with the histidine tag system provides more advantages than the other taggers since it can be performed even under denaturing conditions e.g. 8M urea or 6M guanidine hydrochloride (144). Elution of protein can be done under mild conditions e.g. using metal-chelating agent (EDTA) or competitor (histidine or imidazole).

In this study, the metal-binding tag is applied as a powerful approach for protein purification. The tagger has easily been inserted onto the protein of interest at the gene level. Based on the concept that polyhistidine bind tightly to a number of transition metals including Cu^{2+}, Ni^{2+}, Zn^{2+} and Co^{2+}, therefore, the hexahistidine-tagged GFPuv generated from gene fusion technique can be purified by Immobilized Metal Affinity Chromatography (IMAC) charged with zinc ions. Zinc ions have been

chosen as linker due to the very low adsorptivity of the native GFPuv as compared to copper and nickle ions (151). Although the purification fold of the H_6GFP is not greater than that of the native GFPuv but the H_6GFPuv shows highly purity and the purified protein can easily be obtained in one step purification (table11, figure 42). Furthermore, an enterokinase cleavage site (DDDDK) can also be inserted to allow removal of hexahistidine sequence after purification, in such a way that the fusion partner may interfere or disturb the property of native protein (figure 43). However, neither the metal-binding region nor the enterokinase cleavage site affects both the fluorescent emission and the binding capacity to protease of the chimeric protease-binding GFPuv, (figure 44). These indicate that the metal-binding tag can simply be fused to assist protein purification and the purified chimeric Protease-binding GFPuv can directly be applied as a potential tool for detection in the future.

CHAPTER VI

CONCLUSION

1. The polymer supporting manganese, which was constructed by molecular imprinting technique, has found to be useful as SOD mimic

2. The manganese coordination form in the center among functional monomers has found to play an important role for possessing the highly SOD catalytic activity

3. Both functional monomers, 1-vinylimidazole and methacrylic acid were necessary to maintain the highly catalytic ability of polymer.

4. The genetic construction of chimeric protein encoding GFP having metal-binding tag and protease binding have been successfully constructed.

5. The chimeric proteins possessed metal-binding capability, which could be applied for protein purification by Immobilized Metal Affinity Chromatography (IMAC) charged with zinc ions.

6. The hexahistidine peptide can be specifically removed at the enterokinase cleavage site by the enterokinase enzyme.

7. The protease binding sequence of chimeric H6PBGFP possessed binding avidity to protease, which will be further applied as a tool for detection of *Burkholderia pseudomallei* in the future

REFERENCES

1. Ye L, Mosbach K. The technique of molecular imprinting - Principle, state of the art, and future aspects. J Incl Phenom Macrocycl Chem 2001;41(1-4): 107-13.

2. Haupt K. Imprinted polymers Taylor made mimics of antibodies and receptors. Chem Commun 2003;2:171-8.

3. Piletsky SA, Turner APF. Electrochemical sensors based on molecularly imprinted polymers Electroanalysis. 2002;14(5):317-23.

4. Davidson L, Hayes W. Molecular imprinting of biologically active steroidal systems Curr Org Chem 2002;6:265-81.

5. Shi RX, Guo CH, Zou XH, Zhu CY. The development of research in molecular imprinting technique Prog Chem 2002;14(3):182-91.

6. Andersson LI. Molecular imprinting for drug bioanalysis: A review on the application of imprinted polymers to solid-phase extraction and binding assay. Journal of Chromatography B: Biomedical Sciences and Applications 2000;739:163-73

7. Andersson LI. Molecular imprinting: developments and applications in the analytical chemistry field. Journal of Chromatography B: Biomedical Sciences and Applications 2000;745:3-13

8. Wulff G, Poll HG. Enzyme-Analogue Built Polymers. 23: Influence of the Structure of the Binding Sites on the Selectivity for Racemic Resolution. Makromol Chem 1987;188:741-8.

9. Mosbach K, Yu Y, Andersch J, Ye L.Generation of New Enzyme Inhibitors Using Imprinted Binding Sites: The Anti-Idiotypic Approach, a Step toward the Next Generation of Molecular Imprinting. J Am Chem Soc 2001; 123:12420-1

10. Yu Y, Ye L, Haupt K, Mosbach K. Formation of a Class of Enzyme Inhibitors

(Drugs), Including a Chiral Compound, by Using Imprinted Polymers or Biomolecules as Molecular-Scale Reaction Vessels. Angew Chem Int Ed 2002; 41(23):4460-3

11.   Fridovich I. Superoxide radical and superoxide dismutases. Ann Rev Biochem 1995;64:97-112.

12.   Pauling L. A Theory of the Structure and Process of Formation of Antibodies. J Am Chem Soc 1940;62:2643-57.

13.   Dickey, FH. The Preparation of Specific Adsorbents. Proc Natl Acad Sci USA 1949;35 (5):227-9

14.   Mosbach K, Mosbach R. Entrapment of enzymes and microorganisms in synthetic cross-linked polymers and their application in column techniques. Acta Chimica Scandinavica 1966;20, 2807-10

15.   Takagishi T, Klotz IM. Macromolecule-Small Interactions; Introduction of Additional Binding Sites in Polyethyleneimine by Disulfide Cross-Linkages. Biopolymers 1972;11:483-91.

16.   Wulff G, Sarhan A, Gimpel J, Lohmar.E. Über enzymanalog gebaute Polymere, Zur Synthese von polymerisierbaren D-Glycerinsäurenderivaten. Chem Ber 1974; 107:3364-76.

17.   Wulff G. Biorecognition in Molecularly Imprinted Polymers. Concept, Chemistry, and Application. In Molecular Interactions in Bioseparations, edited by T. Ngo. New York: Plenum Press 1993; 363-81.

18.   Arshady R, Mosbach K. Synthesis of Substrate-selective Polymers by Host-Guest Polymerization. Makromol Chem 1981;182:687-92.

19.   Fujii Y, Kikuchi K, Matsutani K, Ota K, Adachi M, Syoji M, Haneishi I, Kuwana Y. Template synthesis of polymer Schiff base Co(III) complex and formation of specific cavity for chiral amino acids. Chem Lett 1984;1487-90.

20.   Fujii Y, Matsutani K, Kikuchi K. Formation of a Specific Co-ordination Cavity for a Chiral Amino Acid by Template Synthesis of a Polymer Schiff Base Cobalt (III) Complex. J Chem Soc Chem Commun 1985;415-7.

21.   Dhal PK, Arnold FH. Template-Mediated Synthesis of Metal-Complexing

Polymers for Molecular Recognition. J Am Chem Soc 1991;113:7417-8.

22. Dhal PK, Arnold FH. Metal-Coordination Interactions in the Template-Mediated Synthesis of Substrate-Selective Polymers: Recognition of Bis(imidazole) Substrates by Copper(II) Iminodiacetate Containing Polymers. Macromolecules 1992;25:7051-9.

23. Whitcombe MJ, Rodriguez ME, Villar P, Vulfson EN. A new method for the introduction of recognition site functionality into polymers prepared by molecular imprinting: Synthesis and characterization of polymeric receptors for cholesterol. J Am Chem Soc 1995;117(27):7105-11.

24. Shea KJ, Stoddard GJ, Shavelle DM, Wakui F, Choate RM. Synthesis and Characterization of Highly Cross-Linked Polyacrylamides and Polymethacrylamides. A New Class of Macroporous Polyamides. Macromolecules1990;23(21):4497-507.

25. Shea KJ, Dougherty TK. Molecular Recognition on Synthetic Amorphous Surfaces. The Influence of Functional Group Positioning on the Effectiveness of Molecular Recognition. J Am Chem Soc 1986;108 (5):1091-3.

26. Wulff G. Molecular Imprinting in Cross-Linked Materials with the Aid of Molecular Templates - A Way towards Artificial Antibodies. Angew Chem Int Ed Engl 1995;34:1812-32.

27. Tsukagoshi K, Yu KY, Maeda M, Takagi M. Metal Ion-Selective Adsorbent Prepared by Surface-Imprinting Polymerization. Bull Chem Soc Jpn 1993;66:114-20.

28. Rosatzin T, Andersson L I, Simon W, Mosbach K. Preparation of Ca2+ Selective Sorbents by Molecular Imprinting using Polymerisable Ionophores. J Chem Soc Perkin Trans1991;1261-5.

29. Kuchen W, Schram J. Metal-Ion-Selective Exchange Resins by Matrix Imprint with Methacrylates. Angew Chem Int Ed Engl 1988;27(12):1695-7.

30. Efendiev AA. Complexing polymer sorbents and metal polymer complex catalysts with specially designed structure of active centers. Macromol Symp 1994; 80:289-313.

31. Leonhardt A, Mosbach K. Enzyme-mimicking polymers exhibiting specific substrate binding and catalytic functions. React Polym 1987;6:285-90.

32. Kempe M, Glad M, Mosbach K. An approach towards surface imprinting using the enzyme Ribonuclease A. J Mol Recogn 1995;8(1/2):35-9

33. Plunkett S D, Arnold F H. Molecularly imprinted polymers on silica: selective supports for high-performance ligand-exchange chromatography. J Chromatogr A 1995;708:19-29.

34. Zeng X F, Murray G M. Synthesis and characterization of site-selective ion-exchange resins templated for lead(II) ion. Sep Sci Technol 1996;31(17):2403-18.

35. Chen H, Olmstead MM, Albright R L, Devenyi J, Fish RH. Metal-ion templated polymers: Synthesis and structure of N-(4-vinylbenzyl)-1,4,7-triazcyclonanezinc(II) complexes, their copolymerization with divinylbenzene, and metal-ion selectivity studies of the demetalated resins - Evidence for a sandwich complex in the polymer matrix. Angew Chem Int Ed Engl 1997;36(6):642-5.

36. Fish R H. Metal Ion Templated Polymers: Studies of N-(4-Vinylbenzyl)-1,4,7-Triazacyclononane-Metal Ion Complexes and Their Polymerization with Divinylbenzene: The Importance of Thermodynamic and Imprinting Parameters in Metal Ion Selectivity Studies of the Demetalated, Templated Polymers. ACS Symp Ser 1998;703:238-50.

37. Lo HC, Chen H, Fish RH. Synthesis of a [{mono-N-(4-vinylbenzyl)-1,4,7-triazacyclononane}(2)Hg](OTf)(2) sandwich complex, polymerization of this monomer with divinylbenzene, and Hg2+ ion selectivity studies with the demetallated resin. Eur J Inorg Chem 2001;(9):2217-20.

38. Nicholls IA. Thermodynamic Considerations for the Design of and Ligand Recognition by Molecularly Imprinted Polymers. Chem Lett 1995;1035-6.

39. Hosoya K, Shirasu Y, Kimata K, Tanaka N. Molecularly Imprinted Chiral

Stationary Phase Prepared with Racemic Template. Anal Chem 1998;70(5):943-5.

40. Hosoya K, Tanaka N. Development of Uniform-Sized, Molecular-Imprinted Stationary Phases for HPLC. ACS Symp Ser 1998;703:143-58.

41. Kempe M, Mosbach K. Direct resolution of naproxen on a non-covalently molecularly imprinted chiral stationary phase. J Chromatogr 1994;664:276-9.

42. Yilmaz E, Mosbach K, Haupt K. Influence of Functional and Cross-Linking Monomers and the Amount of Template on the Performance of Molecularly Imprinted Polymers in Binding Assays. Anal Comm 1999;36(5):167-70.

43. Yu C, Mosbach K. Insights into the Origins of Binding and the Recognition Properities of Molecularly Imprinted Polymers Prepared Using an Amide as the Hydrogen Bonding Functional Group. J Mol Recogn 1998;11:69-74.

44. Abraham MH. Scales of solution hydrogen bonding: Their construction and application to physicochemical processes. Chem Soc Rev 1993;73-83

45. Ramstrom O, Yu C, Mosbach K. Chiral recognition in adrenergic receptor binding mimics prepared by molecularly imprinting. J Mol Recogn 1996;9:691-6.

46. Sellergren B, Shea KJ. Influence of polymer morphology on the ability of imprinted network polymers to resolve enantiomers. J Chromatogr 1993;(635):31-49.

47. O'Shannessy DJ, Ekberg B, Mosbach K. Molecular Imprinting of Amino Acid Derivatives at Low Temperature (0ºC) Using Photolytic Homolysis of Azobisnitriles. Anal Biochem 1989;177:144-9.

48. Vorderbruggen MA, Wu K, Breneman CM. Use of cationic aerosol photopolymerization to form silicone microbeads in the presence of molecular templates. Chem Mater 1996;8(5):1106-11.

49. Haginaka J, Sakai Y, Narimatsu S. Uniform-Size Molecularly Imprinted Polymer Material for Propanolol. Recognition of Propranolol and its Metabolites. Anal Sci 1998;14(4):823-6.

50. Haginaka J, Sanbe H. Uniform-Sized Molecularly Imprinted Polymers for Beta-Estradiol. Chem Lett 1998;(11):1089-90.

51. Haginaka J, Takehira H, Hosoya K, Tanaka N. Molecularly Imprinted Uniform-Sized Polymer-Based Stationary Phase for Naproxen-Comparison of Molecular Recognition Ability of the Molecularly Imprinted Polymers Prepared by Thermal and Redox Polymerization Techniques. J Chromatogr A 1998;816 (2):113-21.

52. Kempe M. Antibody-Mimicking polymers as chiral stationary phases in HPLC. Anal Chem 1996;68 (11):1948-53.

53. Schweitz L, Andersson LI, Nilsson S. Capillary electrochromatography with predetermined selectivity obtained through molecular imprinting. Anal Chem 1997; 69(6):1179-83.

54. Schweitz L, Andersson LI, Nilsson S. Capillary Electrochromatography with Molecular Imprint-Based Selectivity for Enantiomer Separation of Local Anaesthetics. J Chromatogr A 1997;792(1-2):401-9.

55. Walshe M, Garcia E, Howarth J, Smyth MR, Kelly MT. Separation of the enantiomers of propranolol by incorporation of molecularly imprinted polymer particles as chiral selectors in capillary electrophoresis. Anal Commun 1997;34 (4):119-21.

56. Sellergren B. Direct Drug Determination by Selective Sample Enrichment on an Imprinted Polymer. Anal Chem 1994;66:1578-82.

57. Martin P, Wilson ID, Morgan DE, Jones GR, Jones K. Evaluation of a Molecular Imprinted Polymer for Use in the Solid Phase Extraction of Propranolol from Biological Fluids. Anal Comm 1997;34(2):45-7

58. Muldoon MT, Stanker LH. Molecularly imprinted solid phase extraction of atrazine from beef liver extracts. Anal Chem 1997;69(5):803-8.

59. Matsui J, Okada M, Tsuruoka M, Takeuchi T. Solid Phase Extraction of a Triazine Herbicide Using a Molecularly Imprinted Synthetic Receptor. Anal Comm 1997;34(3):85-7.

60. Mullett WM, Lai EPC. Determination of Theophylline in Serum by Molecularly Imprinted Solid-Phase Extraction with Pulsed Elution. Anal Chem 1998;70 (17):3636-41.

61. Andersson LI, Paprica A, Arvidsson T. A highly selective solid phase extraction sorbent for pre-concentration of sameridine made by molecular imprinting. Chromatographia 1997;46(2):57-62.

62. Andersson HS, Nicholls IA. Molecular Imprinting: Recent Innovations in Synthetic Polymer Receptor and Enzyme Mimics. Recent Res Devel in Pure & Applied Chem 1997;1:133-57.

63. Vlatakis G, Andersson LI, Miller R, Mosbach K. Drug Assay Using Antibody Mimics Made by Molecular Imprinting. Nature 1993;361:645-7

64. Andersson LI, Miller R, Vlatakis G, Mosbach K. Mimics of the Binding Sites of Opioid Receptors Obtained by Molecular Imprinting of Enkephalin and Morphine. Proc Natl Acad Sci USA 1995;92:4788-92.

65. Andersson LI. Application of molecular imprinting to the development of aqueous buffer and organic solvent based radioligand binding assays for S-propranolol. Anal Chem1996;68:111-7.

66. Muldoon MT, Stanker LH. Polymer Synthesis and Characterization of a Molecularly Imprinted Sorbent Assay for Atrazine. J Agric Food Chem 1995; 43:1424-7.

67. Haupt K, Dzgoev A, Mosbach K. Assay System for the Herbicide 2,4-D Using a Molecularly-Imprinted Polymer as an Artificial Recognition Element. Anal Chem 1998;70(3):628-31.

68. Ramstrom O, Ye L, Mosbach K. Artificial Antibodies to Corticosteroids Prepared by Molecular Imprinting. Chem Biol 1996;3(6):471-7

69. Bengtsson H, Roos U, Andersson LI.. Molecular Imprint based Radioassay for Direct Determination of S-Propranolol in Human Plasma. Anal Comm 1997;34 (9):233-5.

70. Ellman J, Stoddard B, Wells J. Combinatorial thinking in chemistry and biology. Proc Natl Acad Sci USA 1997;94:2779-82

71. Terrett NK, Gardner M, Gordon DW, Kobyleki RJ. Steele. Drug discovery by combinatorial chemistry the development of novel method for the rapid synthesis of single compounds. Chem Eur J 1997;3:1917-20

72. Ecker DJ, Crook ST. Combinatorial drug discovery: Which methods will produce the greatest value? Bio/Technology 1995;13:351-60

73. Ramstram O, Ye L, Mosbach K. Screening of a Combinatorial Steroid Library Using Molecularly Imprinted Polymers. Anal Comm 1998;35(1):9-11.

74. Malitesta C, Losito I, Zambonin PG. Molecularly Imprinted Electrosynthesized Polymers: New Materials for Biomimetic Sensors. Anal Chem 1999;71(7)1366-70.

75. Andersson LI, Miyabayashi A, O'Shannessy DJ, Mosbach K. Enantiomeric resolution of amino acid derivatives on molecularly imprinted polymers as monitored by potentiometric measurements. J Chromatogr 1990;516:323-31.

76. Hedborg E, Winquist F, Lundstram I, Andersson LI, Mosbach K. Some studies of molecularly imprinted polymer membranes in combination with field-effect devices. Sensor Actuator A-Phys 1993;(36-38):796-9.

77. Piletsky SA, Parhometz YP, Lavryk NV, Panasyuk TL, El'skaya AV. Sensors for low-weight organic molecules based on molecular imprinting technique. Sensor Actuator B1994;18-19:629-31.

78. Kriz D, Mosbach K. Competitive amperometric morphine sensor based on an agarose immobilized molecularly imprinted polymer. Anal Chim Acta 1995;300:71-5.

79. Kriz D, Ramstram O, Svensson A, Mosbach K. Introducing biomimetic sensors based on molecularly imprinted polymers as recognition elements. Anal Chem 1995; 67:2142-44.

80. Kriz D, Kempe M, Mosbach K. Introduction of molecularly imprinted polymers as recognition elements in conductometric chemical sensors. Sens Actuator B1996; 33:178-81.

81. Chen GH, Guan ZB, Chen CT, Fu LT, Sundaresan V, Arnold FH. A glucose-sensing polymer. Nature Biotechnol 1997;15 (4):354-7

82. Turkewitsch P, Wandelt B, Darling GD, Powell WS. Fluorescent Recognition Sites Through Molecular Imprinting. A Polymer-Based Fluorescent Chemosensor for Aqueous cAMP. Anal Chem 1998;70(10):2025-30.

83. Lai EPC, Fafara A, Van der Noot VA, Kono M, Polsky B. Surface Plasmon

Resonance Sensors Using Molecularly Imprinted Polymers for Sorbent Assay of Theophylline, Caffeine, and Xanthine. Can J Chem 1998;76 (3):265-73.

84. Jenkins AL, Uy OM, Murray GM. Polymer-Based Lanthanide Luminescent Sensor for Detection of the Hydrolysis Product of the Nerve Agent Soman in Water. Anal Chem 1999;71:373-8.

85. Lahav M, Katz E, Doron A, Patolsky F, Willner I. Photochemical Imprint of Molecular Recognition Sites in Monolayers Assembled on Au Electrodes. J Am Chem Soc 1999;121(4):862-3.

86. Kroger S, Turner APF, Mosbach K, Haupt K. Imprinted Polymer Based Sensor System for Herbicides Using Differential-Pulse Voltammetry on Screen Printed Electrodes. Anal Chem 1999;71(17):3698-702.

87. Lerner RA, Benkovic SJ, Schultz PG. At the crossroads of chemistry and immunology: Catalytic antibodies. Science 1991;252:659-67

88. Schultz PG, Yin J, Lerner RA. The Chemistry of the Antibodies Molecule. Angew Chem Int Ed 2002;41(23):4427-37

89. Robinson DK, Mosbach K. Molecular Imprinting of a Transition State Analogue Leads to a Polymer Exhibiting Esterolytic Activity. J Chem Soc Chem Commun 1989;(14):969-70.

90. Muller R, Andersson LI, Mosbach K. Molecularly imprinted polymers facilitating an elimination reaction. Makromol Chem Rapid Commun 1993;14:637-41.

91. Ohkubo K, Urata Y, Honda Y, Nakashima Y, Yoshinaga K. Preparation and catalytic property of L-histidyl group-introduced, crosslinked poly(ethylene imine)s imprinted by a transition-state analogue of an esterolysis reaction. Polymer 1994;35 (24):5372-4.

92. Sellergren B, Shea KJ. Enantioselective ester hydrolysis catalysed by imprinted polymers. Tetrahedron Asymm 1994;5:1403-6.

93. Matsui J, Nicholls IA, Karube I, Mosbach K. Carbon-carbon bond formation using catalytic polymers prepared by molecular imprinting: An artificial class II aldolase. J Org Chem 1996;61:5414-7.

94. Liu XC, Mosbach K. Studies towards a tailor-made catalyst for the Diels-Alder

reaction using the technique of molecular imprinting. Macromol Rap Comm 1997;18 (7):609-15.

95. Wulff G, Gross T, Schvnfeld R. Enzyme Models Based on Molecularly Imprinted Polymers with Strong Esterase Activity. Angew Chem Int Ed Engl 1997;36 (18):1962-4.

96. Liu XC, Mosbach K. Catalysis of Benzisoxazole Isomerization by Molecularly Imprinted Polymers. Macromol Rapid Comm 1998;19(12):671-4.

97. McCord JM, Fridovich I. Superoxide dismutase: an enzymatic function for erythrocuprein. J Biol Chem 1969;244:6049-55.

98. Omar BA, McCord JM. Interstitial equilibration of superoxide dismutase correlates with it protective effect in the isolated rabbit heart. J Mol Cell Cardiol 1991;23:149-59.

99. Droy-Lefaix MT, Drouet Y, Geraud G, Hosfod D, Braquet P. Superoxide dimutase (SOD) and the PAF-antagonist (BN 52021) reduce small intestinal damage induced by ischemiareperfusion. Free Rad Res Commun 1991;12:725-35.

100. Chan PH, Yang GY, Chen SF, Carlson E, Epstein CJ. Cold-induced brain edema and infarction are reduced in transgenic mice overexpressing superoxide dismutase. Ann Neurol 1991;29: 482-6.

101 Yang G, Chan PH, Chen J, Carlson E, Chen SF, Weinstein P, et al. Human copper-zinc superoxide dismutase transgenic mice are highly resistant injury after focal cerebral ischemia. Stroke 1994;25:165-70.

102. Deng HX, Hentati A, Tainer JA, Iqbal Z, Cayabyab A, Hung WY. Amyotrophic lateral sclerosis and structural defects in CU, Zn superoxide dismutase. Science 1993; 261:1047-1051.

103. Rosen DR, Siddique T, Patterson D, Figlewicz DA, Sapp P, Hentati A. Mutations in Cu/Zn superoxide dismutase gene are associated with familial amyotrophic lateral sclerosis. Nature 1993;362:59-62.

104. Brown RHJr. Amyotrophic lateral sclerosis: recent insights from genetics and transgenic mice. Cell 1995;80:687-92.

105. Troy CM, Shelanski ML. Down-regulation of copper/zinc superoxide dismutase

causes apoptotic death in PC12 neuronal cells. Proc Natl Acad Sci USA 1994;91: 6384-7.

106. Greenlund LJS, Deckwerth TL, Johnson EMJr. Superoxide dismutase delays neuronal apoptosis: a role for reactive oxygen species in programmed neuronal death. Neuron 1995;14:303-15.

107. St Clair DK, Oberley TD, Muse KE & St Clair WH Expression of manganese superoxide dismutase promotes cellular differentiation. Free Radic Biol Med 1994;16:275–82.

108. Church SL, Grant JW, Ridenour LA, Oberley LW, Swanson PE, Meltzer PS, et al. Increased manganese superoxide dismutase expression suppresses the malignant human melanoma cells. Proc Natl Acad Sci USA 1993; 90:3113-7.

109. Atzenhofer W, Gunther Regelsberger G, Jacob U, Peschek GA, Furtmuller PG, Hubern R and Obinger C. The 2.0 Aº Resolution Structure of the Catalytic Portion of a Cyanobacterial Membrane-bound Manganese Superoxide Dismutase. J Mol Biol 2002;321:479–89.

110. Gloria EOB, Matthew P, Ramsey C, Anuradha S, Edward HS. Cryo-trapping the Six-coordinate, Distorted-octahedral Active Site of Manganese Superoxide Dismutase. J Mol Biol 2000;296:951-9.

111. Fantone JC, Ward PA. A review: role of oxygen-derived free radicals and metabolites in leukocyte-dependent inflammatory reactions. Am J Pathol 1982;107: 395-418

112. Deitch EA, Bridges W, Berg R, Specian RD, Granger N. Hemorrhagic shock-induced bacterial translocation: The role of neutrophils and hydroxyl radicals. J Trauma 1990;30:942-51.

113. Salvemini D, Marino MH, Seibert K. Activation of the cyclooxygenase pathway by nitric oxide: new concepts of inflammation and therapy. Drug News Perspectives 1996;204-19.

114. Salvemini D, Wang Z-Q, Zweier J, Samouilov A, MacarthurH, MiskoT, CurrieMG, Cuzzocrea S, Sikorski JA, Riley DP. A non-peptidyl mimic of superoxide dismutase with therapeutic activity in rats. Science 1999;286:304-6.

115. Dix TA, Hess KM, Medina MA, Sullivan RW, Tilly SL, Webb TLL. Mechanism of site-selective DNA nicking by the hydrodioxyl (perhydroxyl) radical. Biochemistry 1996;35:4578-4583.

116. Salvemini D, Wang Z-Q, Stern MK, Currie MG, Misko TP. Peroxynitrite decomposition catalysts: Novel therapeutics for peroxynitrite-mediated pathology. Proc Natl Acad Sci USA 1998;95:2659-63

117.   Macarthur H, Westfall TC, Riley DP, Misko TP, Salvemini D. Inactivation of catecholamines by superoxide gives new insights on the pathogenesis of septic shock. Proc Natl Acad Sci USA 2000;97:9753-8.

118. Huber W, Menander-Huber KB, Saifer MGP, Williams LD. Bioavailability of superoxide dismutase: implications for the anti-inflammatory action mechanism of Orgotein. AAS 1980;7:185-95.

119. Flohe L. Superoxide dismutase for therapeutic use: clinical experience, dead ends and hopes. Mol Cell Biochem 1988;84:123-31.

120. Maxwell SRJ. Prospects for the use of antioxidant therapies. Drugs 1995;49: 345-361.

121. Werns SW, Simpson PJ, Mickelson JK, Shea MJ, Pitt B, Lucchesi B. Sustained limitation by superoxide dismutase of canine myocardial injury due to ischemia followed by reperfusion. J Cardiovasc Pharmacol 1988;11:36-44.

122. Omar BA, McCord JM. Interstitial equilibration of superoxide dismutase correlates with it protective effect in the isolated rabbit heart. J Mol Cell Cardiol 1991;23:149-59.

123. McCord JM. Superoxide dismutase: rationale for use in reperfusion injury and inflammation. J Free Rad Biol Med 1986;2:307-10.

124. Chan P H, Yang G Y, Chen S F, Carlson E, Epstein C J. Cold-induced brain edema and infarction are reduced in transgenic mice overexpressing superoxide dismutase. Ann Neurol 1991;29:482-6.

125. Yang G, Chan PH, Chen J, Carlson E, Chen SF, Weinstein P, et al. Human copper-zinc superoxide dismutase transgenic mice are highly resistant injury after focal cerebral ischemia. Stroke 1994;25:165-70.

126 . Zweier JL. Prevention of reperfusion-induced, free radical mediated acute

endothelial injury by superoxide dismutase as an effective tool to delay/prevent chronic renal allograft failure: a review. Transplant Proc 1997;29:2567-8.

127. Shingu M, Takahashi S, Ito M, Hamamatu N, Svenega T, Chibanese Y, Nobunaga M. Anti-inflammatory effects of recombinant human manganese superoxide dimutase on adjuvant arthritis in rats. Rheumatol Int 1994;14:77-82.

128. Andreassen OA, Ferrante RJ, Dedeoglu A, Albers DW, Klivenyi P, Carlson EJ, Epstein CJ, Beal MF. Mice with a partial deficiency of manganese superoxide dismutase show increased vulnerability to the mitochondrial toxins malonate, 3-nitropropionic acid, and MPTP. Exp Neurol 2001;167(1):189-95.

129. Church SL, Grant JW, Ridenour LA, Oberley LW, Swanson PE, Meltzer PS, et al. Increased manganese superoxide dismutase expression suppresses the malignant human melanoma cells. Proc Natl Acad Sci USA 1993;90:3113-7.

130. Safford SE, Oberley TD, Urano M, St Clair DK. Suppression of fibrosarcoma metastasis by elevated expression of manganese superoxide dismutase. Cancer Res 1994;54: 4261-5.

131. Flores SC, Marecki JC, Harper KP, Bose SK, Nelson SK, McCord JM. Tat protein of human immunodeficiency virus type 1 represses expression of manganese superoxide dismutase in HeLa cells. Proc Natl Acad Sci USA 1993;90:7632-6.

132. Edeas MA, Emerit I, Khalhoun Y, Lazizi Y, Cernjavski L, Levy A, et al. Clastogenic factors in plasma of HIV-1 infected patients activate HIV-1 replication in vitro: inhibition by superoxide dismutase. Free Rad Biol Med 1997;23:571-8.

133. Mollace V, Nottet HS, Clayette P, Torco MC, Muscoli C, Salvemini D, Perno CF. Oxidative stress and neuro-aids: triggers, modulators and novel antioxidants. Trends Neurosci 2001;24:411-6.

134. Salminen U, Harjula A L, Maasilta PK, Romanska HM, Bishop AE, Polak JM.

Superoxide dismutase in development of obliterative bronchiolitis. Transplant Proc 2001;33:2477.

135. Barnes JP. Chronic obstructive pulmonary disease. N Engl J Med 2000;343:269-80.

136. Wyde PR, Moore DK, Pimentel DM, Gilbert BE. Recombinant superoxide dismutase (SOD) administered by aerosol inhibits respiratory syncytial virus infection in cotton rats. Antiviral Res 1996 Jul;31(3):173-84.

137. Klivenyi P, St Clair D, Wermer H, Yen H C, Oberly T, Yang L, Beal MF. Manganese superoxide dismutase overexpression attenuates MPTP toxicity. Neurobiol Dis 1998;5:253-8.

138. Lefaix JL. Successful treatment of radiation induced fibrosis using CuZn SOD an Mn SOD: an experimental study. Int J Radiat Oncol Biol Phys 1996;35:305-312.

139. Beyer, W. F., Jr and Fridovich, I. Methods Enzymol. 1990;186:242–9

140. Tian, Y. et al. Biochem. Biophys. Res. Commun. 1993;191:646–53

141. Archibald, F. S. and Fridovich, I. Arch. Biochem. Biophys. 1982;214:452–63

142. LaVallie E R and McCoy J M. Gene fusion expression systems in Escherichia coil Current Opinion in Biotechnology 1995;6:501-6

143. Crowe J, DObeli H, Gentz R, Hochuli E, StLiber D, Henco K: 6 x His—Ni-NTA chromatography as a superior technique in recombinant protein expression/purification. Methods Mol Blot 1994;31:371-87.

144. Hopp TP, Prickett KS, Price V, Libby RT, March CJ, Cerretli P, Urdal DL, Conlon PJ: A short polypeptide marker sequence useful for recombinant protein identification and purification. Biotechnology 1988;6:1205-10.

145. Schmidt TGM, Skerra A: The random peptide library-assisted engineering of a C- terminal affinity peptide, useful for the detection and purification of a functional Ig Fv fragment. Protein Eng 1993;6:109-22.

146. Schatz PJ. Use of peptide libraries to map the substrate specificity of a peptide-modifying enzyme: a 13 residue consensus peptide specifies biotinylatlon in Escherichla coil Biotechnology 1993;11:1138-43.

147. Dalbege H, Dahl HHM, Pedersen J, Hansen JW, Christensen T: A novel

enzymatic method for production of authentic hGH from an Escherichia coli-produced hGH precursor. Biotechnology 1987;5:161-4.

148. Brewer Sl, Sassenfeld HM. The purification of recombinant proteins using C-terminal poly-arginine fusions. Trends Biotechnol 1985;3:119-22.

149. Persson M, Bergstrand MG, Bulow L, Mosbach K: Enzyme purification by genetically attached polycysteine and polyphenylalanine tags. Anal Biochem 1988; 172:330-337.

150. Neff D, De Lalla C, Petrul H, Neff P, Winter G: Calmodulin as a versatile tag for antibody fragments. Biotechnology 1995;13:373-7.

151. Chaga GS. Twenty-five years of immobilized metal ion affinity chromatography: past, present and future. J. Biochem Biophys Methods 2001;49:313–34

152. LaVallie ER, Rehemtulla A, Racie LA, DiBlasio EA, Ferenz C, Grant KL, Light A, McCoy JM: Cloning and functional expression of a cDNA encoding the catalytic subunit of bovine enterokinase. J Bio Chem 1993;268:23311-7.

153. Collins-Racie LA, McColgan JM, Grant KL, DiBlasio-Smith EA, McCoy JM, LaVallie ER: Production of recombinant bovine enterokinase catalytic subunit in Escherichia colt using the novel secretory fusion partner DsbA. Biotechnology 1995; 13

154. Cubitt AB, Heim R. "Understanding, improving and using green fluorescent proteins." Trends in Biochemical Sciences1995;20(11):448-55.

155. Gerdes HH, Kaether C. "Green fluorescent protein: applications in cell biology." FEBS Letters1996;389(1):44-7.

156. Tsien R, Heim R, et al. "Measurement and manipulation of cell signals with photons and designed molecules." Progress in Biophysics and Molecular Biology 1996;65(1):2.

157. Kendall JM, Badminton MN. "Aequorea victoria bioluminescence moves into an exciting new era." Trends in Biotechnology 1998;16(5):216-24.

158. Phillips J, George N. "Structure and dynamics of green fluorescent protein." Current Opinion in Structural Biology1997;7(6):821-7.

159. Naylor LH. (1999). "Reporter gene technology: the future looks bright."
        Biochemical Pharmacology1999;58(5):749-57.

160. Misteli T, Spector DL. "The cellular organization of gene expression."
        Current Opinion in Cell Biology1998;10(3):323-31.

161. Matus A. "GFP in Motion CD-ROM; Introduction: GFP illuminates
        everything." Trends in Cell Biology1999; 9(2):43.

162. Matus A. "GFP moves on." Trends in Cell Biology 2001; 11(5):183.

163. Cormack BP, Valdivia RH, et al. "FACS-optimized mutants of the green
        fluorescent protein (GFP)." Gene 1996;173(1):33-8.

164. Phillips GJ. "Green fluorescent protein-a bright idea for the study of bacterial
        protein localization." FEMS Microbiology Letters 2001;204(1):9-18.

165. Ikawa, M., S. Yamada, et al. "Green mice and their potential usage in biological
        research." FEBS Letters 1998;430(1-2):83-7.

166. Okabe M, Ikawa M, et al. (1997). "Green mice as a source of ubiquitous green
        cells." FEBS Letters 1997;407(3):313-9.

167. Mercuri A, Sacchetti A. "Green fluorescent flowers." Plant Science
        2002;162(4):647-54.

168. Lippincott-Schwartz J, Smith CL. "Insights into secretory and endocytic
        membrane traffic using green fluorescent protein chimeras." Current
        Opinion in Neurobiology 1997;7(5):631-9.

169. Bastiaens PIH, Pepperkok R. "Observing proteins in their natural habitat: the
        living cell." Trends in Biochemical Sciences 2000;25(12):631-7.

170. Miller DL, Bao S. "Ultrasonic enhancement of gene transfection in murine
        melanoma tumors." Ultrasound in Medicine & Biology
        1999;25(9):1425-30.

171. Zhao H,Arnold FH. "Combinatorial protein design: strategies for screening
        protein libraries." Current Opinion in Structural Biology 1997; 7(4):
        480-5.

172. Josenhans C, Friedrich S. "Green fluorescent protein as a novel marker and
        reporter system in Helicobacter sp." FEMS Microbiology Letters
        1998;161(2):263-273.

173. Wouters FS, Verveer PJ. "Imaging biochemistry inside cells." Trends in Cell

Biology 2001;1(5):203-211.

174. White J, Stelzer E. "Photobleaching GFP reveals protein dynamics inside live cells." Trends in Cell Biology 1999;(2):61-65.

175. Li Y, Agrawal A. "Characterization of metal affinity of green fluorescent protein and its purification through salt promoted, immobilized metal affinity chromatography." Journal of Chromatography A 2001;909(2):183-90.

176. Nordstrom T, Senkas A. "Generation of a new protein purification matrix by loading ceramic hydroxyapatite with metal ions-demonstration with poly-histidine tagged green fluorescent protein." J Biotech 1999;69(2-3):125-33.

177. Nock S, Spudich JA. "Reversible, site-specific immobilization of polyarginine-tagged fusion proteins on mica surfaces." FEBS Letters 1997;414(2):233-8.

178. Park SH. and Raines RT. Methods in Enzymology. San diego.2000

179. Overberger CG, Vorchheimer N. Imidazole-containing Polymer. Synthesis and Polymerization of the Monomer 4(5)-Vinylimidazole. 1963; 85

180. Fridovich I, Beyer WF. Assaying for Superoxide Dismutase Activity: Some Large Consequences of Minor Changes in Conditions. Anal Biochem 1987;161:559-66.

181. Maniatis T, Frisch E. Molecular cloning: A laboratory manual. New York, Cold Spring Harbour Laboratory Press. 2000.

182. Petkanchanapong W, Fredriksson S. "Selection of Burkholderia pseudomallei Protease-binding Peptide by Phage Display." Biotech Letter 2000;22:1597-602.

183. Bradford MM. "A rapid and sensitive method for the quantitation of microgram quantities of protein utilizing the principle of protein-dye binding." Anal Biochem 1976;72: 248-54.

184. Laemmli UK. "Cleavage of structural proteins during the assembly of the head of bacteriophages T4." Nature1970;227(259): 680-5.

185. Krall J, Bagley AC, Mullenbach GT, Hallewell RA, Lynch RE. Superoxide

mediates the toxicity of paraquatfor cultured mammalian cells. J Biol Chem 1988;263:1910–4.

186. Ho YS, Vincent R, Dey MS, Slot JW, Crapo JD. Transgenic models for the study of lung antioxidant defense: enhanced manganese-containing superoxide dismutase activity gives partial protection to B6C3 hybrid mice exposed to hyperoxia. Am J Respir Cell Mol Biol 1998;18:538–47.

187. Sohal RS, Agarwal A, Agarwal S, Orr WC. Simultaneous overexpression of copper- and zinccontaining superoxide dismutase and catalase retards age-related oxidative damage and increases metabolic potential in *Drosophila melanogaster*. J Biol Chem 1995;270: 15671–4.

188. Edsmyr F, Huber W, Menander KB. Orgotein efficacy in ameliorating side effects due to radiation therapy. I. Doubleblind, placebo-controlled trial in patients with bladder tumors. Curr Ther Res Clin Exp 1976;19:198–211.

189. Marberger H, Huber W, Bartsch G, Schulte T, Swoboda P. Orgotein: a new anti-inflammatory metalloprotein drug evaluation of clinical efficacy and safety in inflammatory conditions of the urinary tract. Int Urol Nephrol 1974;6:61–74.

190. Goebel KM, Storck U, Neurath F. Intrasynovial Orgotein therapy in rheumatoid arthritis Lancet 1981;1:1015–7.

191. Goebel KM, Storck U. Effect of intra-articular Orgotein versus a corticosteroid on rheumatoid arthritis of the knees. Am J Med 1983;74:124–8.

192. Lund-Olesen K, Menander-Huber KB. Intra-articular Orgotein therapy in osteoarthritis of the knee. A double-blind, placebo-controlled trial. Drug Res 1983;8: 1199–203.

193. Gammer W, Broback LG. Clinical comparison of Orgotein and methylprednisolone acetate in the treatment of osteoarthrosis of the knee joint. Scand J Rheumatol 1984;13:108–12.

194. Mcllwain H. Intra-articular Orgotein in osteoarthritis of the knee: a placebo-controlled efficacy, safety, and dosage comparison. Am J Med 1989;87:295–300.

195. Mazieres B, Masquelier AM, Capron MHA French controlled multicenter study of intraarticular Orgotein versus intraarticular corticosteroids in the treatment of knee osteoarthritis: a one-year followup. J Rheumatol 1991;18:134–7.

196. Sanchiz F. Prevention of radioinduced cystitis by Orgotein: a randomized study. Anticancer Res 1996;16:2025–8.

197. Salvemini D, Riley DP SOD mimetic are coming of age Nature review: Drug discovery 2002;1:367-74

198. Whittaker MM, Whittaker JW Mutagenesis of a Proton Linkage Pathway in Escherichia coli Manganese Superoxide Dismutase. Biochemistry 1997;36:8923.

199. Alexander C, Davidson L, Hayes W Imprinted polymer: artificial molecular recognition materials with application in synthesis and catalysis. Tetrahedron 2003;59:2025-57.

200. Nilsson B, Abrahmsen L. Fusions to *Staphylococcal* protein A. Methods Enzymol 1990;185:144-61.

201. Smith DB, Johnson KS**.** Single-step purification of polypeptides expressed in *Escherichia coli* as fusions with glutathione S-transferase. Gene 1988;67:31-40.

202. Di Guan C, Li P, Riggs PD, Inouye H. Vectors that facilitate the expression and purification of foreign peptides in *Escherichia coil* by fusion to maltose-binding protein. Gene 1988;67:21-30.

203. Schatz PJ. Use of peptide libraries to map the substrate specificity of a peptide-modifying enzyme: a 13 residue consensus peptide specifies biotinylation in *Escherichia coil* Biotechnology 1993;11:1138-43.

204. Vajragupta O, Boonchoong P, Sumanont Y, Watanabe H, Wongkrajanga Y, Kammasuda N. Manganese-Based Complexes of Radical Scavengers as Neuroprotective Agents Bioorganic & Medicinal Chemistry 2003;11(10):2329-37

APPENDIX

1. Reagent for Sodium Dodecyl Sulfate Polyacrylamide Gel Electrophoresis (SDS-PAGE)

1.1 Acrylamide solution (30%T, 2.7% C)

Fifty eight point four grams of acrylamide and 1.6 g of N, $N^{/}$ methylene bisacrylamide were dissolved in 120 ml of distilled water, stirred, warm at 37°C then adjusted to 200 ml with distilled water. The solution was filtered by whatman No1 filter paper, adjusted the pH to 7.0 or less and stored in a dark bottle at 4°C.

1.2 Separating gel buffer (1.5 M Tris-HCl pH 8.8)

Thirty six point three grams of Trizma base was dissolved in 160 ml of distilled water, adjusted to pH 8.8 by conc HCl and added distilled water to 200 ml.

1.3 Stacking gel buffer (0.5 M Tris-HCl pH 6.8)

Three grams of Trizma base was dissolved in 40 ml of distilled water, adjust to pH 6.8 by conc HCl then added distilled water to 50 ml.

1.4 10% Sodium dodecyl sulphate (SDS)

Ten grams of SDS was dissolved in 90 ml of distilled water, heated to 68 ^{o}C and adjusted to pH 7.2 by adding a few drops of conc HCl, and then with distilled water to 100 ml.

1.5 10% Ammonium persulphate

Fifty mg of ammonium persulphate was dissolved in 500 µl of distilled water.

1.6 Sample solubilized buffer (2X) (0.125 M Tris-HCl pH 8.8, 4% SDS, 20% glycerol, 10% 2-mercaptoethanol)

The sample solubilized buffer was prepared by adding 1 ml of 10% SDS, 2 ml of glycerol, 1 ml of 2-mercaptoethanol and 2 mg of Bromophenol blue into 1.5 M Tris-HCl pH 8.8 and then adjusted the volume to 10 ml by adding distilled water. Aliquoted 1 ml of this solution into microcentrifuge tubes and kept at -20 $^{\circ}$C.

1.7 Tank buffer (0.025 M Tris pH 8.3, 0.192 M glycine, 0.1% SDS)

Three grams of Trizma base, 14.4 g of glycine were dissolved in 800 ml of distilled water, added 10 ml of 10% SDS, then adjusted the pH to 8.3 by conc HCl and filled to 1 L with distilled water.

1.8 Staining solution (0.125% Coomassie blue R 250, 50% methanol, 10% acetic acid)

Sixty two point five ml of 1% Coomassie blue, 250 ml of methanol and 50 ml of acetic acid were mixed together and adjusted to 500 ml with distilled water.

1.9 Destaining solution I (50% methanol, 10% acetic acid)

Five hundred ml of methanol and 100 ml of acetic acid were mixed together and adjusted to 1000 ml with distilled water.

1.10 Destaining solution II (5% methanol, 7% acetic acid)

Seventy ml of acetic acid and 50 ml of methanol were mixed together and adjusted to 1000 ml with distilled water.

2.   Luria-Bertani Medium (LB medium)

Compositions of LB broth were of 10 g Tryptone, 5 g yeast extract, 5 g NaCl. All components were dissolved in 800 ml of distilled water. The pH of the medium was adjusted to 7.4 by 1 N NaOH. Then distilled water was added to a final volume of 1 L and autoclaved. To prepare the LB agar, 15 grams of agar was melted in 1 L of LB broth and autoclaved at 121°C, 15 lb/inch^2 for 15 minutes. The LB agar was then

cooled down to 60°C and ampicillin was added when necessary to a final concentration of 100 mg/L before pouring on to sterile plates.

3.   Gel Electrophoresis Buffer (5X) [0.04 M Tris-acetate, 1 mM EDTA, pH 7.5(TAE)].

To prepare TAE buffer (5X), 24.2 g of Tris base was resuspended in 800 ml of deionized water. Then the solution was added with both 5.71ml of glacial acetic acid and 10 ml of 0.5 M EDTA, pH 8.0. The solution was adjusted to 1 L with deionized water.

BIOGRAPHY

NAME	Mr. Theeraphon Piacham
DATE OF BIRTH	22 August 1978
PLACE OF BIRTH	Phichit, Thailand
INSTITUTIONS ATTENDED	Chulalongkorn University, 1996-1999: Bachelor of Science (Medical Technology) Mahidol University, 2000-2002: Master of Science (Medical Technology)
GRANTS	-The Ministry Staff Development Project -UMAP Credit Transfer Scheme - The Swedish Strategic Research Foundation